An analysis of the bed nuclei of the Stria terminalis and related circuitry in the modulation of memory consolidation

Lingg, Ryan Thomas

AN ANALYSIS OF THE BED NUCLEI OF THE STRIA TERMINALIS AND RELATED CIRCUITRY IN THE MODULATION OF MEMORY CONSOLIDATION

by

Ryan Thomas Lingg

A thesis submitted in partial fulfillment
of the requirements for the Doctor of Philosophy
degree in Psychology in the
Graduate College of
The University of Iowa

May 2022

Thesis Committee: Jason Radley, Thesis Supervisor
Ryan T. LaLumiere
Nandakumar S. Narayanan
Rainbo Hultman
John H. Freeman

To my father, who would have been there

To my mother, who always has been there

To my partner, who is always there

To our dogs, who follow anywhere

To our chickens, who do not care

ABSTRACT

Memory consolidation following stressful experiences is a key means of adaptation, allowing a long-term representation of the event to facilitate evaluation of future threats. It is well documented that the consolidation process is enhanced by glucocorticoids, the end-products of the HPA cascade, via activation of cognate receptors in the basolateral amygdala. Nevertheless, there remain lingering questions concerning what changes in endogenous glucocorticoid activity are necessary to enhance memory, which neural systems are involved in this modulation, and whether they overlap with the neural systems implicated in memory generalization. The experiments described here attempt to address this by elucidating neural circuits involved in modulating endogenous glucocorticoid activity and their contribution to memory consolidation and generalization.

Prior work from our laboratory has established a role for the anteroventral subdivision of the bed nuclei of the stria terminalis (avBST) in the modulation of the HPA axis. Moreover, avBST maintains extensive connectivity with a network of limbic cortical circuitry canonically associated with memory consolidation. As such, avBST is well positioned to act within the traditional framework of the consolidation network and as a regulatory locus for the hormonal modulation of memory strength. In chapter 2 we show post-training optogenetic stimulation of avBST bi-directionally modulated long-term retention of a single-trial inhibitory avoidance task via connectivity with separate downstream effectors. Post-training photoinhibition of avBST soma, and its projection to the paraventricular hypothalamus was sufficient to augment long-term retention (by 200%), an effect contingent upon an increased availability of corticosterone produced by the optogenetic manipulation. Separately, post-training photoexcitation of avBST, and its

projection to the ventrolateral periaqueductal gray could diminish long-term retention (by 50%), an effect independent of any changes in HPA activity. Together, these data support a role for divergent avBST centered circuits in the modulation of memory consolidation, whereby biasing avBST activity toward excitation or inhibition engages the capacity to restrict or augment consolidation, respectively.

Chapter 3 addresses the role of a discrete prefrontal projection to BST that is critical for preventing context fear generalization. Generalization of fear is a fundamental adaptive neurobiological process conserved across species that is critical for survival. Organisms utilize environmental information from previous fearful experiences to shape behavioral responses to novel situations where the presence of a threat is uncertain. Provided the perception of threat is high, organisms may express a range of defensive behaviors deemed most likely to navigate the threat successfully. Although generalization is necessary for an organism to predict the presence of threat and select the appropriate behavioral response, in humans, generalization of fear to environments or to cues that bear little similarity to previous fearful experiences is a hallmark of stress-related psychiatric disease. Given the necessity of generalization processes in adapting to complex environmental changes, there is a critical need to better understand the neural systems that restrict fear generalization during periods of uncertainty and the underlying perturbations that lead to the exaggeration of these responses.

Here we used intersectional viral approaches to characterize a subsection of prefrontal input to BST originating from the rostral end of the prelimbic region (rPL) and interrogate its involvement in regulating context fear generalization. We applied electrophysiological and optical methods for monitoring and manipulating neural activity

immediately following training on a modified inhibitory avoidance (IA) procedure to target post-training consolidation processes, as this period is critical for mediating the emergence of long-term fear generalization. We found that rPL provides discrete input to the caudal end of the anterior BST and targets GAD1, but not vGlut2, expressing neurons that in turn provide input to a distributed network of threat processing regions. rPL neuronal ensembles were robustly mobilized following training and were differentially recruited during avoidance testing in a novel context. BST was similarly mobilized during training and avoidance testing. Post-training optical inhibition of the rPL-BST pathway with eNpHR3.0 exaggerated post-training CORT responses and was associated with increased avoidance to a novel chamber 48hrs later, an effect that was not dependent on the increased CORT availability. Separately, we used pre-exposure to a neutral context to encourage later generalization of fear. Here, post-training optical or chemogenetic activation of the rPL-BST pathway with ChR2 (E123A), or hM3dq prevented generalization 48hrs later to the neutral context without affecting avoidance to the training context. We also demonstrate these effects are specific to rPL-BST, and not an rPL-vlPAG projection that maintains collaterals with BST. Together, these data provide evidence for a novel circuit tasked with regulating post-training consolidation processes that contribute to the emergence of generalized fear.

These results outline a BST centric network that is differentially able to modulate the contribution of the neuroendocrine response during memory consolidation and separably capable of mediating the extent of memory consolidation that occurs and whether environmental features extend the generalization of fear to novel situations involving threat.

PUBLIC ABSTRACT

Discrimination between threatening and non-threatening contexts is an adaptive neurobiological process. However, chronic or traumatic stressors may shift responses toward responding to non-threatening contexts as if they contained a threat, a response known as generalization. From a translational perspective, the loss of discrimination, or *over-generalization*, from a stressful to neutral context is one of the core features of stress-related psychiatric diseases. The general goal of this dissertation is to characterize the neural circuits modulating adaptation to environmental threats in the rodent brain and how these affect the ability to discriminate between neutral and threatening contexts in the future. In the first chapter I will discuss the primary research literature relevant to this topic. I will provide background on stress literature and neural circuitry in relation to memory consolidation, a critical process by which organisms create long-term memories. The hypothalamo-pituitary-adrenal (HPA) axis is the canonical neuroendocrine system for stress. Activation of this neuroendocrine cascade produces glucocorticoid hormone secretion that affects a variety of functions in the body and enhances memory consolidation through activation of the neural pathways to be studied in my dissertation. Much prior research has made inroads in understanding the neurobiology of discrimination, however, the neural circuits accounting for how stress perturbs these processes has received less attention. To address this, my work has investigated how a discrete region of the basal forebrain, the bed nucleus of the stria terminalis, mediates the extent with which glucocorticoid hormones contribute to memory consolidation and separably participates in a prefrontal cortex driven network responsible to preventing memory for aversive experiences from generalizing to distinct situations that do not

involve a threat. In this way, the bed nucleus of the stria terminalis is a critical component of how an organism learns about a threat, the extent to which that learning is dependent upon the release of stress hormones, and whether that learning extends to situations of relative uncertainty.

TABLE OF CONTENTS

LIST OF FIGURES

LIST OF ABBREVIATIONS

AAV: Adeno-associated virus

ACTH: adrenocorticotropic hormone

al: anterolateral

ANOVA: Analysis of variance

AP: Anterior/Posterior

av: anteroventral

BLA: basolateral amygdala

BST: Bed nuclei of the stria terminalis

CaMKIIα: Calcium/calmodulin-dependent protein kinase II

CeA: Central amygdala

ChR2: Channelrhodopsin-2

Cm: centimeters

CNS: central nervous system

CORT: corticosterone

CRF: Corticotropin releasing factor

D: day

DEX: dexamethasone

Dv: dorso-ventral

eYFP: Enhance yellow fluorescent protein

GABA: γ-amino butyric acid

GFP: Green fluorescence protein

GR: glucocorticoid receptor

H: Hour

Halo: Halorhodopsin

HPA: hypothalamo-pituitary-adrenal axis

Hz: Hertz

IA: inhibitory avoidance

IL: infralimbic cortex

Kg: kilogram

LE: Long-Evans

LFP: Local Field Potential

MeA: medial amygdala

mg: milligram

Min: minute

ML: Medial/lateral

mPFC; medial prefrontal cortex

ms: millisecond

mW: milliwatt

NA: Numerical aperture

NE: Norepinephrine

nl: nanoliter

nm: nanometer

NTS: nucleus of the solitary tract

PAG: periaqueductal gray

PBS: Phosphate-buffered saline

PCA: principal component analysis

PL: Prelimbic Cortex

PFA: Paraformaldehyde

PFC: prefrontal cortex

PKC: protein kinase C

PNOC: prepronociceptin

Psd: Power Spectral density

PTSD: post-traumatic stress disorder

PVH: paraventricular hypothalamus

S: second

SDS: Sodium dodecyl sulfate

SEM: Standard error of the mean

SOM: somatostatin

µm: micrometer

µg: microgram

vlPAG: ventrolateral periaqueductal gray

vSUB: ventral subiculum

YFP: Yellow fluorescent protein

CHAPTER I:

Introduction

On defining Stress

Stress is a ubiquitous presence during an organism's lifetime, prevalent during exposure to a variety of environmental demands, and yet our understanding of the basic mechanisms that mediate stress are poorly understood. That the relationship between stress and disease is now well-established underscores the critical need for research interrogating stress systems in the development of conditions such as cardiovascular disease and psychiatric illnesses such as depression or PTSD (Hägglöf et al. 1991; Hammen 2005; Kivimäki et al. 2006; Krantz and McCeney 2002; Mazure 1998; Monroe and Simons 1991; Räikkönen et al. 1996; Rozanski, Blumenthal, and Kaplan 1999; Van Praag, de Kloet, and van Os 2004). Outlining the brain pathways that regulate physiological and behavioral responses to stress has advanced considerably in recent years due to technological advancements that allow for exquisitely detailed structural and functional investigation, contributing to our overall understanding of how an organism processes stress to promote adaptive behavior. And yet, the precise neural circuits responsible for coordinating features of stress across multiple domains (i.e., neuroendocrine, autonomic, behavioral) remain unclear. An understanding of the neural circuit components mobilized to regulate feature-specific aspects of the stress response versus those coordinating response-sets (i.e., across domains) and whether these are separable require further interrogation of the brain with increasing precision.

Despite originally a term for the physical interaction between the force applied to a material object and the pressure, or resistance, countering that force (Selye 1936, 1979), “stress” is now colloquially used to refer to any demand, or state of strain, placed on an individual perhaps to the detriment of research on stress due the ambiguity with which the term is applied (as discussed below). Any research on stress requires consideration of what the term is designated to mean within the confines of the research objective. Historically, integration of the term stress into the cultural lexicon can be attributed to one of the founders of the stress research field, Hans Selye (Selye 1936; 1950; 1979), who defined stress as the “*nonspecific response of the body to any demand*”. Selye came to this definition following a series of observations in rodents that included reduced thymus and spleen sizes, in addition to hyperplasia of the adrenal glands, resultant from exposure to a variety of “nocuous agents”. Nocuous agents, or “stressors”, referring to physiological insults such as cold exposure, transection of the spinal cord or other surgical injury, excessive exercise, or drug injections of a diverse make-up (Selye 1936; 1979). Selye referred to this set of observations as a “general adaptation syndrome,” indicative of reduced immune functionality and lessened activation of the endocrine system that appeared consistent across stressors. This generality of effects due to stressor exposure underpinned Selye’s description of stress as “nonspecific,” in that responses of the body occurred similarly regardless of the physiological insult.

The importance of non-specificity (or non-selectivity) in stress is underlined by more recent adaptations to the term in an attempt to refine researcher’s definitions of what constitutes its makeup (Day 2005). Indeed, according to one more recent interpretation produced by Trevor Day, stress is defined as the “*body’s multi-system*

responses to any challenge that overwhelms, or is judged likely to overwhelm selective homeostatic mechanisms" (Day, 2005). A "selective homeostatic mechanism", according to Day, would involve a targeted response directed to a particular organ or subset of nerve cells to achieve an appropriate adjustment in returning to homeostasis (Day 2005). Selye often used the example of an insulin injection to illustrate this, in that insulin specifically is targeted to decrease blood glucose levels (Selye 1936, 1979). By contrast, insulin overdose would be considered a stressor as it can cause hypoglycemia and consequently mobilize adrenal catecholamines and corticosteroids. Adrenal catecholamines and corticosteroid interact with a wide variety of physiological systems and may thus be considered "non-selective." Consequently, the insulin injection performing a selective homeostatic purpose would not be considered a stressor, and thus not involve stress, or stress neurocircuitry. Clearly outlining whether an environmental demand elicits a non-selective response (e.g., adrenal catecholamine or corticosteroid release) allows a determination of whether the demand constitutes stress, and importantly what neural circuits may then be involved.

Stress may be experienced in the form of two broadly conceived insults ranging from physiological (i.e., hemorrhage, insulin overdose) to psychological (i.e., perceived threat to organismal fitness). Indeed, a critical component to Day's definition is its second half; *"judged likely to overwhelm*" (Day 2005). Much of the common use of the term stress likely falls into this category and represents an evaluation of the environmental circumstances that may elicit stress and involves separable neurocircuitry from that responding to physiological insults (Chan & Sawchenko 1994; Sawchenko et al., 1996; Cullinan et al., 1995a; Cullinan et al. 1995b; Li and Sawchenko 1998; Herman and

Cullinan 1997; Bohus et al., 1987). Indeed, while induction of the hypothalamo-pituitary-adrenal (HPA) axis and subsequent release of adrenal hormones is common to all stressors, lesions of the limbic forebrain generally do not alter these stress responses to physiological insults (Herman and Cullinan 1997). Rather, limbic forebrain regions appear particularly sensitive to stressors that involve higher-order evaluative processes (Jankord and Herman, 2008) that weigh past experiences and current environmental demands to select appropriate behavioral responses to navigate stressor presence (i.e., psychological stress). Commonly employed paradigms that evaluate psychological stress in animal models include restraint, context or cued fear conditioning, or footshock. Overall, this processive capacity to evaluate stressor likelihood positions limbic forebrain regions capable of stress response assembly under conditions that likely require mobilization, or suppression when deemed unlikely.

The work of this dissertation aims to outline neurocircuitry involved in conditions of psychological stress, that is - the assembly of neuroendocrine and behavioral responses germane to limbic-forebrain stress neurocircuitry. In particular, I focus on the bed nucleus of the stria terminalis and medial prefrontal cortex as key mediators of psychological stress that inform neuroendocrine output and long-term behavioral adaptations by way of interacting with memory modulatory processes during consolidation. In this introduction I will review:

- The hypothalamic-pituitary-adrenal (HPA) axis response following acute stress
- Stress in memory consolidation
- Stress in fear memory generalization
- The composition of limbic forebrain circuitry in HPA axis regulation

- The role of the bed nuclei of the stria terminalis (BST) in stress and behavior
- Toward a prefrontal – bed nuclei of the stria terminalis network that constrains stress

The hypothalamic-pituitary-adrenal axis response to acute stress

Organismal responses to any challenge that overwhelms, or is judged likely to overwhelm, selective homeostatic mechanisms are diverse, and involve activation of the hypothalamo-pituitary-adrenal axis (HPA) (Day, 2005). The HPA axis is the predominant neuroendocrine system that is mobilized during stress. Corticotropin-releasing factor (CRF), expressed within a subpopulation of paraventricular hypothalamic neurons located at the medial parvicellular region (Antoni 1986; Rivier and Vale 1983), initiate the release of adrenocorticotropic hormone (ACTH) from the anterior pituitary which, in turn, stimulates secretion of adrenal glucocorticoids (cortisol in humans; corticosterone, CORT, in rodents)(Radley, Gosselink & Sawchenko, 2009; Antoni 1986; de Kloet, Oitzl & Joels, 1999; Brown, Rivier, & Vale 1984; Plotsky, Otto, Sutton 1987). These end-products of the HPA cascade, glucocorticoids, act at several limbic-cortical regions and are widely implicated in modulating CNS processing of emotionally relevant stimuli leading to alterations in learning and memory, as well as mediating other physiological processes necessary for responding to stress. Indeed, during stress CORT acts to suppress inflammation and immune function, as well as shift energy reserves toward systems more critical for addressing the presence of a threat, such as cardiovascular systems (Sapolsky 1992), and away from non-essential functions, such as that related to digestive or

reproductive systems (Sapolsky 1992). Additionally, CORT acts to negatively regulate further induction of the HPA axis ((Dallman and Jones 1973; Dallman and Yates 1969; Keller-Wood and Dallman 1984), thereby preventing excessive release of CORT.

Importantly, whereas acute increases in CORT are generally considered adaptive, chronic elevations in CORT are associated with the development of stress-related psychiatric disease in humans (Van Praag, de Kloet & Van Otzl, 2004; Herman and Cullinan, 1997). That the balance of CORT release in acute or long-term conditions may differentially contribute to organismal fitness or disease suggest its regulation is paramount for adaptive behavior. Indeed, suppression of the HPA axis following an acute stressor is carried out by CORT acting at multiple levels of the axis itself (i.e., hypothalamic, pituitary, adrenal) as well as limbic-cortical regions upstream of HPA effector nuclei in the PVH ((Dallman and Jones 1973; Dallman and Yates 1969; Keller-Wood and Dallman 1984; Herman and Cullinan, 1997) that are further tasked with negatively regulating HPA induction. The mPFC, hippocampus, and amygdala are such regions associated with higher-order processing consistent with mediating aspects of psychological stress. Each region contains dense glucocorticoid receptor (GR) levels (Reul & de Kloet, 1985; Chao, Choo and McEwen, 1989) that are bound during periods of high CORT (Ahima and Harlan, 1990; Ahima et al., 1991). Whereas activation of the amygdala leads to increases in CORT (Mason, 1958; Mason et al., 1976; Mason 1972), activation of GR in either mPFC or hippocampus are associated with reducing further HPA responding (discussed more in detail below) (Diorio et al., 1993; Hall and Marr 1975; Porter 1954;). Importantly, each of these regions are implicated in disease pathology during conditions of chronic, or persistent, stress.

On stress in memory consolidation

Originally proposed in 1900 by Müller and Pilzecker, consolidation refers to the hypothesis that memories initially exist in a labile state, susceptible to intervention, that are subsequently strengthened over time resulting in enduring memories (Müller & Pilzecker, 1900; McGaugh, 1999). Characterized as “retroactive interference”, Müller and Pilzecker observed human subjects demonstrated a reduced capacity to remember details when other information was encountered shortly following presentation of the to-be remembered items (Müller & Pilzecker, 1900; McGaugh, 1999). This “forgetting as a result of interference” (Müller & Pilzecker, 1900) marked a predominant theme among memory researchers at the time. Indeed, years prior Bigham (1894) had already showed subjects failed to recall items when the interval between learning and recall was filled with other cognitively demanding tasks (Dewar, Cowan & Della Sala, 2009; Bigham, 1894). Of note, Müller and Pilzecker found this impairment became less pronounced the longer the interval between presentation of the to-be remembered item and the interfering item became, suggesting a stabilization of the memory trace was occurring across time. Along these lines, later work described how cerebral electroconvulsive shock administered to rodents shortly following learning dramatically impaired retention whereas delayed shock administration (i.e., multiple hours) did not (Duncan, 1949); observations further suggesting consolidation involves time-dependent processes.

Decades of subsequent work has shown a variety of drugs administered shortly after learning can facilitate consolidation processes (i.e., supporting memory trace

stabilization) resulting in enhanced recall (McGaugh, 1966; McGaugh, 2000). One of the earliest indications of the potential to facilitate consolidation involved injections of strychnine sulphate (Lashley, 1917) which was shown to improve maze learning in rodents. Work by James McGaugh and colleagues further supported these findings showing a variety of central nervous stimulant injections can facilitate memory consolidation when administered shortly before or after training (McGaugh, 2000). Stimulant injections and their facilitatory effects align well with the notion that emotionally arousing experiences are better remembered than neutral ones.

Emotional experiences mobilize the HPA axis (McEwen & Sapolsky 1995; de Quervain, Schwabe & Roozendaal 2017), and involve the release of adrenal catecholamines and corticosteroids (Dallman & Jones 1973; Dallman 2005; Dallman, Viau, Bhatnagar, Gomez, Laugero & Bell 2002; McIntyre & Roozendaal 2007). That consolidation processes, however, were potently modulated by adrenal hormones released in response to such an event was not well documented until Latané and Schachter (1962) found low doses of epinephrine enhance acquisition of an avoidance response, and later Gold and Van Buskirk (1975) found posttraining injections of epinephrine specifically act to modulate memory consolidation processes. More recent work has highlighted the involvement of noradrenergic signaling in the basolateral amygdala as critical for mediating the influence of posttraining injections of epinephrine (Roozendaal, McGaugh, 1997; Quirarte, Roozendaal, McGaugh, 1997). As epinephrine does not cross the blood-brain barrier, it is thought to interact with the CNS via activation of vagal afferents to the nucleus of the solitary tract (NTS) (Schreurs, Seeling & Schulman, 1986; Aston-Jones & Cohen, 2005; Miyashita & Williams, 2006; Bahtiyar et

al., 2020), by which it enhances the release of norepinephrine (NE) throughout the brain (Williams et al., 1998). Blockade of NE signaling in a variety of regions, including mPFC (Roozendaal et al., 2009), basolateral amygdala (Barsegyan, McGaugh, Roozendaal, 2014; Liang, Chen & Huang, 1995; Izquierdo et al., 1992; Ferry & McGaugh, 1999;) and hippocampus (Bevilaqua et al., 1997; Roozendaal & McGaugh, 2011) generally impairs memory, or blocks the memory enhancing effects of peripherally administered epinephrine.

Adrenocortical hormones (i.e., corticosterone) are also now well documented as involved in modulating memory consolidation (Bohus, 1994; de Quervain et al., 2017; Joels et al., 2011; McEwen and Sapolsky, 1995). Posttraining injections of glucocorticoids can produce dose and time-dependent facilitation of consolidation for many types of learning, including inhibitory avoidance (Flood et al., 1978; Sandi & Rose, 1994), fear conditioning (Sandi & Pinelo-Nava, 2007; Cordero, & Sandi, 1998), and spatial learning (Sandi, Loscertales, & Guaza, 1997). Glucocorticoids readily cross the blood brain barrier and interact with both mineralocorticoid (Type I) and glucocorticoid (Type II) receptors throughout the brain (Bahtiyar et al., 2020; Finsterwald & Alberini, 2014; Lupien and McEwen, 1997; Oitzl & de Kloet, 1992; Roozendaal et al., 1996) to mediate learning processes. Whereas Type I receptors are generally occupied during low corticosterone levels (Ruel & de Kloet,, 1985; de Kloet et al., 2005), such as prior to stress onset, and are primarily expressed with the hippocampus, with lesser densities within the prefrontal cortex and amygdala (Ruel & de Kloet, 1985), Type II GR's are widely dispersed throughout the brain and are predominantly bound during periods of high corticosterone levels, such as immediately following an arousing event (de Kloet et al., 2005; Dallman,

2005). As such, GR's involvement in post-stress processes are likely to predominate with regard to corticosteroid modulation of memory consolidation. In line with this, blockade of GR signaling in either the mPFC (Barsegyan et al., 2010), BLA (Barsegyan et al., 2019), or hippocampus (Roozendaal et al., 1999) prevent the memory enhancing effects of systemic corticosterone administration. Binding of GRs in the central nervous system (CNS) results in a cascade of intra-cellular events to mediate gene-transcription and enhance or inhibit neuronal excitability, depending on the region or level of stress (Finsterwald & Alberini 2014; Diamond, Bennett, Fleshner & Rose 1992; Joëls, & Krugers 2007).

CNS actions of corticosteroids also include interacting with noradrenergic signaling to promote consolidation processes (Roozendaal et al., 1999). Indeed, antagonism of the β-adrenoreceptor subtype in the BLA (Roozendaal, 1999) or mPFC (Barsegyan et al., 2019) prevents the memory enhancing effects of GR agonism in each region. Importantly, the interaction of adreno-medullary and adreno-cortical hormones in the CNS during consolidation appear positioned to support structural and molecular alterations that lead to enduring memories, including morphological alterations (Anderson et al., 2014; Anderson et al., 2016; Anderson et al., 2020; Lesuis et al., 2020) and long-term potentiation (Akirav & Richter-Levin, 2002).

Despite this wealth of information supporting the notion that stress-hormones mediate consolidation processes to preserve emotionally arousing information, however, less well understood are the neural circuits that regulate endogenous hormonal reactivity during consolidation. Much of the historical literature regarding injections of stress hormones or cognate receptor agonists in the CNS involve supraphysiological levels that

may not directly mimic endogenous mechanisms. Regardless, memory consolidation represents a unique period of learning critically mediated by a variety of stress related hormonal and circuit mechanisms that offers a focus for guiding our interrogation of stress neurocircuitry.

Stress in fear generalization

A substantial body of empirical data has shown generalization to be a fundamental behavioral response across a variety of behavioral contexts and sensory modalities, and present among a range of species (Poulos et al., 2016; Lynch et al., 2013; Adolphs, 2013; Dymond et al., 2015). In order to respond adaptively to complex and dynamic environments populated with potential threats, animals must utilize previous experiences that are not identical to the current environmental demand, weighing cues and contextual information that may predict the occurrence of danger. In general, this is accomplished when an animal has learned a specific sensory stimulus, such as context or cue, predicts a particular outcome and thus attributes the outcome to similar sensory stimuli. Much work has been invested to outline the neural circuitry underlying the emergence of a generalized behavioral response suggesting a complex array of interconnected limbic-cortical networks (Dunsmoor & Paz, 2015; Asok, Kandel, & Rayman, 2019; Poulos et al., 2016; Lynch et al., 2013; Adolphs, 2103; Baldi, Lorenzini & Bucherelli, 2004; Dymond et al., 2015). The hippocampus, including both dorsal and ventral axes, are essential in the consolidation of contextual fear memories (Fanselow & Dong, 2010) and the ventral hippocampus has been implicated in discrimination between safe and threatening

contexts (Cullen et al., 2015). The medial prefrontal cortex (prelimbic, and infralimbic regions) maintains extensive connectivity with the hippocampus, and amygdala and has been associated with the emergence of fear generalization when pharmacologically inactivated, and stimulus discrimination when optogenetically activated, an effect that may depend on theta oscillatory coherence between the mPFC and downstream regions (Rozeske et al., 2015; Likhtik et al., 2014). The amygdala is a critical site responsible for not only receiving unconditioned stimulus information (Johansen et al., 2010) but also for coordinating conditioned behavioral responding through an interaction with the midbrain periaqueductal gray (Tovote, Fadok, Luthi, 2015); each important determinants implicated in stimulus generalization (Asok et al., 2018; Ciocchi et al., 2010).

Of note, activation of neuroendocrine and autonomic systems are also implicated in enhancing generalized or precise fear memories, respectively, suggesting an important contribution of peripheral hormonal responses acting at central neural systems to mediate generalization (Donley, Schulkin & Rosen, 2005, Kaouane et al., 2012; Atucha et al., 2017; Lesuis et al., 2020). Of particular interest to our interrogation of stress neurocircuitry is the mobilization of these systems during memory consolidation, and an elaboration on how this might contribute to memory accuracy. However, an overarching framework describing how stress-related signaling, particularly adrenal catecholamines and corticosteroids, contributes to generalization has not been forthcoming and in some cases has presented conflicting information. Indeed, whereas stimulating NE release via systemic injection of the alpha-2 adrenergic antagonist yohimbine during consolidation has been shown to enhance memory accuracy, even up to remote time-points (Roozendaal & Mirone, 2020), optogenetic stimulation of central locus coeruleus NE has

been shown to prevent discrimination (Seo et al., 2021); an effect dependent on β-adrenergic signaling in the dentate gyrus, and seemingly in contrast to the promotion of memory accuracy. That peripheral yohimbine injections are presumed to increase locus coeruleus NE signaling via vagal nerve stimulation (Hulsey et al., 2017) suggests autonomic reactivity contributing to memory accuracy may depend on activation of specific central circuits. Moreover, increased sympathetic activity has been shown to be directly involved in supporting features of stress-related psychiatric disease. Cases of PTSD are consistently associated with hyperactivity of autonomic systems (Sherin 2011), and stimulatory drugs such as yohimbine can contribute to symptomatology (Southwick et al., 1993).

Concerning adrenal-corticosteroids, the relation between HPA reactivity and stress-related diseases in humans that are characterized by high levels of generalized fear behavior (e.g., PTSD) has also been inconsistent. Mason et al. (1986) first reported PTSD was linked to low levels of circulating cortisol, however, this result has not been replicated on multiple occasions (for review see; Fink, 2011). The claim of low circulating cortisol in PTSD also contrasts with a substantial literature showing posttraining CORT injections in rodents enhance memory consolidation (McGaugh, 2000), and decrease memory accuracy (Roozendaal & Mirone, 2020; Lesuis et al., 2021; Kaouane et al., 2012) thereby contributing to disease-like impairments; suggesting hypercortisolism and not hypocortisolism may contribute to disease symptomatology. Further, optogenetic manipulations that suppress CORT release during stress exposure have been shown to reduce the risk of PTSD-like impairments in rodents (Henckens et al., 2017). Pharmacological blockade of training-induced CORT increases with metyrapone has also

been shown to maintain memory accuracy up to remote time-points (Pedraza et al., 2016). While CORT has been shown to enhance neuronal excitability via MR binding (Joels & de Kloet, 1992; Ruel & de Kloet, 1985), interactions with GR can suppress neuronal excitability (Joels & de Kloet, 1992) offering a potential mechanism by which CORT contributes to generalization. Of note, high levels of CORT have been shown specifically to inhibit neural plasticity in the hippocampus (Joels & de Kloet, 1992); a region critical for maintaining memory accuracy (Lesuis et al., 2021; Kaouane et al., 2012). A recent study also showed higher CORT levels produced by more aversive training procedures contributed to enhanced context generalization (dos Santos Correa et al., 2019), and this effect appeared a result of a shift in the occurrence of remote memory generalization to earlier timepoints. Indeed, one proposal for how adrenal catecholamines and corticosteroids interact with memory accuracy and generalization relies on this presumed shift in remote memory generalization to earlier timepoints; an interpretation of systems consolidation theory (Bahtiyar et al., 2020).

Systems consolidation theory posits that initially memories depend on the hippocampus and across time are dispersed throughout neo-cortical regions subsequently becoming less dependent on hippocampal processing (Nadel, Winocur, Moscovitch 2007; Winocur & Moscovitch 2011; Yonelinas, Ranganath, Ekstrom, Wiltgen 2019) and more schematized or gist-based (Robin & Moscovitch 2017); reflecting the time-dependent increase in generalization. NE facilitates interactions between the BLA and hippocampus (Akirav & Richter-Levin 1999; 2002; Ikegaya, Saito & Ave 1995), potentially maintaining hippocampal involvement and preserving memory accuracy, whereas CORT inhibits hippocampal activity and promotes BLA influences on prefrontal

regions (Bahtiyar et al., 2020; Diamond & Rose 1994; Diamond et al., 1992; Roozendaal et al., 2009), potentially facilitating the integration of memories into neo-cortical regions and the subsequent shift toward gist-based representation.

It should be noted, several studies have been critical of systems consolidation theory (Asok, Kandel & Rayman 2019; Rekkas & Constable 2005; Lehman, Lacanilao & Sutherland 2007), as the hippocampus have been shown to be involved in the retrieval of remote memories (Clarke & Sutherland 2013) and neo-cortical regions have been shown to be indispensable during initial encoding and consolidation (Kitamura et al., 2017). Further, systems consolidation theory implicitly presumes the subject learned well enough during the training experience, and it was subsequently only time that transformed the memory toward a gist-based representation.

A counterview that can be traced to early Pavlovian theorists such as Karl Lashley (1946) argue stimulus generalization, particularly in the case of a single trial or learning experience, may instead result from a failure of association during initial training or consolidation. Specifically, during a single trial learning experience conditioning occurs as a function of the “most conspicuous characters” of the event (Lashley, 1946). Generalization therefore represents a failure to attend to the defining characteristic, thereby contributing to what Lashley referred to as an “abstracted” representation. This is perhaps consistent with modern theories of disease states like PTSD as a memory disorder characterized by two predominant components: 1) hypermnesia for the core traumatic event, and 2) an impoverished memory functioning due to diminished encoding abilities (Kaouane et al., 2012; Layton & Krikorian 2002). Posttraining CORT injections have been shown to contribute to both aspects, particularly under high stress conditions,

by way of reducing activity in the hippocampus and increasing activity in the amygdala as mentioned previously. As such, NE and CORT may function to encourage, or inhibit, a subject's capacity to attend to details that ultimately contribute to an accurate or gist-based representation, respectively.

Regardless, as clearly fear generalization encompasses neuronal activation of diverse and interconnected systems performing at times opposing roles, it has been difficult to sort out the specific mechanisms underlying the emergence of a generalized fear behavior. Thus, an important research avenue will be to dissect the functional role of neural circuits that integrate multiple aspects of a threatening event (e.g., neuroendocrine, behavioral) to promote or restrict fear generalization, and whether these aspects are separable or rather inter-dependent. One approach to address this would be to isolate neurocircuitry that directly mediate neuroendocrine and behavioral processes during stress (as discussed below).

Composition of hypothalamo-pituitary adrenal axis regulatory circuits

The defining characteristic of stress neurocircuitry involves an interaction with the hypothalamo-pituitary adrenal axis (Day, 2005), as based on our working definition (discussed previously). Psychological stress relies predominantly on higher-order cognitive processing or associative systems capable of stressor evaluation or anticipation, as has been shown to be mediated by limbic forebrain regions (reviewed in: Jankord & Herman 2008; Herman, Ostrander, Mueller & Figueiredo 2005). Key limbic regions under consideration with regard to stress in memory consolidation and

generalization thus may be further parsed based on network connectivity involving HPA effector neurons within the paraventricular hypothalamus.

The hippocampus contains the highest density of GR receptors in the limbic-forebrain (Chao, Choo, McEwen, 1989; McEwen, Weiss & Schwartz 1968), and maintains an inhibitory role over the HPA axis that is well established. Early lesion work demonstrated removal of the hippocampus elevated glucocorticoid levels in either the absence of stress, or during stress indicating involvement in tonic, and phasic regulation of corticosteroid release (Jacobsen & Sapolsky 1991; Sapolsky et al., 1984). Conversely, electrical stimulation of the hippocampus decreases plasma corticosterone (Dunn & Orr 1984; Rubin, Mandell, Crandall 1966; Saphier & Feldman 1987). The influence of the hippocampus in regulating the HPA axis is further supported by increases in CRF mRNA levels in the PVH resultant from hippocampal lesions (Herman, Dolgas, Carlson 1998; Sapolsky, Armanini, Sutton & Plotsky, 1989). Concerning conditions of psychiatric disease, the hippocampus in particularly impacted by periods of prolonged stress (Herman et al., 1995; McEwen & Magarinos, 1997; McEwen 1999) or corticosteroid administration (Bodnoff et al., 1995; Diamond, Bennett, Fleshner & Rose 1992; Zhang, Zhao, & Wang 2015) which are further associated with dysregulation of the HPA axis. Indeed, humans diagnosed with stress-related disorders (i.e., depression, PTSD) show reduced hippocampal volumes (Wigenfeld, & Wolf 2014; Starkman et al., 1992; Sheline et al., 1996), and in rodents chronic stress administration produces regressive morphological alterations in hippocampal spine densities (Sousa et al., 2000; Chen et al., 2010).

The prefrontal cortex has also been shown to impart inhibitory regulation on the HPA axis (Radley et al., 2009; Radley & Sawchenko 2011; Herman et al., 1995), and promote negative feedback following stress via an interaction with glucocorticoids (Akana, Chu, Soriano, & Dallman 2001). Indeed, most of the PFC is mobilized following exposure to a variety of stressors. PFC regions, including the prelimbic and infralimbic subdivisions exhibit robust induction of the immediate early gene, cFos, following stress (Cullinan et al., 1995; Bland et al., 2005). Early work demonstrated prefrontal cortical interactions with glucocorticoids using autoradiography examining the binding properties for tritiated CORT (^{3}H-CORT) and dexamethasone (^{3}H-DEX) (McEwen, de Kloet, & Wallach, 1976), showing glucocorticoid binding across the prefrontal cortex. Whereas lesions of the PFC do not appear to influence basal levels of CORT or ACTH (Diorio, Viau, Meaney 1993; Figueiredo et al., 2003) as the hippocampus does, pre-stress lesions of the PFC robustly enhance HPA component indices following stress onset including PVH CRF+ mRNA, ACTH, and corticosterone (Radley, Arias & Sawchenko 2006). Interestingly, this inhibitory role over CORT appears to be region and stressor specific, in that lesions of the more ventrally situated infralimbic region have been reported to either not influence post-stress ACTH or CORT (Crane, Ebner & day 2003), or decrease these indices (Sullivan & Gratton 1999). Further, IL lesions appear to differentially alter autonomic-related sympatho-adrenal indices indicating perhaps a preferential role in mediating autonomic reactivity (Verberne et al., 1987; Frysztak & Neafsey 1994). Indeed, optogenetic stimulation of IL has been reported to reduce heart rate, and mean arterial pressure following stress (Wallace et al., 2021). Lesions, or inactivation, of the prelimbic region also do not affect HPA axis responses to ether inhalation (i.e., a physiological stressor) (Figueiredo,

Bruestle, Bodie, Dolgas, Herman 2003), but rather specifically enhance HPA responding to psychological stressors including restraint (Radley, Gosselink, & Sawchenko, 2006) and shock probe defensive burying (Johnson et al., 2019). Increases in HPA axis activity following restraint stress can also be ameliorated via implantation of a CORT pellet within the PFC, indicating the capacity to suppress further HPA responding during stress (Diorior et al., 1993). Regressive morphological alterations are also apparent in prelimbic neurons following chronic stress (Anderson et al., 2014; 2016; 2020), or repeated corticosteroid administration (Anderson et al., 2014; 2016; 2020), an effect that appears largely undifferentiated from similar observations in the hippocampus. That dysfunctional prefrontal cortical activity is commonly associated with conditions of psychiatric disease positions its involvement in the regulation of stress-related processes as critical for adaptive behavior.

In contrast to the predominantly inhibitory role provided by the hippocampus and prefrontal cortex, the amygdala appears to maintain an excitatory role over the HPA axis. Corticosteroid release is enhanced following electrical stimulation of the amygdala (Dunn & Whitener 1986; Feldman, Conforti, Itzik, & Widenfeld 1994); an effect consistent across a variety of species, including rats (Redgate & Fahringer 1973), cats (Mattheson, Branch & Taylor 1971), non-human primates (Mason 1959), and humans (Gallagher, Flanigin, King, & Littleton 1987). Ablation of the amygdala is also associated with reducing the stress response to psychogenic stimuli, but not the physiological stressor ether (Knigge 1961; Feldman & Conforti 1981; Dayas & Day 2002), consistent with the notion that limbic forebrain regions are more preferentially involved in the regulation of the HPA axis under conditions of psychological stress. However, there appears to be a significant subregional

factor to be considered in this regard as well. Indeed, the central amygdala (CeA) is robustly mobilized in response to physiological insults, including hemorrhage (Sawchenko & Ericsson 2000) and drug-induced inflammation (Thrivikraman & Plotksy 1997), but lesions of the CeA do not prevent stress-induced increases in HPA activity following restraint stress (Dayas & Day 1999; Xu, Day & Buller 199) suggesting HPA-related modulation in the CeA is biased toward processing of physiological stressors. The medial amygdala (MeA) shows substantially high levels of cFos immunoreactivity following a variety of psychological stressors, including restraint (Sawchenko & Ericsson 2000), forced swim (Thrivikraman & Plotksy 1997), and predator exposure (Figueiredo et al., 2003), but considerably less to physiological insults such as hypoxia or hemorrhage (Dayas & Day 1999; Thrivikraman & Plotksy 1997) although electrical stimulation of the medial amygdala under anesthesia has been reported to reduce plasma corticosterone responses (Feldman, Conforti & Saphier 1990). To compare, the basolateral amygdala, while being robustly mobilized following a variety of stressors (Sawchenko & Ericsson 2000) and directly involved in mediating the effects of glucocorticoids across the brain during memory consolidation and other fear-related learning processes (Roozendaal & McGaugh 1996; Roozendaal, McEwen & Chattarji 2009; McGaugh 2000), does not appear directly involved in the induction of the HPA axis (Feldman et al., 1994). Rather, the BLA maintains extensive connectivity with the CeA, MeA, and other HPA -modulatory regions to exert top-down facilitatory influences (Dong, Petrovich & Swanson 2001). Conditions of chronic stress also result in contrasting morphological alterations in the BLA, as compared to prefrontal and hippocampal regions. Specifically, chronic stress appears to increase synaptic efficacy and spine densities in rodent BLA neurons (Vyas

et al., 2002a: 2002b; 2006). This increase in synaptic efficacy likely underlies excessive induction of the glucocorticoid response following stress in cases of psychiatric disease (Rosenkranz, Venheim, Padival 2010). Indeed, these observations are consistent with cases of psychiatric disease in humans, where an associated enhancement in amygdala activity is noted in response to fearful stimuli (Sharp 2017; Ressler 2010), particularly among individuals diagnosed with PTSD or major depressive disorder (Liberzon & Sripada 2007), and this is coupled with alterations in measures of corticosteroid release (Wichmann, Kirschbaum, Bohme, Petrowski 2017; Elzinga et al., 2003).

Importantly, HPA modulatory influences provided by hippocampal, prefrontal, and amygdala regions are subserved via indirect relays. Indeed, limbic forebrain regulation of the HPA axis is not achieved via direct innervation of PVH, but rather one or more intermediaries [bed nucleus of the stria terminalis; medial preoptic area; dorsomedial hypothalamus]. Further, extrinsic projections from the prefrontal cortex and hippocampus are largely excitatory (i.e., glutamatergic) necessitating GABAergic structures by which their HPA inhibitory processes are achieved (Gray, Carney, and Magnuson 1989; Herman et al. 2003; Prewitt and Herman 1998; Sawchenko and Swanson 1983; Radley, Gosselink, and Sawchenko 2009; Cullinan, Herman, and Watson 1993). HPA modulation by the amygdala is carried out by GABAergic neurons of the central or medial amygdala subregions. However, similar to prefrontal and hippocampal regions, the CeA and MeA only maintain sparse projections to PVH and these contact predominantly pre-autonomic neurons (Gray, Carney & Magnuson 1989; Dong, Petrovich & Swanson, 2001; Petrovich, Risold & Swanson 1996; Petrovich & Swanson 1997; Price & Amaral 1981).

One candidate relay is the bed nucleus of the stria terminalis (BST). BST is a basal forebrain complex containing upwards of 12-15 different subnuclei that are largely GABAergic (Erlander et al. 1991; Ferraguti et al. 1990; Mugnaini and Oertel 1985) differentiated predominantly by expression of a variety of peptidergic subtypes (Giardino & Pomrenze, 2021) including regions enriched in corticotropin releasing factor (CRF)(Pomrenze, et al., 2015; Pomrenze et al., 2019), somatostatin (SOM)(Bruzsik et al. 2021, prepronociceptin (PNOC)(Rodriguez-Romaguera et al., 2020), among many others (Beyeler & Dabrowska 2020). A comprehensive series of tracer studies conducted by Dong and colleagues outlined extensive direct connectivity with PVH derived from specific BST subregions (Dong and Swanson 2006a; Dong and Swanson 2006b; Dong et al. 2001).

BST modulatory influences on CORT levels had been observed decades earlier when Jon Dunn (Dunn, 1987a) observed electrical stimulation of BST resulted in differential recruitment of HPA responding depending on subregion. Regions dorsal to the anterior commissure and at more rostral levels of BST that received electrical stimulation were reported to produce increases in CORT under anesthesia, whereas regions lateral, and ventral were reported to decrease CORT levels (Dunn, 1987a). Consistent with this, lesions centered in more dorsal regions suppressed HPA responding to context fear conditioning (Sullivan et al. 2004), whereas lesions or inactivation of the ventral or posterior aspect of the structure robustly enhance HPA responses to a variety of stressors including restraint, tail suspension, forced swim (Johnson et al., 2016; Radley & Johnson, 2018; Radley et al., 2009), shock-probe defensive burying (Johnson et al., 2019). In line

with this regional differentiation, these results implicated BST as capable of imparting inhibitory, or conversely facilitatory, control over PVH and mobilization of the HPA axis.

Support for the notion that BST is positioned to subserve limbic forebrain inhibitory control of the HPA axis, particularly that stemming from hippocampal and prefrontal regions, was also demonstrated using a combination of anatomical tracing methods and discrete excitotoxic lesions (Radley et al., 2009). Here, the authors reported that the anteroventral (av) aspect of BST contained stress sensitive GABAergic neurons that projected to PVH, and this neuronal population received convergent input from prefrontal and hippocampal regions. Stress-induced cFos immunoreactivity in avBST was reduced following lesions of the prelimbic region of the prefrontal cortex, or ventral subicular (vSUB) region of the hippocampal formation, and this was couple with enhanced CRF mRNA levels in PVH, and plasma ACTH and CORT in both cases. Interestingly, dual lesions of the vSub and PL appeared to result in additive enhancements of HPA component indices that were similar in magnitude to that of a single lesion of avBST. As such, this study provided evidence for an HPA-inhibitory network that involved prelimbic PFC, hippocampus, and avBST, and that avBST acted to integrate multiple limbic forebrain regulatory mechanisms.

Regarding the HPA-facilitatory effects carried out by the amygdala, an interaction with BST has been implicated but results are generally lacking in specific circuit mechanisms, particularly with regard to the onset of psychological stress. An early study reported electrical stimulation of the MeA enhanced plasma corticosterone responses under anesthesia, and this effect was blocked by bilateral lesion of the BST (Feldman, Conforti & Saphier 1990). CRF administration or corticosterone implants in the CeA have

also been shown to increase CRF mRNA in the PVH (Makino, Gold, & Schulkin 1994; Akana, Chu, Soriano, & Dallman 2001). Yet, despite the now well-established connection between regions of the amygdala and the BST, particularly regarding the modulation of negatively valenced information (Lebow & Chen, 2016; Pomrenze et al., 2019; Kim et al., 2013a), characterization of how these structures interact to mediate mobilization of the HPA axis has not been forthcoming. Regardless, much of the work describing the interaction of these structures implicates it in predominantly HPA faciliatory processes (Dallman et al., 2013), contrasting this projection to the predominantly inhibitory role provided by hippocampal and prefrontal projections to the BST.

The bed nuclei of the stria terminalis in stress and behavior

The BST are widely appreciated to be dynamically involved in the regulation of behavioral responses involving negative affect or threat processing in addition to HPA modulation. Some have argued the structure to be a component of an “extended amygdala” network (Alheid & Heimer, 1988; de Olmos, Beltamino, & Alheid, 2004; Fox, Oler, Tromp do, Fudge, Kalin 2015); regarded as a continuous region stemming from the medial and central nucleus of the amygdala (CEA/MEA) to the rostral pole of the medial and lateral regions of the BST, due to observations of shared cytoarchitectonic and histochemical characteristics implicating it in modulatory features similar between regions. Evidence for this was originally proposed by J.B. Johnston in 1923, and later elaborated upon by de Olmos and Heimer (Alheid & Heimer, 1988; de Olmos, Beltamino, & Alheid, 2004). This model has proved incredibly informative for behavioral researchers

(Davis, Walker, Miles & Grillon 2010; Walker, & Davis, 1997; Walker, Toufexis, & Davis 2003), although more recent examinations of the BST have noted its anatomical and function divergence from much of the amygdala (Swanson, 2000), despite remaining highly interconnected. Indeed, Larry Swanson and colleagues proposed the CEA/MEA and BST anatomically represent ventral differentiations of the striatum and pallidum, respectively, with the CEA/MEA specialized for integration of cortical information to modulate autonomic reactivity (Swanson, 2000), whereas BST is biased toward cerebral regulation of the neuroendocrine system and behavior control column (Swanson, 2000; Canteras, Simerly, Swanson, 1995) as a component of the rostral pallidum. Embryological studies further support this anatomical distinction as GABAergic subpopulations of the pallidum and lateral BST are differentiated from striatal and CEA/MEA developmental origins (García-Lőpez et al., 2008).

Functional divergence of the BST from the amygdala has predominantly been supported in the form of one influential hypothesis for how BST mediates negative affect. Originally proposed by Walker, Davis and colleagues (Walker, & Davis, 1997; Walker, Toufexis, & Davis 2003), it was suggested a dissociation between acute responsiveness to discrete threats were mediated predominantly by the amygdala, whereas the BST appeared necessary for behavioral responses to threats occurring on a longer timescale, consistent with those behaviors that might be associated with the term “anxiety.” This distinction perhaps accords with the anatomical divergence and the bias of CEA/MEA responding to cerebral regulation of autonomic reactivity (i.e., a shorter timescale stress response) as compared to the mediation of the neuroendocrine system performed by the BST (i.e., a longer timescale stress response) (Swanson, 2000). As previously mentioned

regarding BST, however, it is currently appreciated that BST does not react uniformly to stressors, and this is reactivity is not limited to conditions of anxiety-related behaviors. Indeed, BST regions show robust immediate early gene expression following restraint, shock, and predator odor (Rosen, Asok, & Chakraborty 2015; Daniel & Rainnie 2016; Gungor & Parė 2016; Johnson et al., 2016; Radley & Sawchenko 2015; Marcinkeiwcz et al., 2016). Moreover, unconditioned fear responses are often either eliminated, or robustly enhanced following inactivation of the BST; effects that again appear dependent on subregion (Schulz & Canbeyli 2000; Gray et al., 1993; Fendt et al., 2003; Gerwitz et al., 1998; Levita et al., 2004; Hammack et al., 2009; Daniel & Rainnie 2016; Johnson et al., 2016). As such, the BST functions, in parallel with HPA modulation, to generate or restrain unconditioned stress-related behavioral responses.

An updated synthesis of the role of BST in mediating behavioral responses to threatening stimuli, accounting for this functional diversity, has suggested that rather than mediating long-lasting anxiety-like behaviors the BST mediates temporally unpredictable stressors (Ressler, Goode, Evemy, & Maren, 2020; Goode, Acca, Maren, 2019; Goode et al., 2019), or acts as “valence surveillance” (Lebow & Chen, 2016). Support for this idea has been demonstrated by lesions of BST that impair context fear expression when training involved a delayed shock onset (Goode, Acca, & Maren, 2020; Hammack et al., 2015), a randomly generated CS-US pairing, or backward US-CS conditioning (Goode et al., 2019). This hypothesis is also perhaps consistent with work demonstrating that global lesions of the BST prevent cued-fear generalization (Duvarci, Bauer, Pare, 2009). Importantly, that manipulations of the BST can also induce fear responding in variety of stress related paradigms is consistent with the notion that there are functionally distinct

BST subregions that are able to either promote or suppress stress-related behavior, as might be expected of a region tasked with surveilling uncertainty. Indeed, two more recent studies found that separate BST populations residing in proximity exerted opposing capacities in modulation of anxiety-related behavior (Jennings et al., 2013a; Kim et al., 2013a). As such, “valence surveillance” may be the most accurate reflection of the role BST plays during threat processing (Lebow & Chen, 2016), as this would account for its ability to quickly mobilize defense responding in cases where uncertainty regarding threat becomes certain, and conversely prevent defensive behavior under conditions that are deemed non-threatening.

That BST mediates both stress-promoting, and suppressing aspects suggests further anatomical divergence based on limbic forebrain innervation. Prefrontal and hippocampal regions are predominantly involved in HPA-inhibitory regulation suggesting a preferential involvement with BST subregions that act to limit stress-related neuroendocrine and behavioral responding. However, little attention has been placed on circuits that coordinate multiple aspects of an organism’s stress response. Moreover, much of the historical literature has relied on gross anatomical manipulations that produce chronic disruptions in signaling (i.e., global lesions of regions), or correlational observations involving immediate early gene mapping that do not allow for temporally precise, circuit-specific manipulations as would be necessary to disentangle the involvement of specific limbic forebrain HPA regulatory mechanisms.

Toward a prefrontal – bed nuclei of the stria terminalis network in memory consolidation and generalization

The mPFC is indispensable for the refinement of environmental features predictive of stressor likelihood (Sharpe & Killcross, 2018; Antoniadis & McDonald, 2006), and a critical substrate for glucocorticoid actions during memory consolidation (Roozendaal et al., 2009) positioning it as key locus for mediating fear generalization. Lesions of the mPFC impair behavioral selection when conflicting cues are presented (Sharpe & Killcross 2018). mPFC activation reduces fear responding, and prevents generalization to novel cues (Grosso et al., 2018; Likhtik et al., 2014) or contexts (Xu & Südhoff 2013). Moreover, the mPFC projects to the BST in a topographically organized manner exclusively innervating regions implicated in the suppression of HPA-related responding. That the mPFC receives contextual-related information directly from the hippocampus during consolidation, and yet does not maintain a direct path returning to the hippocampus (Vertes 2004) suggests this region maintains a privileged role in coordinating adaptive behavior to mediate generalization. Interestingly, despite this well-established role for integrating hippocampal-dependent context information, and mediating HPA axis mobilization very little work has described the downstream circuits the mPFC utilizes to organize adaptive behavior and promote discrimination between conflicting threatening cues. Indeed, aside from a few recent studies demonstrating mPFC projections to the ventrolateral periaqueductal gray (vlPAG)(Rozeske et al., 2018), and separately the BLA, were involved in promoting discrimination between similarly threatening cues, and necessary for preventing generalization to distinct cues (Likhtik et

al., 2014), the organization of prefrontal circuits mobilized during memory consolidation and how they contribute to long-term expression of fear generalization remains poorly understood, particularly with regard to the mobilization of the HPA axis.

Summary

The recruitment of stress neurocircuitry to mediate memory consolidation processes involve the integration of behavior and neuroendocrine systems to promote adaptive behavior. An ongoing effort to more fully characterize the organization of neural circuits that coordinate this integration is critical for understanding how an organism successfully disambiguates the environmental contingencies that predict threat. These efforts are fundamental for informing therapeutic interventions in cases of neuropsychiatric disease, as much of the extant literature suggest the developmental of stress-related illnesses results from aberrant CNS signaling in stress-modulatory pathways. Therefore, the goal of the current set of experiments is to elaborate on the capacity of the BST to modulate stress-related neuroendocrine and behavioral responses and the contribution of the prefrontal cortex to these. In the following chapters (**FIG. 1.1**), I will present:

- Evidence that the BST mediates memory consolidation via glucocorticoid-dependent and independent pathways (Ch. 2).

- Evidence for involvement of the BST in fear generalization via an interaction with a prefrontal cortical region that is dynamically mobilized during consolidation and disambiguation of threatening and non-threatening contexts. (Ch. 3).

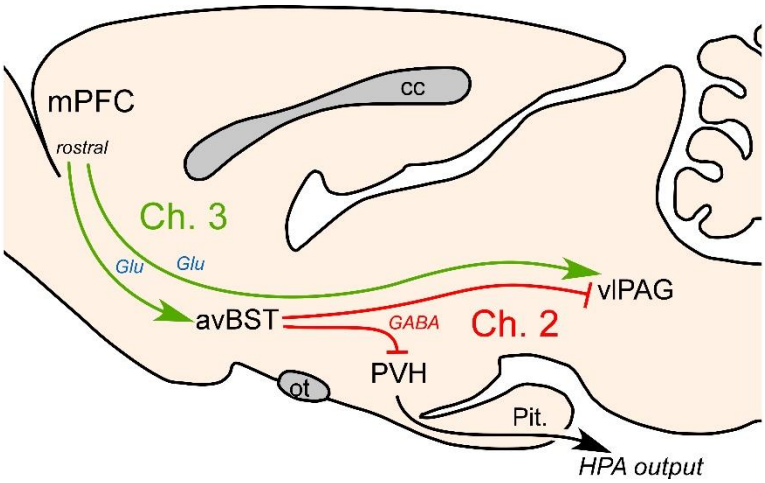

Figure. 1.1. Neural circuit diagram delineating chapter focus. Chapter 3 (green) investigates a pathway from the rostral prelimbic cortex (PL) to the anteroventral bed nuclei of the stria terminalis (avBST) and its involvement in HPA and context fear generalization. Chapter 2 (red) investigates HPA-dependent and independent circuits from avBST that bi-directionally mediate memory consolidation.

The following was previously published in the Proceedings of the National Academy of Science (PNAS)

(Lingg et al. 2020)

CHAPTER II:

Bed Nuclei of the stria terminalis modulate memory consolidation via glucocorticoid-dependent and -independent circuits

Abstract

There is extensive evidence that glucocorticoid hormones enhance memory consolidation, helping to ensure that emotionally significant events are well remembered. Prior findings suggest that the anteroventral region of bed nuclei of the stria terminalis (avBST) regulates glucocorticoid release, suggesting the potential for avBST activity to influence memory consolidation following an emotionally arousing learning event. To investigate this issue, male Sprague-Dawley rats underwent inhibitory avoidance training and repeated measurement of stress hormones, immediately followed by optogenetic manipulations of either avBST or its projections to downstream regions, and 48 h later were tested for retention. The results indicate that avBST inhibition augmented posttraining pituitary-adrenal output and enhanced the memory for inhibitory avoidance training. Pre-treatment with a glucocorticoid synthesis inhibitor blocked the memory enhancement as well as the potentiated corticosterone response, indicating the dependence of the memory enhancement on glucocorticoid release during the immediate posttraining period. In contrast, posttraining avBST stimulation decreased retention yet had no effect on stress hormonal output. Subsequent experiments revealed that inhibition

of avBST input to the paraventricular hypothalamus enhanced stress hormonal output and subsequent retention whereas stimulation did not affect either. Conversely, stimulation, but not inhibition, of avBST input to the ventrolateral periaqueductal gray impaired consolidation, whereas neither manipulation affected glucocorticoid secretion. These findings indicate that divergent pathways from avBST are responsible for the mnemonic effects of avBST inhibition versus stimulation and do so via glucocorticoid-dependent and -independent mechanisms, respectively.

Introduction

Emotionally arousing experiences produce lasting memories (McGaugh 2003; McGaugh 2013), an effect mediated, at least in part, by activation of adrenal stress hormones including cortisol (corticosterone, or CORT, in rodents) and epinephrine (McGaugh 2000; Gold & van Buskirk 1978; Gold & van Buskirk 1975; Sandi & Pinelo-Nava 2007; Roozendaal, McEwen, & Chattarji 2009; McGaugh & Roozendaal 2002; de Kloet, Oitzl, & Joels 1999). These hormones influence memory consolidation processes that occur during the immediate post-learning period and depend on the basolateral amygdala for their memory-modulatory effects. For example, amygdala lesions or noradrenergic receptor blockade in the amygdala prevent the memory-enhancing effects of systemically administered CORT and epinephrine (Liang, Juler, & McGaugh 1986; Quirarte, Roozendaal & McGaugh 1997; Fery, Roozendaal, & McGaugh 1999; Roozendaal & McGaugh 1996; Roozendaal et al., 2006). The basolateral amygdala, in turn, modulates memory consolidation through its interactions with other brain regions,

including the bed nuclei of the stria terminalis (BST). Prior work indicates that the memory-modulatory ability of the amygdala depends on concurrent activation of the BST (Liang & McGaugh 1983a; Liang & McGaugh 1983b; Liang, Chen, & Chen 2001), suggesting that the BST acts “downstream” from the amygdala in influencing memory consolidation.

The BST is a complex of heterogeneous regions with distinct functions (Lebow & Chen 2016; Gungor & Pare 2016; Daniel & Rainnie 2016; Rodriguez-Sierra, Turesson, Pare 2013; Crestani et al., 2013). Whereas previous studies focused on the dorsal BST, findings from our laboratory suggest that a different subregion, the anteroventral subdivision (avBST), regulates the *acute* behavioral and physiological responses to stressors and emotional arousal (Radley & Johnson, 2018; Johnson et al., 2016). The avBST is well-positioned to modulate neuroendocrine responses to stress (Choi et al., 2007; Cullinan, Herman & Watson 1993; Radley & Sawchenko, 2011; Radley, Gosselink, & Sawchenko 2009). It provides a GABAergic input to effector neurons in the paraventricular hypothalamic nucleus (PVH) that modulate the hypothalamic-pituitary-adrenal (HPA) axis and thereby regulate peripheral glucocorticoid levels in response to a variety of aversive experiences (Crestani et al., 2013; Radley & Johnson 2018; Johnson et al., 2019; Choi et al., 2008; Dong, Petrovich, Watts, & Swanson 2001). Thus, avBST and its projections to PVH may serve as a critical central regulator of CORT release during the posttraining period of memory consolidation. The avBST also projects to the periaqueductal gray (PAG) (Johnson et al., 2016; Dong & Swanson 2006a; 2006b; Wright & McDannald 2019), and recent findings implicate the PAG more directly in memory consolidation following aversive experiences, either itself as a nodal point or as a relay to limbic cortical consolidation networks (Cole & McNally 2009; Arico, Bagley, Carrive,

Assareh, & McNally 2017; Johansen, Tarpley, LeDoux, & Blair 2010; Boyden, Zhang, Bamberg, Nagel, Deisseroth 2005).

Together, these findings suggest a rather distinct role for the avBST, compared to the dorsal regions of BST previously investigated. To address this issue, the present study used an optogenetic approach in rats to control activity of avBST neurons and its projections to PVH and ventrolateral PAG following training in a single-trial inhibitory avoidance (IA) task. CORT and adrenocorticotropic hormone (ACTH) levels were assessed before and after training. Rats' retention of IA learning was measured two days after training. The findings indicate that the avBST→ PVH and avBST→ ventrolateral PAG pathways are capable of modulating memory consolidation, via glucocorticoid-dependent and -independent mechanisms, respectively.

Methods

Animals and treatments. Adult male Sprague-Dawley rats (225–250g at time of arrival; Charles River Labs) were used. Animals were maintained on a 12:12 light/dark cycle (lights on at 0600) in an AAALAC-approved vivarium with ad libitum access to food and water. Rats were acclimated to the vivarium housing conditions for 7 d prior to surgery. All procedures were in accord with the National Institutes of Health's Guide for the Care and Use of Laboratory Animals and were approved by the University of Iowa Institutional Animal Care and Use Committee.

Surgeries. Rats were anesthetized with 4% isoflurane in oxygen, placed in a stereotaxic frame (Kopf Instruments), and received a pre-surgical analgesic (2 mg/kg meloxicam, s.c.). Surgical anesthesia was maintained with 1.5–2% isoflurane. A midline incision was made down the scalp and a craniotomy was performed above the region of interest. Rats received bilateral microinjections (350 nl/ side) of virus solution directed at avBST (anteroposterior, AP: -0.10 mm relative to bregma; mediolateral, ML: ±1.20 mm; dorsoventral, DV: -7.45 mm). The virus solution contained AAV5 coding either eArch3.0-eYFP, eNpHR3.0-eYFP, ChR2(E123A)-eYFP, or eYFP alone, all of which were under the control of the human synapsin-1 promoter (Chow et al., 2010, Alheid & Heimer, 1988). Optical fibers (200-µm diameter, 0.37 N.A.; Thorlabs) secured inside of steel ferrules (PlasticsOne) were implanted either immediately dorsal to avBST (AP: -0.10 mm; ML: 2.35 mm; DV: -6.60 mm; 8°), avBST terminal fields in PVH (AP: -1.55mm; ML: 1.65 mm; DV: -7.00 mm; 10°), or above the ventrolateral PAG (AP: -7.85 mm; ML: 1.80 mm; DV: -5.20; 10°) and then secured with dental cement and surgical screws. After 3-6 weeks recovery, rats began the behavioral procedures.

Hormone Assays. Two days prior to IA training, rats received implants with indwelling jugular catheters (Ericsson, Kovacs, Sawchenko 1994; Radley, Arias, Sawchenko 2006). Sealed jugular catheters (polyethylene PE 50) with a SILASTIC (Dow-Corning) tip containing sterile heparin-saline (50 U/ml) were implanted under isoflurane anesthesia. The internalized SILASTIC tip was positioned at the atrium and was exteriorized at the interscapular region of the neck. At 0600 on day 1 of the experiment (i.e., a time chosen since it coincides with the onset of the diurnal trough of the circadian CORT cycle)

(Ericsson, Kovács, & Sawchenko 1994), rats were brought to the procedure room and jugular catheters were connected to 1-ml syringes filled with sterile heparinized saline. Catheters were flushed with heparinized saline prior to blood collection. After 90 min of habituation and prior to the onset of behavioral training, blood samples were collected prior to IA training (0 min), and at 10, 30, 60, and 90-min intervals thereafter to monitor elevations in stress hormone levels. Upon collection, each sample was immediately placed in a chilled conical vial containing 15 µl EDTA/ aprotinin, centrifuged for 20 min, and plasma was fractionated for storage at -80 °C. A two-site radioimmunoassay (MP Biomedicals) incorporating rabbit antisera raised against ACTH-BSA with ^{I25}I-ACTH-BSA serving as a tracer was used for measurement of plasma ACTH. Intraassay and interassay coefficients of variation for ACTH radioimmunoassay were 3% and 7%, respectively. Similarly, plasma CORT was measured without extraction using rabbit antisera raised against CORT-BSA with ^{I25}I-CORT-BSA serving as tracer (MP Biomedicals), with intra/ interassay coefficients of 5% and 10%, respectively, and a sensitivity of 8 ng/ml. Catheter viability was consistently >80% across all experiments. Rats with failed catheter patency were still included in behavioral analyses.

Drug Treatment. One experiment involved systemic injections of metyrapone 90 min prior to IA training, to reversibly inhibits steroid 11β-hydroxylase in the adrenal cortex (Sigma). The dose of metyrapone (50 mg/kg, s.c.) was selected as based on prior knowledge of its capacity to suppress stress-induced elevations in plasma CORT, without leading to significant impairments in memory consolidation following IA training (Roozendaal, Carmi & McGaugh 1996; Roozendaal, Bohus, McGaugh 1996). To reach

the appropriate concentration, the drug was dissolved in 40% polyethylene glycol and diluted with 0.9% saline.

Behavioral Procedures. All rats were trained on the single-trial step-through IA task (Roozendaal, Carmi & McGaugh 1996; Huff, Miller, Deisseroth, Moorman, LaLumiere 2013; LaLumiere, Buen, McGaugh 2003). The IA apparatus was a trough-shaped box segmented into one-third (30 cm) an illuminated white plastic bottom and the remaining two-thirds (60 cm) darkened stainless steel. The 60 cm darkened stainless steel portion of the apparatus was connected to a shock generator, and timer. A retractable stainless-steel door separated the two compartments.

Prior to experimentation, rats were handled for 3 min daily, and habituated for 1 hour to the procedure room each day for 7 days. During IA training (day 1), rats were placed in the enclosed lit compartment to allow for a brief period of acclimation (~10 s). The door was then opened to allow free exploration of the apparatus. Upon entry into the darkened compartment, the retractable door was closed to prevent the rat from returning to the lit side. When the rat reached the end of the dark compartment, it received a single inescapable footshock (1.0 mA, 2-s duration for rats transduced with ChR2 in avBST neurons; 0.8 mA, 1-s duration for experiments involving transduction with Arch and Halo; different footshock intensities were used to prevent floor and ceiling effects, respectively) (Huff et al., 2013; Liu, Chen, & Liang 2009; Chen, Bambah-Mukku, Pollonini, Alberini 2012; Roozendaal, Williams, & McGaugh 1999). Thereafter, the rat was left in the dark compartment for 20 s and then removed for optical manipulation and further blood collection. For retention testing 48 h later, rats were placed back into the lit compartment

of the IA chamber with the door retracted. Rats' latency (in seconds) to cross into the dark compartment was measured and used as the index of retention with a maximum latency of 600 s.

Optical procedures. Surgically implanted optic ferrules were connected to an insulated optical fiber directed from a 561-nm (Laser century), or 473-nm light source (OptoEngine). Laser output was adjusted to direct 10 mW at the tip of the implanted optical fibers, which is sufficient to activate opsins within a 0.46-mm radius of spherical illumination below the termination of the fiber optic (Huff et al., 2013, Yizhar, Fenno, Davidson, Mogri, Deisseroth 2011). In all experiments, illumination began 20 s following application of footshock and continued for 10 min. For Arch and Halo experiments, continuous 561-nm light illumination was used. Experiments involving avBST cell body inactivation were carried out using Arch, and Halo was used for pathway inactivation, as based on evidence that illumination of Arch at axon terminals over a several minute period may paradoxically increase spontaneous transmitter release (Yizhar, Fenno, Davidson, Mogri, & Deisseroth 2011). For ChR2 experiments, trains of 5-ms pulses at either 20 Hz or 40 Hz (Master-9 pulse generator) were used. Experiments involved the use of controls receiving the same illumination parameters as their respective experimental counterparts, unless otherwise noted.

Optrode recordings. In a separate experiment, rats were injected with viral solutions for the transduction of Arch, Halo, or ChR2 in avBST neurons. Four weeks later, the same rats underwent an additional stereotaxic surgery for the implantation of a combined

microwire array/optical fiber, or optrode (MicroProbes for Life Science), and recording of optically evoked excitation or inhibition of AAV-transduced avBST neurons or separately, post-synaptic characterization of single unit PVH and vlPAG neuronal activity following avBST terminal excitation and inhibition. Following initial induction of anesthesia, animals received an intraperitoneal injection of ketamine (100 mg/kg) and xylazine (10 mg/kg) and subsequently maintained at surgical level anesthesia with additional injections of ketamine (30 mg/kg), as necessary. The scalp was then retracted, and skull leveled between bregma and lambda before commencement of craniotomy above the avBST, PVH, or vlPAG of the right hemisphere. Insertion of the ground wire was performed in a separate hole and secured to skull screws. The optrode was positioned above avBST, PVH, or PAG and slowly lowered (0.1 mm/min) into the most dorsal aspect of each region (avBST: DV -7.2mm; PVH: DV -7.45mm; vlPAG: -5.2mm relative to dura).

Using an online oscilloscope and audio monitor to identify single neurons, neuronal recordings were made using a multielectrode recording system (Plexon). Recordings were made with the following parameters: avBST neuron recording experiments: 0-15 min, laser off; 15-30 min, either 473 nm laser pulsed at 20 Hz with 10% duty cycle, or 561 nm laser on; 30-45 min, laser off. PVH neuron recording experiments: 0-5 min, laser off; 5-10 min (20 s laser off – 20 s laser on – 20 s laser Off); 10 – 20 min laser on; 20-21 min laser off. vlPAG neuron recording experiments: 0-1 min, laser off; 1-2 min 1 Hz to 20 Hz ramping 473 nm laser on with 10% duty cycle; 2-5 min 473 nm laser pulsed at 20 Hz with 10% duty cycle. After the initial recording, the optrode was lowered in 0.15-mm increments for a total of 4 recordings. After the recording session, the hardware was removed, and animals were prepared for histology (see below). To analyze signals offline

and for the removal artifacts, the Plexon Off-line Sorter program was used. All cells that fired at rates >0.1 Hz were analyzed. Principle component analysis (PCA) and waveform shape were used for spike sorting. All single units exhibited (1) consistent waveform shape, (2) separable clusters in PCA space, (3) average amplitude >3 times background activity, and (4) refractory periods of <2 ms. Custom MATLAB routines were used to analyze neuronal activity.

Histology and tissue processing. Rats were anesthetized with pentobarbital (Fatal Plus; 100 mg/kg, i.p.) and transcardially perfused at a rate of 55 ml/min with 100 ml of 0.9% NaCl, followed by 900 ml of ice-chilled 4% paraformaldehyde (PFA). Brains were then dissected and postfixed in 4% PFA at 4°C for 4 h prior to transfer into a 20% sucrose/ potassium phosphate buffer cryoprotectant for overnight storage. Coronal sections (30 µm) were collected in a 1:5 series on a sliding microtome (Leica). In all cases, sections were stored in a cryoprotectant solution at -20°C. Verification of viral expression, and placement of optical probes was performed by visualization of YFP expression under epifluorescence with a compound light microscope (Leica) and confirmed based on the cytoarchitectonic characteristics for the structures of interest (Paxinos & Watson 2006, Swanson 2004). Rats with incorrect placement of virus and/or optic probes were excluded from subsequent analyses.

Hybridization histochemistry. In situ hybridization was performed using antisense oligonucleotide probes from RNAscope (Advanced Cell Diagnostics, Newark, CA) (Wang et al., 2012; Sharpe et al., 2017; Li et al., 2015). This variation of in situ hybridization

utilizes DNA Z-blocks containing complimentary 18-25 bp target RNA sequences, a spacer sequence, and a 14-base oligonucleotide tail that allows single-cell resolution of targeted mRNA with a high degree of specificity. Probes targeting GAD1 (ACDBio catalog #316401), vGlut2 (ACDBio catalog #317011), and CRF (ACDBio catalog #318931) were obtained and hybridization was performed using RNAscope Fluorescent Multiplex v2 (Advanced Cell Diagnostics). Visualization was performed using fluorophores (Fluorescein, Cyanine 3, Cyanine 5) with fluorescent signal enhancement using a modified tyramide signal amplification method (Perkin Elmer). Slides were counterstained with DAPI (Thermo Fisher) and cover slipped with ProLong Gold antifade reagent.

Immunohistochemistry. Localization of antigens were performed on free-floating sections. Primary antisera raised against anti-GFP (rabbit polyclonal; Thermo Fisher) and GAD-65 (mouse monoclonal; University of Iowa Developmental Studies Hybridoma Bank) were visualized respectively with goat anti-rabbit (Alexa 488; Thermo Fisher) or goat anti-mouse (Alexa 568; Thermo Fisher). CRF was immunolocalized using an antiserum raised against rat CRF (rC68, rabbit polyclonal; Paul Sawchenko, The Salk Institute of Biological Studies), followed by incubation with biotinylated goat anti-rabbit IgG and streptavidin conjugated Alexa 633 (Thermo Fisher).

Statistics. Plasma levels of stress hormones were analyzed using a repeated measures two-way ANOVA with blood collection time point (0, 10, 30, 60, 90 min) as the within-subjects variable, and optogenetic treatment as the between-subjects factor. Post-hoc pairwise comparisons using Fisher's LSD were used when appropriate (i.e., $p < 0.05$). All

main analyses were considered significant at $p < 0.05$. Integrated hormone levels (i.e., AUC), and retention latency data were analyzed using an unpaired t-test. Data are expressed as mean ± SEM.

Data Availability. The data presented in this report are available in Datasets S1-S3.

Results

Anteroventral BST bi-directionally modulates memory consolidation via HPA-dependent and independent mechanisms

Adult male Sprague-Dawley rats received microinjections in avBST with adeno-associated virus (AAV5) containing the inhibitory opsin enhanced archaerhodopsin 3.0 or excitatory channelrhodopsin-2 (E123A) (Arch and ChR2, respectively; (Boyden, Zhang, Bamberg, Nagel, Deisseroth 2005; Chow et al., 2010), both fused to enhanced yellow fluorescent protein (YFP) and under the human synapsin-1 promoter. These injections were targeted to produce expression in a population of GABAergic projection neurons within the division of BST considered as “ventrolateral” by De Olmos and colleagues (Alheid & Heimer 1988; de Olmos, Beltamino, Alheid 2004) or within fusiform, dorsomedial and subcommissural subdivisions according to the nomenclature of Dong and Swanson (Dong, Petrovich, Watts, Swanson 2001; Dong & Swanson 2004b; Dong & Swanson 2006a; 2006b). Designation of this BST region as “anteroventral” is based upon these different taxonomic regimes and its exclusivity from other BST regions dorsal and posterior to the anterior commissure. In order to activate or inactivate neuronal cell

bodies, optical fibers were implanted above the avBST (**FIG. 2.1A**). IA training consisted of a standard IA apparatus, in which the rat was placed into a brightly lit compartment, and then upon crossing into the darkened compartment, received a single inescapable footshock (0.8 mA, 1 s duration). In an initial experiment (**FIG. 2.1B**), rats expressing either Arch or YFP in avBST received illumination of avBST for 10 min with 561-nm light immediately after IA training. Blood samples were collected from indwelling jugular catheters in both groups immediately prior to training (0 min) and at 10, 30, 60, and 90 min posttraining.

Radio-immunometric analysis of plasma levels of ACTH and CORT revealed posttraining increases in both groups, with Arch rats displaying a greater enhancement relative to YFP controls. For ACTH, repeated-measures ANOVA revealed an interaction between group and time ($F_{4,92} = 3.32$, $p = 0.014$) and main effects of group ($F_{1,23} = 14.89$, $p = 0.001$) and time ($F_{4,92} = 17.54$, $p < 0.001$). Posttraining avBST inhibition increased integrated ACTH responses (area under curve, AUC; $t_{23} = 3.43$, $p = 0.002$) and increased ACTH levels at 10 and 30 min ($p = 0.003$ and 0.012, respectively) relative to the YFP control values (**FIG. 2.1C**). Analysis of plasma CORT revealed main effects of group ($F_{1,23} = 7.71$, $p = 0.011$) and of time ($F_{4,92} = 101.34$, $p < 0.001$) (no group by time interaction). Posttraining avBST inhibition produced an increased integrated CORT response (AUC; $t_{23} = 2.92$, $p = 0.008$) and increased CORT levels at 60- and 90 min time points ($p = 0.016$ and 0.040, respectively), as compared with YFP control rats (**FIG. 2.1D**). Two days after training, rats were assessed for IA retention by being placed back in the lit compartment, and their latency to enter the darkened compartment was utilized as an index of retention. Rats that had received avBST inhibition displayed significantly higher retention latencies

compared to YFP controls (t_{25} = 2.50; p = .019) (**FIG. 2.1E**). To address the possibility that posttraining inhibition produced long-lasting changes in avBST that account for the altered retention, an additional group of rats expressing Arch or YFP received a 10-min illumination period of avBST 3 h after IA training. However, there was no significant difference in the retention latencies between the groups (**FIG. 2.1F**).

Given that posttraining administration of glucocorticoids has been shown to enhance memory for IA training (Roozendaal & McGaugh 1996a, Roozendaal, Portillo-Marquez, & McGaugh 1996; Roozendaal & McGaugh 1996b), the memory modulatory effect of avBST inactivation may be regulated through its potentiating effects on adrenocortical output. To address this possibility, a follow up experiment was carried out repeating the same design as shown in **FIG. 2.1B**, except both groups of rats received pretreatment with the corticosterone synthesis inhibitor, metyrapone, 90 min before IA training. Previous work indicates that a 50 mg/kg (s.c.) dose of metyrapone given 90 min prior to IA training attenuates the induction of glucocorticoids without altering retention on its own (Roozendaal, Carmi, & McGaugh, 1996). IA training significantly increased ACTH levels, with potentiation of this response in rats receiving avBST inhibition with Arch **(FIG. 2.1G)**. A repeated-measures ANOVA revealed a main effect for time ($F_{4,56}$ = 4.82, p = 0.002) and a nonsignificant trend for avBST inhibition to potentiate the ACTH response ($F_{1,14}$ = 4.21, p = 0.059; no group by time interaction). Additionally, avBST significantly increased integrated ACTH values compared to YFP controls (t_{14} = 2.43, p = 0.029). However, metyrapone blunted the CORT response following IA training and prevented its potentiation following avBST inhibition (**FIG. 2.1H**). Repeated-measures ANOVA revealed a main effect only for time ($F_{4,60}$ = 14.92, p = 0.001), but not for group ($F_{4,60}$ =

0.1, p = 0.8), interaction ($F_{4,60}$ = 0.6, p = 0.6), or effect of inhibition on integrated CORT (AUC: t_{15} = 0.1, p = 0.9). Moreover, metyrapone pretreatment prevented the retention-enhancing effects following avBST inhibition, as retention latencies did not significantly differ between Arch-expressing and YFP control rats (**FIG. 2.1I**).

The next experiment involved activating the avBST in rats expressing either ChR2 or YFP for 10 min with 473-nm light (20 Hz, 5-ms pulse width), immediately following IA training. For this, the shock amplitude was increased (1.0 mA, 2 s) to ensure sufficiently high retention latencies to observe impairments in retention (46-49), as the foregoing results suggest that posttraining stimulation of avBST may *attenuate* retention. As before, IA training significantly increased plasma CORT and ACTH in both groups, as indicated by main effects of time (ACTH: $F_{4,76}$ = 14.84, p < 0.001; CORT: $F_{4,76}$ = 84.55, p < 0.001). However, no main effects of group (ChR2 vs. YFP controls) or interaction were observed, nor were any differences found in integrated values for either ACTH or CORT (**FIG. 2.1J, K**). Nevertheless, rats receiving avBST stimulation with ChR2 had significantly attenuated retention latencies compared to YFP controls (t_{20} = 2.90; p = 0.009) (**FIG. 2.1L**). As with the optical inhibition experiment, a control experiment was conducted in which rats expressing either ChR2 or YFP in avBST received the same laser illumination (20 Hz for 10 min) 3 h after IA training. However, there was no significant difference in the retention latencies between the groups (**FIG. 2.1M**). Altogether, the findings of these initial experiments indicate that the mnemonic effects of avBST inhibition versus stimulation occur via glucocorticoid-dependent and -independent mechanisms, respectively.

Opsin functionality was verified in rats (n = 2) bearing Arch and ChR2 expression in the avBST. Optrode recordings of avBST were performed both before and during laser illumination (**FIG. 2.2**). Illumination at 561-nm for 15 min suppressed the activity of Arch-expressing neurons (**FIG. 2.2C**). Similarly, 5-ms pulses (20 Hz for 15 min) of 473 nm light increased phasic firing rates of avBST neurons (**FIG. 2.2D**). Previous work found no effect of 15-min of either means of illumination on neuronal responses in avBST of rats not expressing the opsin (Johnson et al., 2016), indicating that illumination alone has no effect on neural activity.

Circuit basis for avBST enhancement of memory consolidation

That avBST inhibition potentiated posttraining levels of plasma ACTH in the face of constrained CORT levels suggested a mechanism of HPA axis modulation that is more purely neuronal rather than dependent on glucocorticoid negative feedback. This raised the possibility that the memory-enhancing effect of posttraining avBST inactivation were due to disruption of its GABAergic input to (i.e., disinhibition of) HPA effector neurons in the PVH and subsequent enhancement of downstream glucocorticoid release. To investigate this, avBST neurons were transduced with the inhibitory opsin enhanced halorhodopsin 3.0 (Halo) fused to YFP (Han, & Boyden 2007), and implanted optical fibers bilaterally above PVH (**FIG. 2.3A-C)**. Immediately following IA training (0.8 mA, 1 s), half of the rats injected with Halo received continuous illumination of avBST axons in PVH with 561-nm light for 10 min, and the other half (i.e., control group) received no illumination.

In rats with viral injections centered in the avBST, YFP-fluorescent terminals formed a dense innervation of the PVH that ramified within the parvicellular divisions and provided relatively sparse innervation outside of the nuclear boundary (**FIG. 2.3B**). Confocal laser-scanning microscopic analysis in PVH revealed extensive colocalization of YFP-fluorescent puncta with the GABA synthetic enzyme GAD-65 (**FIG. 2.3D-F**). In the medial parvicellular division of PVH, these dual-labeled puncta were noted to reside in close apposition to CRF-immunoreactive secretory neurons (**FIG. 2.3F**). The GABAergic signature of this pathway is consistent with the fact that most neurons in avBST are GABAergic, with very few glutamatergic neurons (**FIG. 2.3G, H**) (Kudo et al., 2012, Giardino et al., 2018), and is similar to previous observations (Johnson et al., 2016, Culinan, Herman, & Watson 1993; Radley, Gosselink, & Sawchenko 2009).

IA training significantly increased plasma ACTH and CORT levels in each group, with inhibition of avBST axons in PVH potentiating these responses (**FIG. 2.4A, B**). For ACTH, there were main effects of time, group, and an interaction for time and group ($F_{4,92}$ = 20.04, p < 0.0001; $F_{1,23}$ =6.36, p = 0.019; $F_{4,92}$ = 3.21, p = 0.016; respectively). For CORT, there were main effects for time and group ($F_{4,92}$ = 68.15, p < 0.001; $F_{1,23}$ = 6.38, p = 0.019). Analysis of integrated ACTH and CORT responses revealed significant increases in the inhibition group (t_{23} = 2.29, p = 0.031; t_{23} = 2.49, p = 0.020) (inset in **FIG. 2.4A, B**). Comparisons of hormone differences at select time points after training found increased ACTH values at 10 min and 60 min (p = 0.009 and 0.021, respectively) and increased CORT values at 10 min and 90 min (p = 0.009 and 0.046) in rats receiving illumination. Consistent with the increased HPA response, illumination of avBST axons in the PVH significantly increased retention latencies when assessed 48 h

later (t_{26} = 2.14; p = 0.042) (**FIG. 2.4C**). To verify the postsynaptic effects of avBST→ PVH pathway optogenetic inhibition, rats (n = 2) received avBST microinjections of AAV expressing Halo. Four weeks later, optrode recordings in the PVH were performed both before and during laser illumination in the PVH (**FIG. 2.4D**). Inhibiting avBST axons in the PVH reliably increased PVH spiking, indicating an inhibitory relationship between avBST and its postsynaptic target.

To determine whether the memory-impairing effects of avBST stimulation (i.e., **FIG. 2.1L**) also occur via this pathway, avBST neurons were transduced with ChR2 fused to YFP or with YFP alone in the control group, and optical fibers were implanted bilaterally above PVH. Following IA training (1.0 mA, 2 s), rats received 473-nm light (20 Hz, 5-ms pulse width) to PVH for 10 min to stimulate ChR2-transduced avBST axons, with YFP controls receiving the same illumination. Although IA training increased plasma CORT and ACTH in both groups, avBST→ PVH pathway stimulation with ChR2 did not produce any differential effects (**FIG. 2.4E, F**). Similarly, there were no differences in latencies during the 48-h retention test (**FIG. 2.4G**).

A divergent pathway from avBST accounts for its memory-attenuating effects

Together, the results described above suggest that the memory-attenuating effects of avBST stimulation depends on a separate pathway. Recent evidence suggests that the PAG is a more central player in fear learning circuitry than previously appreciated (Wright & McDannald 2019; Cole & McNally 2008; Arico et al., 2017; Johansen, Tarpley, Ledoux, & Blair 2010; Assareh, Bagley, Carrive, & McNally 2017), raising the possibility that avBST stimulation impairs retention via projections to this region.

To investigate this issue, avBST neurons were transduced with either ChR2-YFP or YFP-only and implanted optical fibers above the ventrolateral PAG (**FIG. 2.5A-C**). Immediately following IA training (1.0 mA, 2 s), both ChR2 and YFP control rats received illumination of the axonal pathway from avBST to PAG with 473-nm light (20 Hz, 5-ms pulse width) for 10 min. Analysis of YFP innervation of PAG confirmed previous reports that the avBST preferentially innervates the ventrolateral subdivision, with a dearth of input to more lateral and dorsal regions (Dong, Petrovich, Watts & Swanson 2001; Dong & Swanson 2004b). Immunohistochemical analysis in PAG revealed extensive colocalization of YFP-fluorescent puncta with the GABA synthetic enzyme GAD-65 (**FIG. 2.5D-F**). IA training increased plasma CORT in both groups, with pathway stimulation producing no significant differences relative to YFP controls (**FIG. 2.5G**). Nevertheless, posttraining stimulation of this pathway decreased retention latencies as compared with YFP controls (t_{20} = 2.48; p = 0.022) during the 48-h retention test (**FIG. 2.5H**). Optrode recordings in the PAG were performed to verify the postsynaptic effects of avBST→ PAG pathway stimulation using the same stimulation parameters as above. Rats (n = 2) received microinjections of AAV expressing ChR2 and, 4 weeks later, received 20 Hz pulses (5 ms width) of 473 nm light in the PAG. Stimulating avBST axons in the PAG transiently decreased neuronal responses (**FIG. 2.5I**), indicating that there may be an inhibitory relationship between avBST and PAG.

A final experiment examined whether the memory-enhancing effects observed following avBST inhibition could also occur through the pathway involving the ventrolateral PAG. avBST neurons were again transduced with Halo fused to YFP or with YFP alone in the control group. Following IA training (0.8 mA, 1 s), rats received

continuous 561-nm light to the ventrolateral PAG for 10 min to inhibit Halo-transduced avBST axons, with YFP controls receiving the same illumination. Posttraining inhibition of this pathway did not alter adrenocortical output on the day of training (**FIG. 2.5J**) and did not alter retention 48-h thereafter (**FIG. 2.5K**).

Discussion

The present findings indicate that the avBST bidirectionally modulates consolidation of IA memory via divergent neural pathways. Optogenetic avBST inhibition for 10 min after IA training increased pituitary-adrenal responses during the posttraining period, as measured by CORT and ACTH, and enhanced retention when tested 2 d later. Pretreatment with a glucocorticoid synthesis inhibitor blocked the memory enhancement and CORT increase without altering the ACTH response, indicating that this memory-modulatory effect was mediated, at least in part, via HPA activation. However, posttraining avBST stimulation decreased retention without altering HPA output. Subsequent experiments then targeted the avBST inputs to the PVH and PAG. Posttraining inhibition of the avBST→PVH pathway mimicked the effects of avBST inhibition alone, increasing HPA output and enhancing retention, with stimulation of this pathway producing no effects. In contrast, stimulation of the avBST→PAG pathway attenuated retention without altering HPA output, with inhibition of this pathway producing no effects. Together, these results reveal a role for the avBST in modulating memory consolidation through distinct pathways using HPA-dependent and -independent mechanisms, respectively.

Glucocorticoids, avBST, and PVH

A substantial body of work indicates that systemic glucocorticoid administration enhances memory consolidation for many different forms of learning in rodents, including contextual and auditory fear conditioning (Medina et al., 2007; Kaouane et al., 2012; Hui et al., 2004; Corderon, Merino, Sandi 1998; Cordero, Sandi 1998), spatial and novel-object recognition (Roozendaal & McGaugh 1996; Roozendaal et al., 2003; Okuda, Roozendaal, McGaugh 2004; Sandi, Loscertales, Guaza 1997), and inhibitory avoidance (Roozendaal, Williams, McGaugh 1999; Sandi, & Rose 1994). Similarly, in humans, oral administration of cortisol and increased cortisol secretion induced by cold-pressor stress enhance memory consolidation for emotionally arousing stimuli (Buchanan, & Lovallo 2001; Cahill, Gorski, Le 2003). Prior work indicates that the memory-modulatory capability of peripheral stress hormones depends, in part, on activity in the BLA. Following emotionally arousing events, glucocorticoids enhance neuronal excitability in the BLA and memory consolidation (Duvarci, Parė 2007). Electrophysiological recordings of the BLA following IA training reveal time-dependent increases in neuronal activity that crest with plasma glucocorticoid concentrations, at around 30 min post-footshock (Pelletier, Likhtik, Lilali, Parė 2005). The ability of the BLA to influence memory consolidation, in turn, depends on concurrent activity in other brain structures, including the BST (Liang & McGaugh 1983a; Liang & McGaugh 1983b; Liu, Chen, & Liang 2009; McGaugh, McIntyre, & Power 2002; LaLumiere, McGaugh, & McIntyre 2017). Such work appears to position the BST as *downstream* from the BLA in memory modulation.

Earlier work investigating the role of BST in learning regarded it as having a singular function and focused exclusively on dorsal aspects of this structure. More recently, heterogeneity in BST functions have been parcellated relative to dorsal (Kim et al., 2013a), posterior (Henckens et al., 2017), and ventral (Johnson et al., 2016; Jennings et al., 2013a) regions, and these may be further distinguished by distinct neurochemically defined subpopulations within and spanning across these regions (Giardino et al., 2018; Fetterly et al., 2019; Pomrenze, Fetterly, Winder, & Messing 2017; Marcinkiewcz et al., 2016). The present study targeted the avBST region, as opposed to dorsal BST, because evidence suggests that avBST is capable of potently modulating adaptive responses to stressors, particularly HPA axis activity (Choi et al., 2007; Radley, Gosselink & Sawchenko 2009; Choi et al., 2008; Radley & Sawchenko 2015; Cullinan, Ziegler, & Herman 2008). This suggested the possibility that avBST could influence memory consolidation as an *upstream* regulator of stress responses.

Indeed, the first central finding of the present study reveals a novel role for the avBST in regulating memory consolidation. In particular, the results indicate that avBST activity alters consolidation via the regulation of glucocorticoid secretion through its GABAergic input to the HPA effector region of the PVH. This suggests that, in contrast to studies on the dorsal aspects of BST, avBST acts *upstream* from BLA-dependent processes by regulating glucocorticoid secretion. Interestingly, inhibition, but not stimulation, of the avBST→ PVH pathway altered memory consolidation and HPA output. Thus, the current findings suggest that activity of this circuit is necessary, but not sufficient, to restrain the extent of HPA output following an aversive experience which, in turn, reduces the strength of the resulting memory of the experience. Along these lines,

diminished activity in this pathway may provide an endogenous mechanism for augmenting HPA output and memory consolidation following an emotionally arousing event.

As each major BST subdivision expresses the type II glucocorticoid receptor (McEwen, de Kloet, Rostene 1986; Aronsson et al., 1988; Ahima & Harlan 1990), this raises the possibility that HPA axis activation influences avBST and its modulation of memory consolidation. However, the present results indicate that posttraining avBST inhibition was accompanied by increases in plasma ACTH even when metyrapone administration prevented the footshock-induced increase in CORT, suggesting that the ability of avBST to regulate the HPA axis involves some degree of independence from feedback influences of CORT (**Fig. 1G**) (e.g., see Kim, Han & Iremonger 2019). This supports the idea that the memory-modulatory influences of avBST occur via a circuit-based mechanism involving PVH rather than via glucocorticoid feedback. Nevertheless, the possible involvement of BST-glucocorticoid receptor effects on memory consolidation at later times after training warrants consideration in future studies.

avBST and PAG

The second central finding from the present study is that avBST inputs to the ventrolateral PAG also influence memory consolidation and do so in a manner *independent* of HPA axis modulation. These results build on recent evidence implicating the PAG more directly in learning than previously appreciated (Wright & McDannald 2019; Johansen, Tarpley, LeDoux & Blair 2010; McNally, Johansen, & Blair 2011), although the precise role of the PAG in aversive learning is still not clear. Whereas past studies suggest

that the ventrolateral PAG is involved in the expression of conditioned freezing responses and defensive behaviors (LeDoux, Iwata, Cicchetti, Reis 1988; Tovote et al., 2016), there is also a growing appreciation for the role of the ventrolateral PAG in the acquisition of fear conditioning. A current perspective is that the ventrolateral PAG relays aversive instructive signals, presumably to other brain regions (e.g., the BLA during auditory Pavlovian fear conditioning) to enable learning-related plasticity (McNally, Johansen, & Blair 2011). This view is based upon evidence that ventrolateral PAG modifies aversive stimuli-evoked activity in the BLA (Johansen, Tarpley, LeDoux & Blair 2010), whereas chemogenetic, optogenetic, and pharmacological manipulations of the ventrolateral PAG disrupt acquisition of conditioned fear (Wright & McDannald 2019; Arico, Bagley, Carrive, Assareh, & McNally 2017; Johansen, Tarpley, LeDoux & Blair 2010; Assareh, Bagley, Carrive, & McNally 2017; McNally, Johansen, & Blair 2011; Watson, Cerminara, Lumb, & Apps 2016). Another recent study found that enhanced activity in the ventrolateral PAG reflects an increased probability of threat onset (e.g., footshock) (Wright & McDannald 2019). As the present results found that stimulation of GABAergic avBST inputs to the ventrolateral PAG impaired retention, this raises the possibility that such activity disrupts the ability of the PAG to convey this instructive signal as part of a memory consolidation process and warrants more careful consideration of this novel circuit for future studies. However, inhibition of this pathway did not alter consolidation, suggesting a lack of activity in this pathway at least in the present experimental circumstances.

One outstanding question concerns the temporal sequence for how the avBST→ ventrolateral PAG pathway modulates memory consolidation. As the present study involved manipulations of the avBST→ ventrolateral PAG pathway after IA training,

this more directly implicates the ventrolateral PAG in memory consolidation that is neither directly connected with acquisition or expression and points to the avBST as an important upstream modulatory influence. Indeed, it appears that the same circuits and structures (e.g., PAG) that generate defensive behaviors and stress-adaptive responses are also important *after an aversive event* for influencing memory consolidation.

Nonetheless, the present findings support the ability of avBST activity to modulate memory consolidation in a bidirectional manner. Although activity in this structure appears to be both necessary and sufficient for enhancing and attenuating retention, respectively, a surprising finding was that each effect depended on distinct pathways involving PVH and the ventrolateral PAG, respectively. Recent evidence implicates these pathways in the modulation of endocrine and behavioral stress-adaptive behaviors (Radley & Johnson, 2018; Johnson et al., 2016), whereas diminished activity may account for some of the endocrine and behavioral disturbances that are common in stress-related psychiatric disorders. The fact that all manipulations in the current study were given during the posttraining period enables the distinction between the role of the circuits in adapting to exposure to the stressor and their role in altering mnemonic processes following an aversive learning event. Nevertheless, additional work is needed to assess whether the avBST and related circuitry have distinct roles in stress adaptation and memory modulation under naturalistic conditions. Considering the persistence or over-saliency of memories that occurs in a variety of stress-related pathologies such as post-traumatic stress disorder, avBST dysfunction may provide a novel mechanism connecting stress susceptibility to the mnemonic components of stress-based disorders.

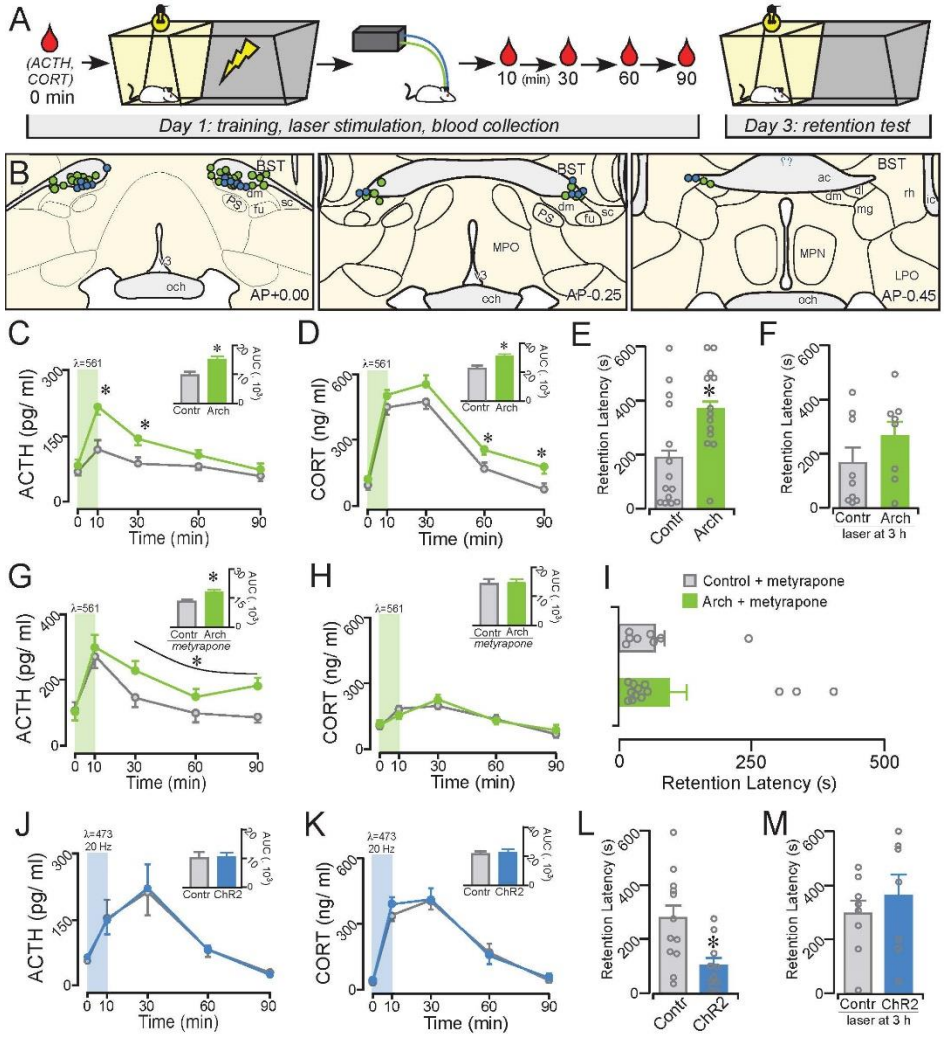

Figure 2.1. Posttraining manipulation of avBST activity bi-directionally modulates IA memory consolidation.

A: Diagram illustrating the experimental timeline. Posttraining inhibition and stimulation of avBST were conducted in serial experiments and were compared with AAV5-YFP control rats receiving identical illumination, respectively. ***B***: Examples of fiber optic implants targeted toward the region immediately dorsal to the avBST for illumination. Circles represent rats from separate experiments, first for Arch inhibition (green, n=13; n=11 for metyrapone + Arch group in ***G-I***), and next for ChR2 activation (blue, n=10) of avBST neurons. Coronal atlas images adapted from Swanson (92). ***C, D***: Shown are mean ± SEM of plasma ACTH (***C***) and CORT (***D***) in control and Arch groups before (0 min) and at various intervals following IA training. Both hormones are significantly increased in the Arch group at various intervals following illumination. *Inset in* ***C, D***: Integrated ACTH and CORT responses (area under the curve, AUC) were also significantly increased in the Arch versus YFP groups. ***E, F***: Inhibition of avBST neurons

in the Arch group immediately posttraining increased retention latencies when measured 48 h later (***E***), but not when inhibition was administered 3-h posttraining (***F***). ***G, H***: Mean ± SEM of plasma ACTH and CORT in control and Arch groups before (0 min) and at various intervals following IA training following pretreatment with a glucocorticoid synthesis blocker (metyrapone). Inhibition of avBST with Arch potentiated the increase in plasma ACTH levels, whereas CORT levels were not distinguishable between Arch and control groups due to pre-treatment with metyrapone. *Inset in* ***G, H***: Integrated ACTH and CORT responses (area under the curve, AUC) in Arch and YFP groups. ***I***: Posttraining inhibition of avBST neurons failed to enhance retention latencies when assessed 48 h later. ***J, K***: Plasma levels of ACTH (***J***) and CORT (***K***) were not significantly altered by posttraining activation of avBST neurons with ChR2. ***L, M***: ChR2 rats displayed significantly decreased retention latencies relative to YFP controls (***L***) when assessed 48 h later, whereas stimulation with ChR2 at 3-h posttraining had no effect (***M***). *, $p < 0.05$.

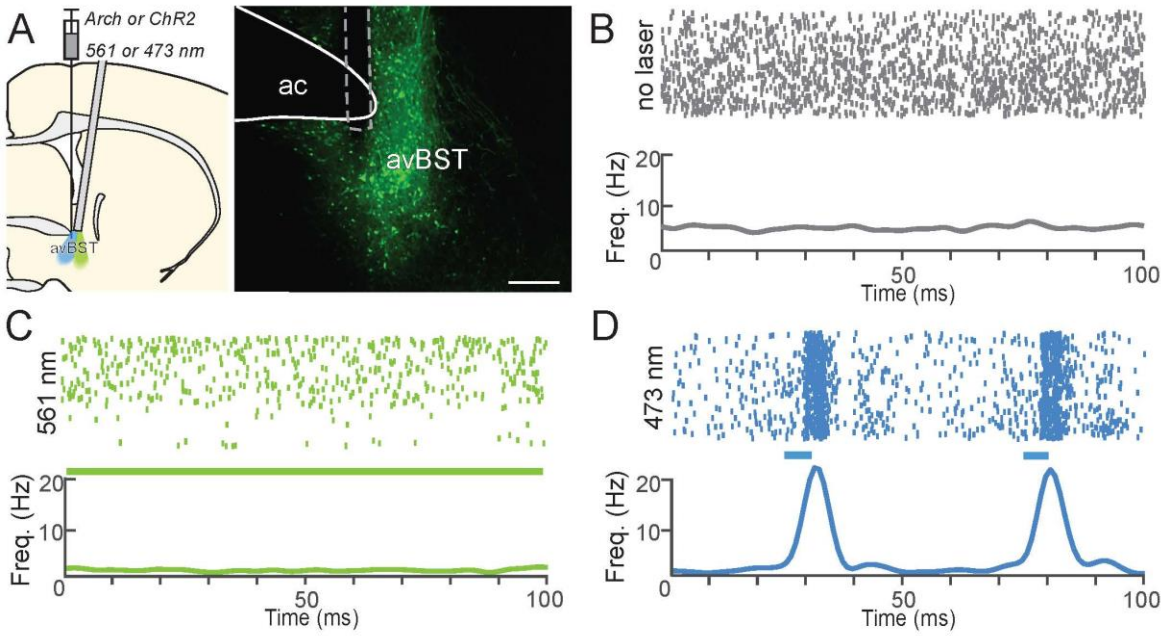

Figure 2.2. Characterization of avBST neuronal activity before and during optogenetic manipulations.
A: Schematic diagram (left) illustrating AAV injection and optrode placement during the recording during inhibition and excitation (green and blue, respectively). Epifluorescent image (right) displays an implant (dashed line) for neurophysiological activity recordings made ventral to the anterior commissure (ac). Scale bar, 300 µm: ***B***: Raster plot (top) and summary histogram (bottom) of action potentials over a 15-min recording session in the absence of illumination. ***C***: Raster plot (top) of action potentials in the same neuron as above (in ***B***), in the presence of continuous 561-nm light over a 15-min recording session. The summary histogram (bottom) reveals a decrease in frequency relative to baseline activity above. ***D***: Raster plot (top) of action potentials in the presence of 20-Hz pulses of 473-nm light over a 15-min recording session, and summary histogram (bottom), illustrating light-evoked neuronal activity. Blue bars indicate 5-ms laser pulse.

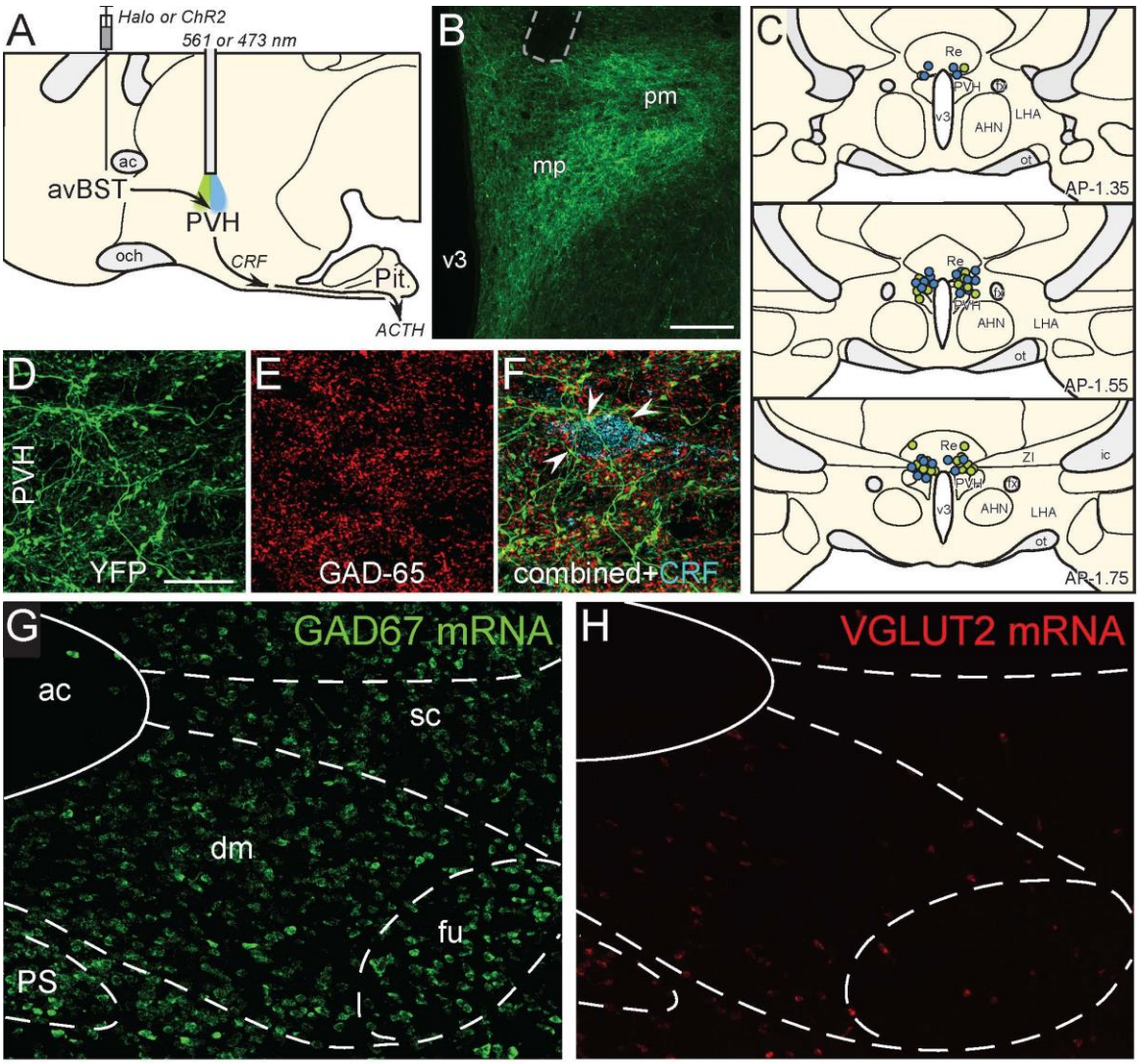

Figure 2.3. Role of avBST–GABAergic input to PVH in the enhancement of memory consolidation.

A: Midsagittal diagram depicting AAV5 microinjection into avBST and fiber optic placement above PVH to assess avBST→ PVH pathway involvement in the posttraining modulation of HPA activity and consolidation of IA learning. ***B***: Fluorescent image illustrating the distribution of YFP-labeled terminal fields in PVH following injection in avBST. Fiber optic implant is shown by dashed gray outline in the upper left. Scale bar: 200 µm ***C***, Examples of fiber optic implants targeted toward the region immediately dorsal to the PVH for illumination. Different colored circles represent rats from separate experiments, first for Halo inhibition (green, n=15), and next for ChR2 activation (blue, n=15) of the avBST→ PVH axonal pathway. ***D***: Confocal fluorescent images depict YFP immunoreactivity in the medial parvicellular subdivision of PVH following AAV injection in avBST, and GAD-65, the 65 kDa form of GAD, a synthetic enzyme for GABA (***E***). ***F***: Composite of images in ***D*** and ***F***, with the addition of immunolocalization of CRF (cyan). Numerous instances of YFP+/ GAD+ puncta were noted to make appositions

with CRF-labeled neurons (arrowheads). ***G, H***: Fluorescent images showing *in situ* hybridization of GAD67 (***G***) and VGLUT2 (***H***) mRNA in avBST and its vicinity. ac, anterior commissure; dm, avBST dorsomedial subdivision; fu, avBST fusiform subdivision; PS, parastrial nucleus; sc, avBST subcommissural subdivision. Scale bar (in *D*): *D-F*, 20 µm; *G-H*, 100 µm.

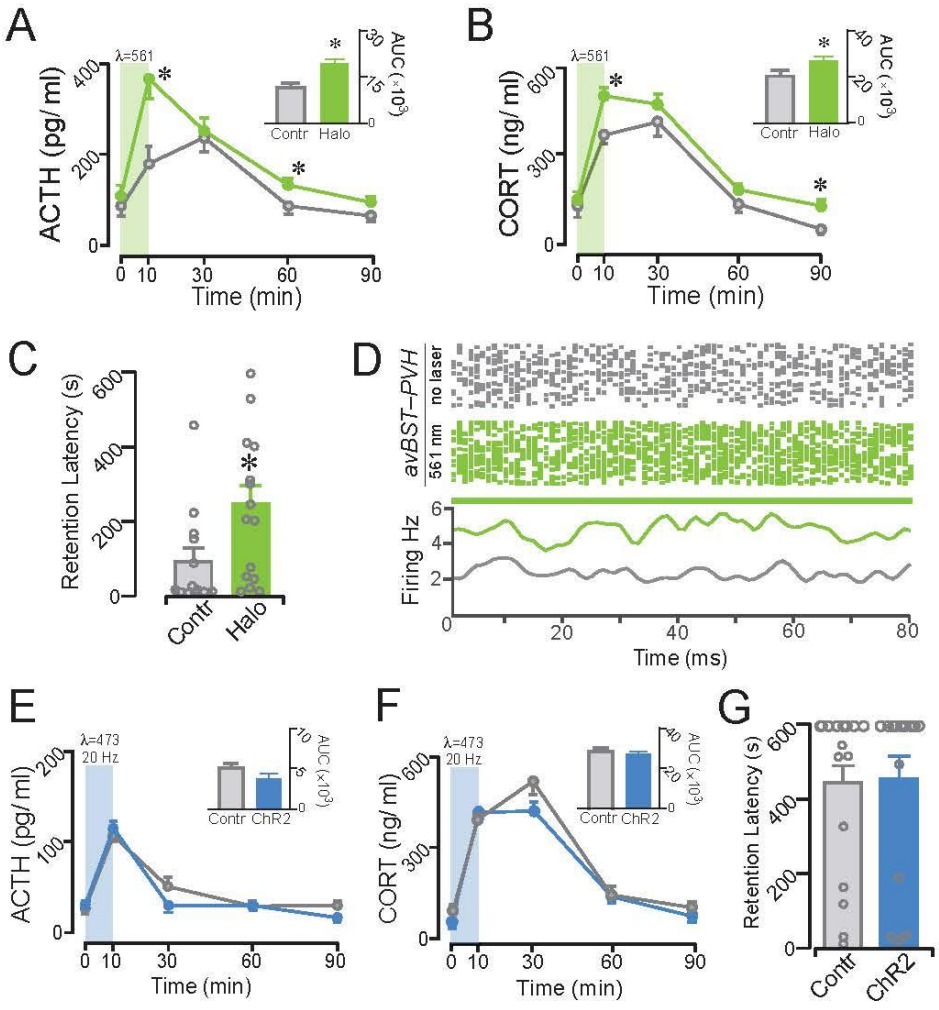

Figure 2.4. **Functional evidence that avBST→ PVH pathway inactivation enhances memory consolidation.**

A, B: Mean ± SEM of plasma ACTH (***A***) and CORT (***B***) in no-laser control and laser Halo groups before (0 min) and at various intervals following IA training. Both hormones are significantly increased in the Halo group at various intervals following illumination. *Inset in* ***A, B***: Integrated ACTH and CORT responses (area under the curve, AUC) were also significantly increased in the Halo versus control groups. ***C***: Posttraining inhibition of avBST neurons enhanced retention when measured 48 h later. ***D***: Raster plots (*top*) of action potentials over a 15-min recording session in the absence (gray) and presence (green) of 561-nm illumination. The summary histogram (*bottom*) reveals an increase in frequency relative to baseline activity above. ***E-G***: avBST→ PVH pathway stimulation with ChR2 failed to alter posttraining levels of plasma ACTH (***E***) and CORT (***F***), or retention latencies (***G***) when assessed 48 h later. *, $p < 0.05$.

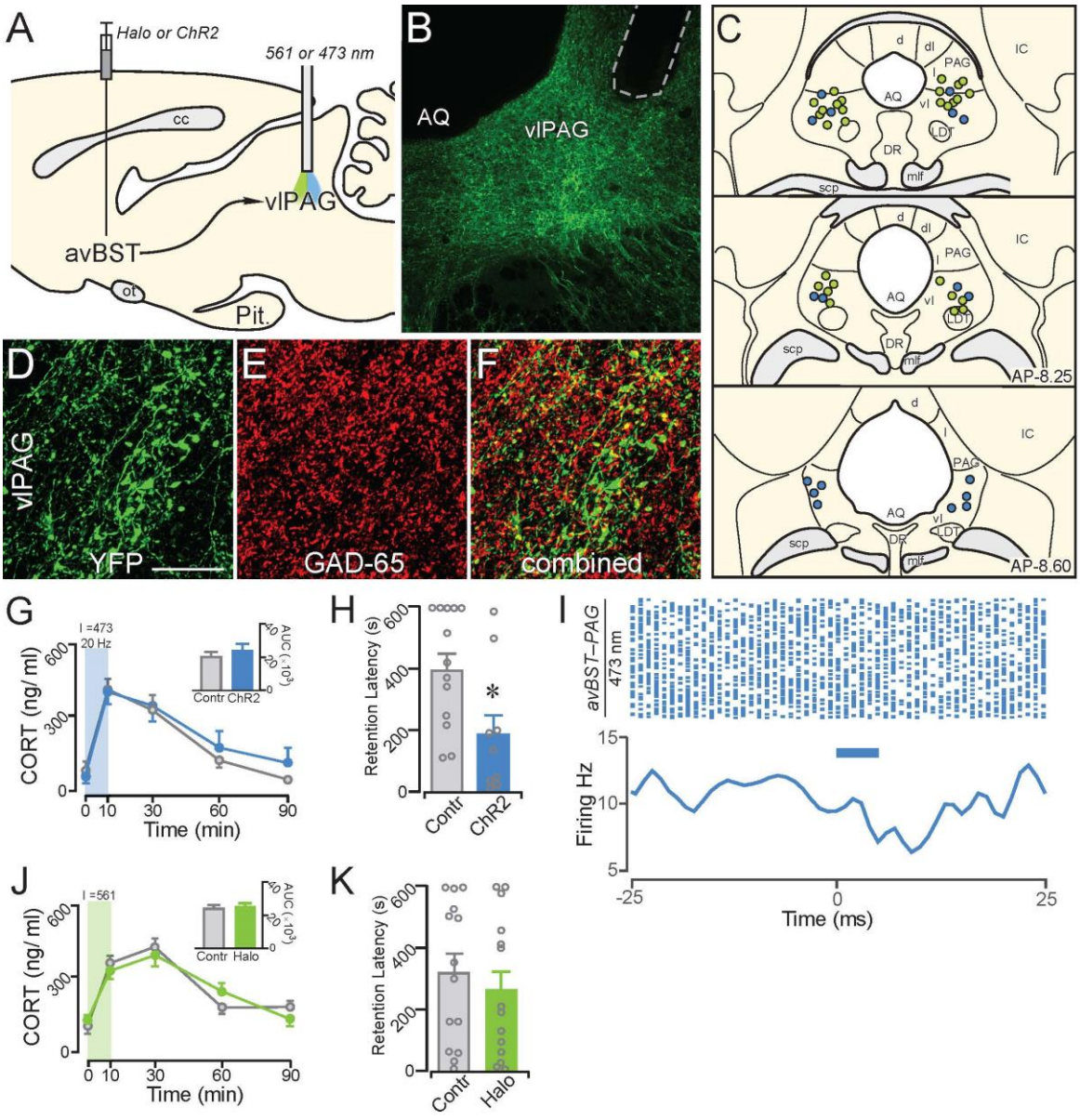

Figure 2.5: Circuit basis for avBST attenuation of memory consolidation.
A: Midsagittal diagram depicting AAV5 microinjection into avBST and fiber optic placement above PAG. ***B***: Fluorescent image illustrating the distribution of YFP-labeled terminal fields in ventrolateral PAG following injection in avBST. Fiber optic implant is shown by dashed gray outline. ***C***: Examples of fiber optic implants targeted toward the region immediately dorsal to the ventrolateral PAG for illumination. Different colored circles represent rats from separate experiments, first for stimulation with ChR2 (blue, n=9) and next for inhibition with Halo (green, n=14) of the avBST→ ventrolateral PAG axonal pathway. ***D-F***: Confocal fluorescent images show YFP immunoreactivity in the ventrolateral PAG following AAV injection in avBST (***D***), GAD-65 immunofluoresence (***E***), and a composite of these images (***F***) illustrating instances of YFP+/ GAD+ colocalization. Scale bar (in *D*): *B*, 250 µm; *D-F*, 20 µm. ***G***: Mean ± SEM of plasma CORT in YFP and ChR2 groups before (0 min) and at various intervals following IA training. *Inset in* ***G***:

Integrated CORT responses (AUC). ***H***: Posttraining stimulation of the avBST→ ventrolateral PAG pathway with ChR2 attenuated retention latencies, when measured 48 h later. ***I***: Raster plot (top) of action potentials in the presence of 20-Hz pulses of 473-nm light over a 15-min recording session, and summary histogram (bottom), illustrating light-evoked neuronal activity. Blue bars indicate 5-ms laser pulse. ***J, K***: avBST→ PVH pathway inhibition with Halo failed to alter either posttraining levels of plasma CORT (***I***), or retention latencies (***J***) when assessed 48 h later. *, $p < 0.05$.

CHAPTER III:

Evidence for involvement of a prefrontal-bed nucleus of the stria terminalis circuit in constraining contextual fear memory generalization

Abstract

Generalization of fear is an adaptive neurobiological process conserved across species. Nevertheless, dysregulation of the neural systems that mediate fear generalization has been implicated in the development of a variety of stress-related psychiatric illnesses, including PTSD. In stress-related psychiatric disease, excessive fear generalization is characterized by an enhanced memory for the core traumatic event, and a disrupted disambiguation of peritraumatic elements (i.e., cues or contexts) producing an excessive fear to environmental stimuli which have never been explicitly associated with danger. It is well documented that the end-products of the hypothalamo-pituitary-adrenal axis (HPA), glucocorticoids (cortisol in humans and corticosterone [CORT] in rodents), have an important modulatory role in memory consolidation and contribute to fear generalization. However, little is known about the stress-modulatory systems that regulate endogenous glucocorticoid activity and how these are engaged to mediate fear generalization. Our prior work combining optogenetic, behavioral, and neuroendocrine approaches highlight the bed nuclei of the stria terminalis (BST) as an important interface between HPA-related information processing and prefrontal cortical regions tasked with the regulation of emotional memory. Here we used intersectional viral approaches to characterize a subsection of prefrontal input to BST originating from the rostral end of the prelimbic region (rPL) and interrogate its involvement in regulating context fear generalization. We applied optical and electrophysiological methods for

monitoring and manipulating neural activity immediately following training on a modified inhibitory avoidance (IA) procedure to target posttraining consolidation processes, as this period is critical for mediating the emergence of long-term fear generalization. We found that rPL is broadly mobilized following IA training and provides discrete input to the caudal end of the anterior BST and targets GAD1, but not vGlut2, expressing neurons that in turn provide input to a distributed network of threat processing regions. BST is similarly robustly recruited following footshock training, and posttraining optical inhibition of the rPL-BST pathway in adult male Long-Evans (LE) rats with eNpHR3.0 exaggerated posttraining CORT responses and was associated with increased avoidance to a novel chamber 48hrs later. Separately, we used pre-exposure to a neutral context to encourage later generalization of fear. Here, posttraining optical activation of the rPL-BST pathway with ChR2 (E123A) prevented generalization 48hrs later to the neutral context without affecting avoidance to the training context. Together, these data provide evidence for a novel circuit tasked with regulating posttraining consolidation processes that contribute to the emergence of generalized fear.

Introduction

Generalization of fear is a fundamental adaptive neurobiological process conserved across species that is critical for survival. Organisms utilize environmental information from previous fearful experiences to shape behavioral responses to novel situations where the presence of a threat is uncertain. Provided the perception of threat is high, organisms may express a range of defensive behaviors deemed most likely to navigate the threat successfully. Although generalization is necessary for an organism to predict the presence of threat and select the appropriate behavioral response, in humans, generalization of fear to environments or to cues that bear little similarity to previous fearful experiences is a hallmark of stress-related psychiatric disease. Given the ubiquity of generalization processes in adapting to complex environmental changes, there is a critical need to better understand the neural systems that restrict fear generalization during periods of uncertainty and the underlying perturbations that lead to the exaggeration of these responses.

Severity of threat encounter, prior stress and enhanced stress-hormone responding contribute toward the saliency of an event and modulate later generalization (dos Santos Corrêa et al., 2019; Bahtiyar et al., 2020; Asok, Kandel & Rayman 2018). The medial prefrontal cortex (mPFC) is involved in the regulation of affective memory (Xu & Südhoff 2013; Cullen et al., 2015; Antoniadis & McDonald, 2006; Gilmartin, Balderston & Helmstetter 2014) and shows alterations in activity (Yuen, Karatsoreos, Feng, McEwen & Yan 2009) and morphology (Anderson et al., 2016; Anderson et al., 2020) following either prior stress or increased stress-hormone responding. Moreover, the mPFC projects

to the lateral and ventrolateral periaqueductal gray (l/vlPAG)(Vertes 2004) and the bed nucleus of the stria terminalis (BST)(Johnson et al., 2019; Radley, Gosselink & Sawchenko 2009; McDonald, Shammah-Lagnado, Shi, & Davis 1999; Chiba, Kayahara, & Nakano 2001; Dong, Petrovich, & Swanson 2001), two structures involved in the acquisition (Wright & McDannald 2019; McNally, Johansen, & Blair 2011; Hammack, Todd, Kocho-Schellenberg, & Bouton 2015; Goode & Maren 2017; Zimmerman & Maren 2011; Bjorni, Rovero, Yang, Holmes, & Halladay 2020), consolidation (Lingg et al., 2020; Bruzsik et al., 2021) and expression (Ressler, Goode, Evemy, & Maren 2020; Goode, Ressler, Acca, Miles, & Maren 2019) of fear during periods of uncertainty. In addition, both the vlPAG and BST are involved in the regulation of stress hormone responding through direct GABAergic projections to the paraventricular hypothalamus (Floyd, Keay, Arias, Sawchenko, & Bandler 1996; Johnson et al., 2016; Johnson et al., 2019; Radley, Gosselink & Sawchenko 2009; Radley & Sawchenko 2015; Herman, Cullinan, & Watson 1994a; Herman, Cullinan, & Watson 1994b). Thus, the mPFC is well positioned to integrate context information regarding threat with stress hormonal status through an interaction with the BST and/or vlPAG to disambiguate environmental stimuli most relevant for predicting threat.

Historically, fear generalization in rodents has been investigated using either context or auditory-fear conditioning (Asok, Kandel, & Rayman 2019; Lashley & Wade 1946). During conditioning an aversive stimulus is paired with a particular context or tone. When tested later, rodents will exhibit high levels of fear-related behavior (e.g., freezing, avoidance) when re-exposed to the context or tone associated with the aversive stimulus (Maren 2001). If the rodent is exposed to a stimulus that shares similar features (Rozeske

et al., 2015; Rozeske et al., 2018; Maren 2001) or is temporally linked (Cai et al., 2016) with the original context or tone, a similarly high degree of fear behavior will be produced, indicative of fear generalization. Conversely, a reduction in fear behavior is evident if the rodent is exposed to a context/tone that is sufficiently different, or not temporally linked (Cai et al., 2016) from the original aversive one and this distinction may be termed fear discrimination. Prior work has shown that lesions of the prefrontal cortex before conditioning impair context fear discrimination (Antoniadis & McDonald 2006), and more recently that prefrontal projections to the vlPAG are involved in mediating the expression of fear discrimination (Rozeske et al., 2018). However, the prefrontal projections that are involved in the initial consolidation of an aversive event and how perturbations to this process mediate later generalization and whether this is associated with alterations in neuroendocrine responding remain unknown.

Here we sought to disentangle the circuit and hormonal processes underlying the emergence of fear generalization using an inhibitory avoidance paradigm modified for context discrimination. We identify a role for a prefrontal to bed nucleus of the stria terminalis projection (mPFC-BST) in preventing context fear generalization and gating posttraining neuroendocrine responses.

Methods

Subjects. Adult male Long-Evans or Sprague-Dawley rats, 225-250g at time of arrival (Charles River Laboratories) were used for all experiments. Upon arrival, rats were acclimated for at least 7 days prior to surgery in an AALAC-approved vivarium with ad

libitum access to food and water. All procedures were approved by the University of Iowa Institution Animal Care and Use Committee and in accordance with National Institutes of Health Guide for the Care and Use of Laboratory Animals.

Surgeries. Optogenetic/Fiber Photometry Experiments. Rats were anesthetized with 4% isoflurane in oxygen, then placed in a stereotaxic frame (Kopf Instruments) and received a presurgical analgesic (2mg/kg Meloxicam, s.c). Surgical anesthesia was maintained at 1.5-2% isoflurane. Rats received bilateral microinjections (350nL per side) of adeno-associated virus solution directed at avBST (anteriorposterior, AP: -0.18mm relative to bregma; mediolateral: ±1.20mm; dorsoventral, DV: -6.75mm) and rostral prelimbic [rPL; (AP): 3.85mm; (ML); 0.85mm; (DV); 3.00mm]. Following AAV injection, steel ferrules (Plastics One) fitted with fiber optics (200 µm diameter, 0.37 NA; Thorlabs) for optogenetic experiments were placed bilaterally immediately dorsal to avBST [(AP): -0.18mm; (ML): 2.35; (DV): -6.55mm; 6°] and then secured with dental cement and surgical screws. Fiber photometry experiments involved unilateral AAV injections, and optic placements directed at the same rPL or avBST coordinates. Rats were allowed to recover for >5wks, and then were habituated to a holding room where blood collection occurred and handled daily by an experimenter for 1 week prior to behavioral procedures.

Hormone assays. Two days prior to IA training, rats were implanted with indwelling jugular catheters as described elsewhere (Ericsson, Kovács, & Sawchenko 1994; Radley, Arias & Sawchenko 2009). Under isoflurane anesthesia, polyethylene (PE-50) tubing containing sterile heparin-saline (50 U/mL) were implanted with its internal SILASTIC

(Dow Corning) tip positioned at the atrium and the remaining length exteriorized at the nape in the interscapular region. On the experiment day, and at the beginning of the circadian trough (0600 hr), rats were brought to a procedure room where the jugular catheters were connected to 1mL syringes containing sterile heparin-saline. Following >90 min habituation, blood samples (~200 µL) were taken prior to IA training (0 min) for baseline estimation of corticosterone (CORT) and adrenocorticotropic (ACTH) hormone levels. Subsequent samples were taken immediately following IA training at repeated intervals (+10min, 30, 60, 90). Each sample was immediately place in a chilled 1.5mL microcentrifuge tube containing 15 µL EDTA/aprotinin and centrifuged for 20 min prior to plasma fractionation and storage at -80°C. Plasma ACTH were measured using a two-site radio-immunometric assay (MP Biomedicals) with I-125 as a tracer. Intra- and inter-assay coefficients of variation were 3% and 10%, respectively. Assay sensitivity was 1.5pg/mL. Plasma CORT was measured without extraction with rabbit antisera raised against corticosterone-BSA with ^{125}I-corticosterone-BSA as a tracer (MP Biomedicals). Intra- and inter-assay coefficients of variation were 5% and 10%, with a sensitivity of 8ng/mL.

Behavioral Procedures. All rats were trained on a single-trial step-through inhibitory avoidance (IA) task (Medina et al., 2007; Huff et al., 2013), with modified procedures to assess discrimination and generalization, as based on (Atucha & Roozendaal 2015; Atucha et al., 2017). Multiple IA apparatuses were used, each of a similar general design, albeit with distinct contextual modifications. General features of the IA apparatus were a

trough-shaped box segmented into two compartments; one illuminated white plastic bottom and the remaining area darkened stainless steel. The darkened stainless-steel portion of the apparatus was connected to a shock generator, and timer. A retractable stainless-steel door separated the two compartments. IA chambers were made distinct with the following features: #1 had no context modifications and was cleaned with 70% Ethanol prior to training and testing for each animal, #2 had six 2-inch white strips of tape separated by ~2-inches placed on each wall of the darkened compartment and was cleaned with a citrus scented surface cleaner. Fiber photometry and electrophysiological experiments utilized IA chambers that had larger walls to accommodate head-stage equipment.

Discrimination Test: Prior to experimentation, rats were handled for 3 min daily, and habituated for 1 hr to the procedure room for 7d. During training (Day 1), rats were placed in the enclosed lit compartment of the shock IA chamber and briefly allowed to acclimate (~10s). The retractable door was then opened to allow free exploration of the entire apparatus. Upon entry into the darkened chamber, the door was closed to prevent the rat from returning to the lit side. The rat was then allowed 20s prior to receiving a single inescapable footshock (0.8mA, 1-s duration). The rat remained in the chamber for 20s and then removed for optical manipulation and further blood collection. 48hrs later, rats were placed in the lit compartment of either the original training context, or the modified context (in a pseudo-randomized way) with the door retracted. Rats' latency (in seconds) to cross into the darkened compartment was measured and used as an index of retention with a maximum latency of 600s. Rats were immediately transferred to an adjacent room for testing in the remaining context.

Generalization Test: Rats were handled prior to experimentation, as described above. During training (Day 1), rats were placed in the lit compartment of the contextually modified IA chamber with door retracted and allowed 1 min to explore the entire chamber. Rats were then transferred to an adjacent room containing the shock IA chamber and were subsequently placed into the lit compartment prior to being allowed entry into the darkened compartment and footshock training. A more intense shock (0.8mA, 2s duration) was used here to help bias animal responding toward generalization (dos Santos Corrêa et al., 2019; Kaouane et al., 2012). The rat was left in the dark compartment for 20s prior to removal and optical manipulation. For avoidance testing 48hr later, rats were placed in the lit compartment of the contextually modified IA chamber first. Rats' latency (in seconds) to cross into the darkened compartment was measured. Immediately following, rats were transferred to the shock IA chamber and similarly tested for latency to enter.

Photoillumination Parameters. Rats bearing ChR2-DIO microinjections and mCherry control counterparts received 473nm laser light (OptoEngine) pulses at 20Hz (5ms width; Master-9 pulse generator). Halorhodopsin (HALO) and control animals received constant 561nm laser light (Laser Century). Laser power for all experiments was adjusted to deliver ~10mW power at the tip of the implanted fiber optic, which has been reported to be sufficient to activate opsins within a 0.46 radius sphere below the termination of the fiber tip (Huff et al., 2013; Yizhar, Fenno, Davidson, Mogri, & Deisseroth 2011).

Neurophysiological recordings and analyses. A multi-electrode recording system (Plexon, Dallas, TS) was used for neuronal ensemble recordings. In each animal, the common average reference (CAR) was used for referencing, preserving 16 electrodes per animal.

The Plexon Off-Line Sorter program was used for neuronal preprocessing. Spike activity was analyzed for all cells that fired at rates above 0.1 Hz. Principal component analysis (PCA) and waveform shape were used for manual spike sorting. Units selected for additional analyses had (1) consistent waveform (Emmons, de Corte, Kim, Parker, Matell, & Narayanan 2017), (2) distinct clustering in PCA space, and (3) refractory period of <2ms. Analysis of neuronal activity was performed using custom routines in MATLAB. FP activity was performed with Brainstorm (Tadel et al. 2011), which is documented and freely available for download online under the GNU general public license (**http://neuroimage.usc.edu/brainstorm**).). FP data were down sampled to 100Hz and band-pass filtered to select between 0.7Hz to 30Hz for further analysis. Power spectral densities were calculated using Welch's method and time frequency data was calculated using a Morlet wavelet transformation. Values were averaged across animals (n = 3 or 4, depending on event) by electrode number, yielding 16 data points per event of interest.

A separate group of rats bearing either dual viral preparation for excitation or inhibition of the rPL-BST pathway (See Table 1 for Virus List) underwent neuronal recording procedures for verification of opsin functionality. At least 4 wks after viral microinjection, animals underwent stereotaxic surgery for implantation of a 16-wire microelectrode with optical fiber, or "optrode" (MicroProbes for Life Science). Rats underwent a surgical level of anesthesia induced by intraperitoneal injection of ketamine

(100mg/kg) and xylazine (10mg/kg). Supplementary injections of ketamine (30mg/kg) were given as needed. For optrode implantation, the scalp was retracted, and skull leveled between bregma and lambda. A craniotomy was made above either rPL or avBST of the right hemisphere. An additional hole for a single skull screw was made for connection to ground wire.

The optrode was slowly lowered (0.1mm/min) into the dorsal-most aspect of either the rPL or avBST. Neuronal recordings were made using a multielectrode recording system (Plexon). To determine whether regions were modulated by photoillumination, we recorded with the following parameters: 0-10 min, no laser on; 10-20 min, 473nm laser pulsed at 20Hz with 10% duty cycle or 561nm laser on; 20-30min no laser on. The optrode was then advanced ventrally by 0.3mm three times for a total of four recordings. After the recording session, the optrode was removed and animals were prepared for histology.

Fiber Photometry. Synapse software controlling a RZ10x lock-in amplifier (Tucker-Davis Technologies) were used to acquire fiber photometry data. 465nm and 405nm LEDs were used as light sources for illumination of GCaMP8s or GCaMP7f to record calcium-dependent and isosbestic changes, respectively. Light intensities were set to obtain ~50 µW power at the tips of optic fibers. Experimental timestamps (e.g., avoidance latency, footshock) were acquired using TTL pulses generated by the recording apparatus. Raw data were transferred to Z-Score ΔF/F values and aligned to experimental timestamps by using the open-source analysis software (pMAT) (Bruno et al., 2021). Further analyses of fiber photometry data were performed using custom routines in MATLAB.

Histology and Tissue Processing. Upon completion of experiments, rats were anesthetized with pentobarbital (Fatal Plus; 150mg/kg i.p) and then perfused with 100mL 0.9% NaCl, then 660mL of ice-cold 4% paraformaldehyde (PFA) at a rate of 55mL/min. Brains were then harvested and postfixed in 4% PFA at 4°C for 6 hr, then placed in cryoprotectant (20% Sucrose/KPBS) for an additional 18hrs. Coronal sections (30 µm) were collected in a 1:5 series on a sliding microtome (Leica). In all cases, sections were stored in a cryoprotectant solution at -20°C. Verification of viral expression and placement of optical probes was performed by visualization of mCherry expression under epifluorescence with a compound light microscope (Leica) and confirmed based on cytoarchitectonic characteristics for the region of interest (Paxinos & Watson, 2006; Swanson 2004). Rats with incorrect placement of virus or optic probes were excluded from subsequent analyses.

Hybridization Histochemistry. In situ hybridization was performed using RNAscope (Advanced Cell Diagnostics) (Wang et al., 2012). Probes targeting GAD1 (ACDBio catalog #316401), vGlut2 (ACDBio catalog #317011), and mCherry (ACDBio catalog #513201) were obtained and hybridization was performed using RNAscope Fluorescent Multiplex v2 (Advanced Cell Diagnostics). Visualization was performed using fluorophores (Fluorescein, Cyanine 3, Cyanine5) with fluorescent signal enhancement using a modified tyramide signal amplification method (Perkin-Elmer). Slides were counterstained with DAPI (Thermo Fisher) and cover slipped with ProLong Gold antifade reagent.

Immunohistochemistry. Free-floating sections of coronal tissue were used for localization of antigens. Primary antisera raised against anti-GFP (rabbit polyclonal; Thermo Fisher), mCherry (chicken polyclonal; Abcam), GAD-65 (mouse monoclonal; University of Iowa Developmental Studies Hybridoma Bank) were visualized respectively with goat anti-rabbit (Alexa 488; Thermo Fisher), goat anti-chicken (Alexa 555; Thermo Fisher) or goat anti-mouse (Alexa 680; Thermo Fisher). CRF was immunolocalized using an antiserum raised against rat CRF (rC68, rabbit polyclonal; Paul Sawchenko, The Salk Institute of Biological Studies, La Jolla, CA), followed by incubation with biotinylated goat anti-rabbit IgG and streptavidin-conjugated Alexa 633 (Thermo Fisher).

Statistics. Plasma levels of stress hormones were analyzed using a repeated measure two-way ANOVA with blood collection time point (0,10,30,60,90min) as the within-subjects variable, and optogenetic treatment as the between-subjects factor. Post hoc pairwise comparisons using Fisher's least significant difference were used when appropriate. Integrated hormone levels (i.e., AUC) were analyzed using an unpaired t-test. Avoidance latency data were analyzed with a repeated measures ANOVA with context and optogenetic treatment as factors. All main analyses were considered significant at $P<0.05$.

Results

Anatomical characterization of prefrontal – BST circuits

We initially sought to characterize the projection patterns from prefrontal subfields (infralimbic, IL; prelimbic, PL) to the BST using adeno-associated viral tracing and distinguish a subset of rostral prelimbic neurons that have been previously implicated in modulation of stress (Johnson et al., 2019) and avoidance (Diehl et al., 2018; Martínez-Rivera et al., 2022) from the well-characterized input stemming from the IL region (Vertes 2004). We microinjected green fluorescent protein (GFP)(IL) and mCherry (PL) expressing viral vectors (AAV5) under the CAMKIIα promoter into both IL and PL subfields in adult male rats to outline innervation patterns of BST (**FIG. 3.1**). Expression of viral vector injections were evaluated based on cytoarchitectonic parcellations of each region and adjacent cortical regions (Swanson 2004; Kretteck & Price, 1977; Vogt & Peters 1981; Radley et al., 2006; Van de Werd & Uylings, 2008). Prior work has shown that more rostral and ventrally lying areas of PL exhibit moderate to dense innervation of BST (Reynolds & Zahm 2005; Sesack et al., 1989; McDonald, Shammah-Lagnado, Shi, & Davis, 1999; Radley et al., 2006; 2013; Dong, Petrovich & Swanson), whereas more dorsal and caudal regions of PL exhibit sparse-minimal innervation of BST (Shin, Geerling & Loewy 2008; Vertes 2004). As such, we targeted injections in PL to produce expression in deep-layer glutamatergic projection neurons near the rostral end of the PL (rPL) subfield (~AP coordinates: +3.85mm, relative to bregma in the rat) (Johnson et al., 2019) (**FIG. 3.1**). Microinjections in IL were based on prior work outlining input from this region to BST (Shin, Geerling, & Loewy 2008; Vertes 2004). Evaluation of injection sites in both

regions revealed minimal overlap as for cases exhibiting the most rostral placement in PL, IL is not present (**FIG. 3.1A**). Due to the ventrally lying position of IL, however, microinjections into this area necessarily pass through the caudal PL, limiting specificity in this regard.

BST is a basal forebrain complex made up of at least 12-15 different subnuclei (for review see; Lebow & Chen, 2016; Giardino & Pomrenze 2021) which have typically been defined based on their spatial properties. While recent work has highlighted the limitations of this approach (Giardino and Pomrenze, 2021), inspection of GFP-IL and mCherry-rPL projections revealed distinct differences in innervation patterns of BST based on their spatial organization. As has been noted previously, injections in IL produced abundant labeling across most of the BST with dense innervation of medial and lateral groups of the anterior BST division (Vertes 2004) (**FIG. 3.1F, H, L.**) and posterior BST (**FIG. 3.1O**). Injections in the rPL, however, produced virtually no labeling in the medial group of the anterior BST, consistent with observations made by many other groups (Vertes 2004; McDonald, Shammah-Lagnado, Shi, & Davis, 1999; Radley et al., 2006; 2013; Dong, Petrovich & Swanson) (**FIG. 3.1E, H**). Rather, injections in the rPL produced innervation patterns of BST most consistent with targeting regions of BST at AP coordinates of -0.26mm to -0.46mm relative to bregma in the rat (**FIG. 3.1K**). This area generally corresponds to the anterolateral/anteroventral division (Dong, Petrovich, & Swanson 2001; Dong & Swanson 2004b; Dong & Swanson 2006a; Dong, Petrovich, Watts, & Swanson 2001), including subcommisural, fusiform and rhomboid subdivisions described by Swanson and colleagues. A similar pattern was previously characterized as the posterior division of the lateral BST (McDonald, Shammah-Lagnado, Shi, & Davis, 1999).

Indeed, near the accumbens transition zone (Heimer and Alheid, 1991) at the rostral end of BST moderate labeling was noted almost entirely restricted within the anterolateral/subcommisural subgroup (**FIG. 3.1E**), along with a substantial innervation of the neighboring ventral striatum. Progressing caudally, rPL fibers were again mostly absent from medial subregions dorsal to the anterior commissure (i.e., ad, oval, CC), but remained moderately dense within the anterolateral and anteroventral subdivisions (**FIG. 3.1K**) coursing medially from the internal capsule and descending ventro-caudally into the substantia innominata (SI).

To further substantiate the findings of our anterograde tracing experiments and characterize the distribution of BST projection neurons stemming from rPL, we microinjected the retrogradely transported AAV2-retro-GFP (Tervo et al., 2016) into the ventral aspect of BST and imaged GFP+ neurons across the prefrontal cortex (**FIG. 3.2**). In agreement with our anterograde tracing experiments, we found a paucity of labeling at caudal levels of PL despite substantial numbers of GFP+ neurons within the IL (**FIG. 3.2D**). At more rostral levels of PL (AP = +3.85mm - +4.85mm in the rat, relative to bregma) we found consistent labeling of GFP+ nuclei predominantly within deep layers (**FIG. 3.2D**). We noted an additional population of BST projecting nuclei within the medial orbital region (mOFC) (**FIG. 3.2D**) that continued rostrally in parallel with the rPL population; a projection which has been previously described in the primate (Fox et al., 2010). Additionally, we confirmed a similar pattern using more conventional retrograde tracer microinjections of Fluorogold (FG) in BST (**FIG. 3.3**).

We then used an intersectional trans-neuronal approach (Zingg et al., 2017) in combination with fluorescent in-situ hybridization (FISH) to identify the cellular phenotype

of BST neurons receiving input from rPL. To target post-synaptic BST neurons receiving input from rPL, we microinjected an AAV1 containing Cre that has trans-neuronal properties (Zingg et al., 2017) in rPL and a cre-dependent AAV expressing mCherry vector in BST (**FIG. 3.4A**). We noted restricted labeling of an isolated cell population within the ventral aspect of BST (**FIG. 3.4B-D**). We used a commercially available FISH procedure (RNAscope) for multi-fluorescent labeling of vGLUT2, GAD1, and mCherry target RNA probes. Inspection of fluorescent RNA labeling revealed extensive colocalization between mCherry and GAD1 fluorescent labels (**FIG. 3.4G-H**) and minimal overlap with vGLUT2 (**FIG. 3.4J**.) indicating most of the input stemming from the rPL region is directed toward GABAergic BST neurons within the avBST subgroup. Further analysis of the trans-neuronal network revealed largely preferential targets within the hypothalamus (**FIG. 3.5**). Indeed, the lateral hypothalamus (LH) and paraventricular hypothalamus (PVH) ($F_{6,19}$=9.21, p = 0.0005) (**FIG. 3.5 A-C**) exhibited greater levels of fluorescent density values as compared to a number of other regions. Bonferroni-corrected multiple comparisons indicated increases for LH and PVH fluorescent density values as compared to other regions exhibiting fluorescent values including the central amygdala (CeA) (LH: p = 0.0028; PVH: p = 0.01), midline thalamus (LH: p = 0.006; PVH: p = 0.02), vlPAG (LH: p = 0.006; PVH: p = 0.02), and parabrachial nucleus (LH: p = 0.02; PVH: p = 0.06). The ventral tegmental area (VTA) was also noted as an output region, although this was not significantly differentiated from any other region imaged.

rPL involvement in threat processing

To confirm the involvement of rPL in threat processing, we recorded neuronal ensembles in rPL during inhibitory avoidance training (IA) and testing (**FIG. 3.6A-B**). We first demonstrated that un-surgerized rats were able to discriminate between two contextually distinct IA chambers during an avoidance test 2 days following IA training (t_{19} = 3.3, p =0.004) (**FIG. 3.6C**). We then implanted a separate sample of rats (n=4) with a 16-wire microelectrode into rPL. For rats with microarray implants, on day 1, we recorded a 25 min pre-training session prior to rats being placed in the lit compartment of an inhibitory avoidance chamber modified for recording of neural activity. Upon entry into the adjacent darkened area, rats received a single inescapable footshock (0.8mA/1s) and were subsequently left in the chamber for an additional 5 minutes. Rats were then removed, and a further 25 minutes of recording commenced in the animal's homecage. 48hrs later (D3), neuronal recordings commenced during a 10 min avoidance test in the safe chamber (D3-safeCTX). Here we logged initial latency to cross into the adjacent darkened area. Rats were subsequently returned to their homecage and allowed a period of rest before being placed in the original training context (D3-Shock-CTX) for additional avoidance testing. As training and testing are single trial events, for analysis we turned to principal component analysis (PCA) to characterize patterns of neuronal responses and inspected field potential (FP) activity during each phase of experimentation. Neurons were manually sorted and further separated based on waveform characteristics to exclude putative interneurons. Neurons with a waveform half-peak width greater than 0.15 ms and peak-to-trough duration greater than 0.25 ms were used for further analysis (**FIG. 3.6D**) [average frequency: 5.72Hz, SEM: 0.36] (Emmons et al., 2017). Consistent

with a role for rPL in threat processing on D1, we observed the predominant components (PC1 and PC2) exhibited patterns consistent with an increased activity following footshock (**FIG. 3.6E**). We confirmed single-unit responses aligned with these components in a proportion of overall units isolated (**FIG. 3.6F-G**). Further, consistent with PC analyses and single unit data, inspection of FP activity during training also revealed significant overall increases in peak power-spectral density (PSD) values across theta (4-8Hz)(t_{15} = 3.17, p = 0.0064), alpha (8-12Hz)(t_{15} = 3.84, p = 0.0016)(FIG XX), and beta (12-30Hz)(t_{15} = 3.44, p = 0.0037)(**FIG. 3.6H**) oscillatory bands in the 300s following shock, as compared to the 300s prior. Lower-frequency delta activity (1-4Hz) was not different post-shock (t_{15} = 1.23, p = 0.24), as compared to pre-shock (**FIG. 3.6H**). These results suggest rPL is broadly mobilized in response to IA training.

Additional analyses on D3 during avoidance testing revealed distinct differences in rPL activity associated with latency to enter the adjacent darkened area that occurred as a function of chamber (**FIG. 3.7**). Interestingly, rPL activity appeared to be mobilized predominantly prior to entry into the adjacent darkened compartment specifically for D3-SafeCTX (**FIG. 3.7D**). This pattern was not evident D1 during training (**FIG. 3.7C**) or D3 testing in the original training context (**FIG. 3.7E**). An analysis of the area under the curve (AUC) prior to latency revealed a significant main effect of latency ($F_{2,107}$ = 4.54, p = .013), post hoc tests revealed this effect was largely driven by a significant increase in AUC values for D3-SafeCTX as compared to D1 (p = 0.005) and trending increase for D3-SafeCTX as compared to D3-ShockCTX (p = 0.039) (**FIG. 3.7F**). We then conducted an additional PC analysis for activity surrounding each latency event. PC analyses here indicated 3 predominant components (**FIG. 3.8A-C**) that accounted for 15 – 22% of the

variation in unit responses across all latency events (i.e., D1, D3-SafeCTX, D3-ShockCTX), including one component (i.e., PC3, **FIG. 3.8C**) that exhibited a similar pattern to that observed in averaged Z-scored values for D3-SafeCTX (**FIG. 3.7D**). Further PC analyses for latency values revealed increased PC coefficient values for unit responses associated with D3-SafeCTX in relation to PC3 (**FIG. 3.8G**). A repeated measures ANOVA confirmed a main effect of Latency ($F_{2,107}$ = 3.272, p = .042), and PCA coefficient ($F_{2,214}$ = 6.37, p = .002) (**FIG. 3.8D-H**), with PC3 values significantly greater for D3-SafeCTX as compared to D3-ShockCTX (p = 0.023) and trending increase for D3-SafeCTX as compared to D1 (p = 0.06). Moreover, we noted a higher proportion of units from D3-SafeCTX loading on the upper 25% of PC3 coefficient values ($\chi^2_{(2)}$ =7.01, p = .030) (**FIG. 3.8H**) as compared to D1 or D3-Shock-CTX. We did not observe any differences for units loading on PC1 (($\chi^2_{(2)}$ =1.06, p = .59), or PC2 ($\chi^2_{(2)}$ =4.19, p = .12) indicating these were consistent across training and testing regardless of chamber.

Inspection of FP activity across each latency event also revealed a unique activity-related signature associated with D3-SafeCTX with regard to increased average PSD values in the theta oscillatory (4-8Hz) band immediately prior to latency to enter (**FIG. 3.8I-L**). Specifically, a repeated measures ANOVA indicated a main effect of Latency event ($F_{2,30}$ = 7.31, p = 0.003) on average theta PSD values. Of note, D3-SafeCTX showed increased theta PSD values compared to both D1 (p = 0.007) and D3-Shock-CTX (p = 0.01) (**FIG. 3.8L**). No other frequency band (i.e., delta, alpha, beta) exhibited a similar pattern prior to latency. These results indicated that during avoidance testing, rPL activity may be mobilized distinctly prior to latency to enter the adjacent darkened area of the “safe” context, suggesting a potential role in differentiating this environment from

previous experiences and/or preventing avoidance to an environment that has not been explicitly paired with an aversive event. That this pattern of activity also appeared to be coupled to increased theta oscillations is consistent with prior work demonstrating increased mPFC theta in animals that differentiated between aversiveness and safety in a cued-fear conditioning task (Likhtik et al., 2014; Stujenske, Likhtik, Topiwala, Gordon 2014).

BST involvement in threat processing

To then determine the involvement of BST in IA, we used fiber photometry to monitor calcium-bound fluorescent changes during footshock administration in the IA task. Here, we microinjected AAV-GCaMP8s in BST and positioned an optical fiber immediately dorsal to the right BST (**FIG. 3.9**). Three weeks after viral injection/optic implant, rats underwent standard (IA) training (Cahill & McGaugh, 1998; Huff et al., 2013). Upon entry into the darkened compartment of an IA chamber rats received a single 0.8mA/1s footshock. Calcium bound fluorescence was monitored prior to and following footshock. Entry into the darkened compartment on day 1 (D1) was not associated with any changes in calcium-mediated fluorescence in the BST (**FIG. 3.9D**), similar to that observed in rPL previously. However, footshock training rapidly increased BST activity, as demonstrated by peak dF/F (Z) values post footshock as compared to pre footshock ($t_4 = 3.35$, $p = 0.03$) (**FIG. 3.9C**), consistent with a role for this region in threat processing. 48hrs later we tested the involvement of BST in latency to avoid a novel chamber. We focused on the “safe” context here, as our recording data with rPL indicated a distinct pattern of activity during this testing period. Rats were placed in the lit compartment of a

safe context and BST activity was recorded for 10 minutes. We again logged initial latency to cross into the darkened compartment for peri-event analysis of calcium activity. Similar to our recording data of rPL activity, we noted a significant increase in BST activity immediately prior to entry into the darkened compartment of the safe chamber on D3 that was not present on D1 in the original training context as demonstrated by a repeated measures ANOVA for dF/F (Z) area under the curve ($F_{3,12}$ = 6.38, p = 0.008) (**FIG. 3.9E-F**). Specifically, whereas BST activity prior to latency on D1 was no different than D1 post latency (p = 0.64), activity on D3 prior to latency was significantly greater than D3 post latency (p < 0.001). These results were consistent with a mixed effects model of BST activity across time that indicated a significant main effect of time ($F_{81,405}$ = 2.01, p <0.0001) and significant time*latency interaction ($F_{81,241}$ = 1.72, p = 0.001). Overall, these results indicated that BST is mobilized in response to footshock, and prior to latency to cross into a safe chamber 48hrs later in a similar manner to that which was observed from recording of rPL neuronal activity. We additionally conducted a simple linear regression analysis for dF/F (Z) AUC and latency to enter Safe-CTX to assess the relationship between BST activity in the 20s prior to latency, and total avoidance time and noted an overall significant regression [(R^2 = 0.91), $F_{1,3}$ = 28.66, p = 0.013] (**FIG. 3.9G**). It was found that pre-latency dF/F (Z) AUC was significantly associated with latency time (s). Interestingly, a greater dF/F (Z) AUC value was associated with increased avoidance latency times suggesting a greater mobilization of BST was necessary to encourage latency to enter for animals that had longer avoidance latencies. Note that the window of interest for BST activity was limited to the 20s prior to latency, and that the average latency value for D3-SafeCTX was 58.25s (SEM = 32.71s). As such, the data would not

be consistent with an interpretation that BST activity was promoting avoidance as the increase in BST activity occurred immediately prior to latency regardless of total avoidance time.

We also reasoned this change in activity could have also been associated with generic changes in environment and the transition from one context to another, or other motivational properties associated with dimly lit areas and so conducted an additional experiment where rats were placed in a three-chamber apparatus with two contextually distinct components and a middle area separating the two (**FIG. 3.9H-K**). Here we logged transitions between each compartment. Analysis of changes in fluorescence revealed no similar differences in BST activity as a function of context transitions.

rPL-BST projection in preventing context fear generalization

As our recording data demonstrated that both regions were mobilized in response to footshock training, indicating an involvement in the initial encoding and/or consolidation of the training event, and our previously published work (Lingg et al., 2020) suggested the involvement of BST during the posttraining consolidation period, we focused our remaining experiments on this posttraining period for intervention. We first tested whether posttraining activity in the rPL-BST projection was necessary to prevent generalization to a novel context. To that end, we used an intersectional optogenetic approach to photoinhibit rPL-BST projection fibers immediately after IA training for 10 minutes (**FIG. 3.10**). We confirmed in vivo the efficacy of this viral approach, wherein rats were implanted with a 16-wire microelectrode containing optic fiber (termed: “optrode) in BST and received 10 minutes of 561nm laser light. Photoinhibition of rPL fibers in BST reduced

neuronal activity (**FIG. 3.10C**). We then microinjected a separate group of rats with the same viral preparation and implanted bilateral optic fibers above BST. On the training day, rats were placed in an IA chamber and upon entry into the darkened compartment received a single footshock (0.8mA/1s). Rats were then placed back into their homecage and received 10 minutes of rPL-BST photoinhibition with constant 561nm laser light. Blood samples were taken prior to and following training to measure circulating corticosterone levels as well. Rats were then brought back to assess avoidance in both the training context and the novel contextually modified chamber 2 days later. As expected, based on our prior work (Johnson et al., 2019), an RIA for CORT revealed an augmented stress hormone response for rPL-BST^{Halo} rats, as compared to rPL-BST^{mCherry} controls ($F_{1,23}$ = 4.91, p = 0.037) on the training day (**FIG. 3.10D**). Integrated area under the curve analysis of CORT values confirmed a significant overall increase in CORT for rPL-BST^{Halo} rats, as compared to rPL-BST^{mCherry} (t_{23} = 2.32, p = 0.03) (**FIG. 3.10E**). Moreover, on D3 posttraining, a repeated measures ANOVA revealed a significant main effect of context ($F_{1,23}$ = 17.61, p <0.001) and significant virus*context interaction ($F_{1,23}$ = 5.41, p = 0.029) for latency (**FIG. 3.10F**). Specifically, whereas rPL-BST^{mCherry} rats displayed low avoidance to the novel context and high avoidance to the training context (**FIG. 3.10F**) (p < 0.001), rPL-BST^{Halo} rats displayed similarly high levels of avoidance to both contexts (**FIG. 3.10F**) (p = 0.17). Avoidance to the safe context was also significantly higher in rPL-BST^{Halo} rats than rPL-BST^{mcherry} (p = 0.035). Assessment of a discrimination index (DI; A/(A+B)) further supported these findings, as rPL-BST^{Halo} rats showed significantly reduced DI values (t_{23} = 2.43, p = 0.023) (**FIG. 3.10G**) compared to rPL-BST^{mCherry}. These results indicated that posttraining inactivation of rPL-BST augmented

corticosterone responses and produced later generalization in the form of increased avoidance in a novel chamber.

As a wealth of research support the notion that posttraining increases in CORT can produce generalization (Lesuis et al., 2021; Kaouane et al., 2012; Roozendaal & Mirone 2020; Kolodziejczyk & Fendt 2020; dos Santos Corrêa et al., 2021; Bahtiyar et al., 2020), we sought to determine whether the increased posttraining CORT levels seen here were responsible for producing the observed generalized response. We confirmed that posttraining systemic injections of CORT (3mg/kg) do indeed enhance avoidance, and promote generalization, 48hrs later in the inhibitory avoidance paradigm as indicated by a main effect of CORT injection ($F_{1,11}$ = 7.11, p = 0.02) on avoidance latency (**FIG. 3.11B**), in line with what others have shown. To then address the possibility that generalization produced by rPL-BST posttraining photoinhibition was dependent upon changes in CORT, we carried out a follow-up experiment repeating the same design (as shown in **FIG. 3.8**), except that we blocked the training-induced increase in CORT with adrenalectomy (ADX) (**FIG. 3.9**). We performed ADX two weeks prior to training and administered CORT in the drinking water (25mg/dl) to account for diurnal variations in plasma CORT levels. This procedure maintains a circadian CORT rhythmicity (**FIG. 3.9D**; Gourley et al., 2012) while blocking any stress-induced increases (**FIG. 3.9E**). We then footshock trained rats (0.8mA/1s), and again administered a 10-minute posttraining photoinhibition of rPL-BST. Here, we again noted a significant main effect of context ($F_{1,21}$ = 9.26, p = 0.006) and significant context*virus interaction ($F_{2,21}$ = 3.88, p = 0.037). Specifically, rPL-BST$^{mCherry\text{-}Sham}$ rats displayed high avoidance to the training context and low avoidance to the novel context 48hrs after training (**FIG. 3.9B**) (p = 0.003). rPL-

BST$^{mCherry\text{-}ADX}$ rats also displayed high avoidance to the training context and low avoidance to the novel context (**FIG. 3.9B**), although had more difficulty distinguishing between contexts (p = 0.10). We noted no significant differences in avoidance between mCherry-ADX and mCherry-Sham groups (**FIG. 3.9B**) in either the training context (p = 0.16) or novel context (p = 0.98), although average latencies for the training context were generally lower in the mCherry-ADX rats, as compared to the mCherry-Sham [Mean mCherry-ADX = 141s; Mean mCherry-Sham = 295s], which likely contributed to the decreased difference between novel and training context latencies for mCherry-ADX animals. In contrast to our control groups, however, rPL-BST$^{Halo\text{-}ADX}$ rats displayed high avoidance to both chambers (**FIG. 3.9B**), similar to the previous inhibitory experiment (**FIG. 3.8**). While avoidance for rPL-BST$^{Halo\text{-}ADX}$ in the training context was no different than either rPL-BST$^{mcherry\text{-}sham}$ (p = 0.55) or rPL-BST$^{mcherry\text{-}ADX}$ (p = 0.35), avoidance for the novel context was significantly higher than both control groups (p = 0.004, p = 0.002, respectively). Moreover, rPL-BST$^{Halo\text{-}ADX}$ rats were also unable to discriminate between the two contexts, as avoidance was similar for both (p = 0.83) We confirmed this result by inspection of discrimination index values, which also indicated a reduced discrimination for rPL-BST$^{Halo\text{-}ADX}$ as compared to controls (**FIG. 3.9C**) ($F_{2,21}$ = 10.63, p <0.001). Post hoc test revealed, rPL-BST$^{Halo\text{-}ADX}$ had significantly lower DI values than both rPL-BST$^{mcherry\text{-}sham}$ (p <0.001) and rPL-BST$^{mcherry\text{-}ADX}$ (p = 0.002), while control groups were no different from each other (p = 0.27). These results suggest that taking the rPL-BST projection offline immediately following an aversive event produces an augmented generalization via a glucocorticoid-independent mechanism. We also confirmed a successful ADX procedure in this group of rats by removing CORT in the

drinking water after completion of avoidance testing and then administering a 30 min restraint test followed by blood collection (**FIG. 3.9E**). We noted a significant main effect of blood sample ($F_{2,44}$ = 104.13, p <0.001) and significant sample*ADX interaction ($F_{2,44}$ = 114.96, p <0.001). Here, despite ADX and Sham animals showing similar AM (p = .22) and PM (p = .24) values, with PM values being greater than AM (p < 0.001) (**FIG. 3.9D**), Sham rats mounted a robust CORT response following restraint whereas ADX rats did not (p <0.001) (**FIG. 3.9E**). These results are consistent with the interpretation that CORT in the drinking water allowed for a diurnal circadian rhythm for ADX rats that was no different than sham animals, but ADX prevented stress-induced increases in CORT. Overall, both experiments utilizing posttraining inhibition of the rPL-BST pathway specifically influenced avoidance to the novel chamber 48hrs later and had no effect on avoidance to the training chamber, regardless of adrenocortical status, indicating that while the rPL-BST pathway is necessary for learning about specific features of the training experience that may be utilized to differentiate an aversive event from a novel one, this pathway does not appear to influence the overall strength of avoidance to the training context.

rPL-BST projection mediates disambiguation of a pre-exposed neutral chamber from a shock-associated chamber

To then determine whether the rPL-BST projection could prevent context fear generalization, we adapted prior work with the inhibitory avoidance paradigm (Atucha & Roozendaal, 2015; Atucha et al., 2017) to allow us to shift rodent behavioral responses toward context generalization. We used context pre-exposure, wherein a rat is placed in

a neutral/safe inhibitory avoidance chamber for a short period, prior to footshock training in a separate contextually distinct inhibitory avoidance chamber (Cai et al., 2016; Huff, Wright-Hardesty, Higgins, Matus-Amat, & Rudy 2005) to facilitate context generalization (**FIG. 3.10**). Enhanced context generalization using the pre-exposure model has been suggested to result from pattern completion processes within the hippocampus (O'Reilly, Randall, & Rudy 2001) and has been reported in both rats (Atucha et al., 2017) and mice (Keiser et al., 2017). To assess the involvement of the rPL-BST pathway in mediating context generalization, we microinjected AAV2-retro-Cre into the ventral aspect of BST, and then either an AAV-DIO-mCherry or AAV-DIO-ChR2(E123A)-mCherry in rPL. Rats then had fiber optics positioned bilaterally above BST. Histological verification of mCherry+/GFP+ nuclei in prefrontal cortex of all rats indicated a predominance of overlap at rostral levels, and not caudal levels of mPFC (**FIG. 3.10C**) as expected. A subset rats received viral preparation and an optrode implant into BST. We then optically evoked excitatory neuronal responses in each region with 473nm laser light (20Hz, 5ms pulse width) across a 10-minute period. Photo-stimulation of rPL-BST fibers in BST with ChR2 consistently evoked excitatory short latency neuronal responses (**FIG. 3.10G**). Optically evoked excitatory BST responses were observed <5ms after light pulses, supporting our prior trans-neuronal experiments suggesting rPL-BST connections are mono-synaptic (**FIG. 3.3**). To assess stress hormonal fluctuations during inhibitory avoidance training, we again fitted rats with indwelling jugular catheters two days prior to context pre-exposure and footshock training. During training, rats were placed in an inhibitory avoidance chamber and allowed to explore the entire chamber for one minute. Rats were then immediately transferred to a contextually modified inhibitory avoidance chamber,

and upon entry into the darkened compartment received an inescapable high intensity (0.8mA/2s) footshock (**FIG. 3.10**). We used a higher intensity shock here to facilitate the likelihood that rats would generalize during avoidance testing, as has been reported elsewhere (dos Santos Corrêa et al., 2019; Kaouane et al., 2012). The rat was then returned to its home cage and posttraining photostimulation was carried out for 10 minutes. Blood samples were collected at varying intervals immediately prior to and following training to characterize stress hormonal output. Avoidance for each chamber was assessed 2- and 28-days following training.

On D1, rats readily enter the darkened compartment of each chamber (**FIG. 3.10I**) regardless of viral treatment. However, on D3 rPL-BST^{mCherry} control rats exhibit similarly high avoidance to both the neutral pre-exposed chamber and the contextually distinct training chamber (**FIG. 3.10I**) indicating enhanced generalization between chambers. Interestingly, rPL-BST^{ChR2} rats continued to have low avoidance to the neutral pre-exposed chamber (**FIG. 3.10I**), similar to D1, and yet had high avoidance levels for the aversive chamber indicating an enhanced discrimination between contexts. rPL-BST^{Chr2} rats displayed a similar pattern, albeit to a lesser degree, 28 days later (**FIG. 3.10I**). A repeated measures ANOVA supported these observations, as we noted a main effect of Day ($F_{5,105}$ = 16.18, p <0.0001) and a significant Day*Virus interaction ($F_{5,105}$ = 2.46, p = 0.038). Whereas rPL-BST^{mcherry} rats did not exhibit differences in avoidance latency on D3 between contexts (p = 0.1), rPL-BST^{ChR2} rats exhibited significantly lower avoidance for the pre-exposed neutral chamber (p < 0.001), as compared to the shock chamber. 28 days later, rPL-BST^{ChR2} rats continued to have significantly lower avoidance for the pre-exposed chamber (p = .037), while rPL-BST^{mcherry} rats exhibited similarly high levels of

avoidance to both chambers (p = .74). We calculated a discrimination index for each day and confirmed an increased discrimination at D3 for rPL-BST^{ChR2} rats, as compared to rPL-BST^{mCherry} rats (t_{21} = 2.37, p = .028) (**FIG. 3.10J**). D28 DI values were not different between groups (t_{21} = 1.53, p = 0.14), which appeared to be perhaps related to the overall decreases in avoidance for the shock chamber between D3 and D28 for rPL-BST^{Chr2} rats (p = 0.03). Avoidance for the shock chamber was not different between rPL-BST^{mcherry} and rPL-BST^{Chr2} rats at either D3 (p = 0.55) or D28 (p = 0.69). We noted both groups exhibited a robust increase in CORT responses posttraining ($F_{5,105}$ = 48.91, p < 0.001) (**FIG. 3.10H**) but observed no differences between groups as a function of viral preparation ($F_{1,21}$ = 0.002, p = .964). We then confirmed these results by repeating the above experiment using an intersectional chemogenetic strategy (**FIG. 3.11**), which produced broadly the same behavioral pattern at D3, again without affecting HPA status. As such, posttraining activation of rPL-BST did not appear to influence the overall strength of avoidance for the shock context, but rather mediated the disambiguation between features of the pre-exposed neutral context from the subsequent shock-training context and did so without altering CORT reactivity. D28 testing from our optogenetic experiment also suggested this effect persisted for at least 28 days, although this may have been indirectly the result of the enhanced discrimination exhibited by rPL-BST^{ChR2} rats on D3 and subsequent reconsolidation processes (Alberini & Ledoux 2013), rather than directly a product of posttraining photostimulation on D1.

Posttraining rPL-vlPAG photoexcitation does not prevent context generalization

We then sought to address the specificity of these results by targeting an additional projection stemming from the rPL region. As has been demonstrated previously (Vertes 2004; Hoover & Vertes 2011), rPL has dense projections throughout the brain and targets a variety of structures involved in the processing of threat-related information, including the vlPAG. Indeed, we noted a degree of collateralization in our dual-viral approach between rPL-BST and rPL-vlPAG (**FIG. 3.12A**) and further demonstrated a small population of dual-projecting nuclei within rPL (**FIG. 3.12B**) indicating our experiments using excitatory viral strategies may have involved activation of this projection via antidromic stimulation in the case of our optogenetic targeting, or as a collateral activation in our chemogenetic manipulation resultant from systemic CNO administration. To address the possibility that collateral activation was driving the enhanced discrimination, we injected either AAV-YFP or AAV-ChR2 into rPL and positioned bilateral optic fibers above vlPAG (**FIG. 3.12C**). We confirmed in vivo excitation of rPL-vlPAG^{ChR2} with 473nm laser light increased activity in vlPAG neurons (**FIG. 3.12E**). We then trained rats on the pre-exposure model, and stimulated ChR2 expressing rPL fibers in vlPAG for 10 minutes posttraining. On D3 we noted rPL-vlPAG^{YFP} rats had difficulty distinguishing between the neutral pre-exposed chamber and the training chamber (**FIG. 3.12F**), as expected based on our other experiments. Importantly, rPL-vlPAG^{ChR2} rats also displayed an inability to distinguish between the two chambers that was no different than their control counterparts (**FIG. 3.12F**). Indeed, a repeated measures ANOVA demonstrated no effect of either context ($F_{1,16}$ = 3.67, p = 0.14), viral preparation ($F_{1,16}$ = 0.03, p = 0.86) or interaction ($F_{1,16}$ = 0.20, p = 0.65). We confirmed no difference in discrimination index values between

groups (**FIG. 3.12G**; $t_{16} = 0.47$, $p = 0.65$). Taken together with the previous results, these data suggest the enhanced discrimination produced by posttraining rPL-BST photoexcitation is not likely a result of collateral excitation with rPL-vlPAG.

Discussion

Our results demonstrate, using single-unit recordings, fiber photometry, and optogenetic manipulations, aversive processing in the rPL and BST during the immediate aftermath of an event contribute to long-term behavioral expression of generalized avoidance. Moreover, our results indicate the rPL-BST pathway is both necessary and sufficient for preventing context fear generalization independent of associated changes in adrenocortical status. Single-unit and fiber photometry data showed IA training robustly mobilized activity in both rPL and BST, respectively. Optogenetic rPL-BST inhibition for 10 min after IA training increased corticosterone responses during the posttraining period and enhanced avoidance to a novel context when tested 2 days later. Blockade of stress-induced increases in corticosterone using adrenalectomy were unable to prevent the enhanced avoidance to the novel context, indicating this effect was not mediated via HPA activation. Posttraining optogenetic and chemogenetic stimulation of rPL-BST was sufficient to prevent generalization to a neutral pre-exposed chamber. We also noted a unique activity related signature for both rPL and BST that was associated with an increase prior to entry into an adjacent darkened area in a novel chamber during testing that was coupled with increased theta power in rPL suggesting these structures contribute not only to the initial processing of an aversive event, but during avoidance testing to

distinguish the novel area from the previous aversive area or prevent inappropriate avoidance. Together, these results reveal a role for the rPL-BST pathway in modulating posttraining consolidation processes that ultimately contribute to the long-term expression of fear generalization.

mPFC, BST, and fear discrimination

Prior work examining the medial prefrontal cortex in threat processing have demonstrated involvement in responding to fear (Sotres-Bayon & Quirk 2010; Rozeske et al., 2018; Likhtik et al., 2014; Sangha, Diehl, Bergstrom, & Drew 2020), however this work has largely focused on the role of prefrontal regions in the expression of fear and discrimination. mPFC activity is associated with the inhibition of fear to an auditory CS- (Likhtik et al., 2014), and pre-training lesions of mPFC prevent context discrimination (Antoniadis & McDonald 2006). More recently, Rozeske and colleagues (Rozeske et al., 2018) demonstrated recruitment of prelimbic PFC neuronal ensembles during the transition between fearful and non-fearful contexts. Activation of a subset of this neuronal population that projected to the vlPAG was necessary to prevent generalization to a non-fearful context, and moreover this pathway was sufficient to promote discrimination between similarly fearful contexts.

Prior anatomical work has shown vlPAG projecting neurons in the prelimbic region are localized within more rostral areas (Vertes 2004; Floyd, Price, Ferry, Keay, & Bandler 2000); an area we have previously demonstrated projects to the BST and is involved in inhibiting passive coping responses (Johnson et al., 2019). Work carried out by Martínez-Rivera et al., (2022) has also demonstrated this rostral prelimbic area is associated with

decreasing persistent avoidance during extinction training, an effect consistent with previously published work from this same group demonstrating activation of the rPL subregion decreases avoidance during retention in a platform mediated avoidance task (Diehl et al., 2018; 2020). Our experiments generally support these findings and indicate the rPL-BST pathway as being important for mediating posttraining consolidation processes that contribute to future generalization. Our *in vivo* recording data demonstrated an rPL neuronal ensemble that is robustly mobilized during footshock training, and a predominance of rPL activity during avoidance testing in a novel context is explained by an increased rPL activity and associated increased theta power prior to entry into an adjacent darkened area suggesting during testing this region may be mobilized to prevent inappropriate avoidance. Moreover, posttraining optogenetic excitation and inhibition of rPL-BST were able to prevent and augment future generalization, respectively.

Interestingly, our optogenetic targeting of the rPL-vlPAG pathway immediately following IA training did not influence future generalization. While our optogenetic experiments did not explicitly target IA memory expression, our in vivo data demonstrate rPL is mobilized during both encoding/consolidation and expression suggesting it is possible that rPL mobilizes distinct projections during different phases of learning, and prefrontal innervation of vlPAG, or other regions, may be more directly involved in mediating the expression of discrimination. Indeed, previous work has shown increased theta coupling between the prefrontal cortex and basolateral amygdala during cued-fear discrimination, suggesting a role for this pathway in mediating the expression of discrimination and preventing inappropriate fear responding (Likhtik et al., 2014). Whether

posttraining optogenetic modulation of the rPL-BST pathway disrupts either rPL or BST activity during retention will be a necessary question for the future, although we have previously shown that delayed optogenetic modulation of BST (+3hrs after training) was unable to alter IA memory consolidation (Lingg et al., 2020), suggesting there is a period immediately after training that is uniquely susceptible to intervention.

Several studies have shown involvement of the BST in threat processing, including IA training (Liang, Chen, & Chen 2001; Liang & McGaugh 1983a; Liang & McGaugh 1983b; Liu, Chen, & Liang 2009; Liu & Liang 2009; Lingg et al., 2020; Bruzsik et al., 2021), context and auditory fear conditioning (Goode, Ressler, Acca, Miles, & Maren 2019; Goode & Maren 2017; Ressler, Goode, Evemy, & Maren 2020; Bjorni et al., 2020), as well as mediating coping responses (Johnson et al., 2016; 2018; Radley & Johnson 2018) and anxiety-related behaviors (Glangetas et al., 2017Giardino et al., 2018; Jennings et al., 2013a; Pomrenze et al., 2019). Work has highlighted the extensive heterogeneity of BST functions which appear to largely depend on subregion and neurochemical phenotype (Giardino & Pomrenze, 2021). Indeed, whereas optogenetic or chemogenetic activation of more dorsal regions of BST, such as the oval BST (Kim et al., 2013a), are generally implicated in anxiogenic responses (Giardino et al., 2018; Jennings et al., 2013a; Pomrenze et al., 2019) or promoting aversion (Yu et al., 2021), more ventral and posterior regions have been implicated in preventing threat-related behaviors or in producing anxiolytic responses (Henckens et al., 2017), along with gating of the HPA axis thereby limiting stress-related neuroendocrine output (Johnson et al., 2016; 2019; Radley, Gosselink & Sawchenko 2006). Overall, a prevailing theme for involvement of BST in threat processing is an association mediating uncertainty (Goode & Maren, 2017) or

integration of information with a negative valence (Lebow & Chen, 2016), which is likely reflective of the functional heterogeneity displayed by BST subregions; flexibility in responding to threats requires the capacity to switch between promoting and inhibiting fear-related behavior depending on environmental contingencies or threat predictability.

One critical component of our findings here was that posttraining modulation of rPL-BST activity did not alter avoidance responses to the original training context, suggesting this pathway, and/or the subset of BST neurons receiving input from rPL, is uniquely situated to mediate how aversive experiences may relate to novel situations. Although contrasted to the effects seen here, prior work has suggested a similar involvement of BST in selectivity of conditioned responding (Duvarci, Bauer, & Paré 2009). Specifically, global BST (i.e., encompassing dorsal and ventral components) pre-training lesions prevented inappropriate avoidance to a CS-. More selective targeting has shown posttraining blockade of DR2 receptors in the oval BST impaired discrimination between a CS+ and CS- (de Brundel et al., 2016), whereas posttraining chemogenetic excitation of somatostatin neurons in the BST promoted context fear generalization (Bruzsik et al., 2021). Separately, optogenetic activation of the anteroventral BST or CRFR2+ neurons in the posterior BST have been shown to prevent context fear memory altogether (Lingg et al., 2020; Henckens et al., 2017). These contrasting results likely reflect the complexity of processing in BST, as different BST subregions or peptidergic subtypes, are likely recruited in distinct manners to integrate aversive information and promote adaptation. While our work suggests rPL largely targets GAD1 expressing neurons in the ventral BST, GAD1 expressing BST neurons broadly encompasses a variety of peptidergic subtypes (Giardino & Pomrenze 2021), suggesting the possibility

for further heterogeneity. Further work will be necessary to disentangle the specific BST GABAergic subtypes that interact with descending prefrontal innervation.

That the time-course of HPA-related hormonal induction occurs over a period of several minutes, and a substantial body of work support HPA-related hormonal processes in mediating memory consolidation (Li & Sawchenko 1998; Hui et al., 2004; Roozendaal, McEwen, & Chattarji 2009; Roozendaal, Bohus & McGaugh 1996; Cahill & McGaugh 1998), BST regions that project to HPA effector neurons in the PVH are uniquely situated to mediate posttraining consolidation processes. Prior anatomical work has suggested the predominance of BST input to PVH is found within ventral (i.e., fusiform, anterolateral, anteroventral, rhomboid nucleus) (Dong & Swanson 2006a; Dong & Swanson 2006b; Dong, Petrovich, Watts, & Swanson 2001) and posterior regions (i.e., principal division) (Dong & Swanson 2004a). Our anatomical work and fiber photometry data endorse the notion that the ventral BST is robustly mobilized during IA training, and rPL projects to an isolated population of ventral BST neurons that in turn projects to PVH. Here, posttraining photoinactivation of the rPL-BST pathway also enhanced CORT responses along with the increased generalization confirming a role for rPL-BST in mediating HPA responding, likely via the disynaptic connection with PVH described elsewhere (Johnson et al., 2019; Radley 2012; Radley & Sawchenko 2015; Radley, Gosselink, & Sawchenko 2006; Herman et al., 2003; Spencer, Buller & Day 2005). That the observed generalization produced by rPL-BST photoinactivation was not dependent upon this increased CORT response suggest modulation of the HPA axis is conducted in parallel to an as yet unspecified mechanism that more directly contributes to processing of the training event.

Glucocorticoids and fear generalization

It is well established that the glucocorticoid hormone, corticosterone (CORT), is involved in mediating memory consolidation for emotionally arousing stimuli (for further review see: Roozendaal, McEwen, & Chattarji 2009; McGaugh & Roozendaal 2002; McGaugh 2000). Posttraining administration of CORT, or dexamethasone (i.e., a synthetic glucocorticoid), enhance long-term memory for training experiences that are emotionally arousing, including inhibitory avoidance (Flood et al., 1978; Kovács, Telegdy Lissák 1977; Roozendaal & McGaugh 1996), contextual and auditory fear conditioning (Sandi & Pinelo-Nava 2007), as well as spatial and novel-object recognition (Sandi et al., 1997). Actions of CORT during the posttraining period have been reported to predominantly activate the Type II glucocorticoid receptor (i.e., GR) (Finsterwald & Alberini 2014; Oitzl, & de Kloet 1992) within the BLA, hippocampus, and mPFC, as local administration of a GR agonist into either of these regions enhances memory consolidation for many types of stressful experiences (Barsegyan et al., 2019; Roozendaal et al., 1999). These actions critically depend upon noradrenergic signaling in the BLA, and the functional network connectivity between the BLA and other regions (Roozendaal et al., 2006). Indeed, several studies have demonstrated that blockade of noradrenergic signaling (Barsegyan et al., 2014; Hatfield & McGaugh 1999), or functional inactivation of the BLA impair consolidation or prevent the memory enhancing effects of CORT. In general, these results position posttraining CORT administration as sufficient for enhancing memory strength.

More recently, interest has been directed to resolving the role of CORT not only in modulating memory strength, but rather mediating the balance between memory

specificity and generalization (Roozendaal & Mirone 2020; Bahtiyar et al., 2020). Indeed, it has been reported that posttraining systemic CORT administration enhances generalization to a novel environment (Kolodziejczyk & Fendt 2020; Roozendaal & Mirone 2020; Lesuis et al., 2021; dos Santos Corrêa et al., 2019) or cue (Kaouane et al., 2012), and this is associated with alterations in both amygdala and hippocampal activity (Kaouane et al., 2012). Our results using systemic posttraining CORT administration support these findings. Specifically, posttraining administration of CORT enhanced generalization to a novel context, suggesting that CORT functions as sufficient to enhance generalization. Of note, prior work has suggested memory accuracy is not mediated by fluctuations in CORT but may rather be linked more closely with noradrenergic signaling (Bahtiyar et al., 2020; Seo et al., 2021).

Here, blockade of stress-induced elevations in CORT with ADX was also unable to prevent generalization produced by rPL-BST pathway inactivation. These results were surprising as our prior work has shown that posttraining photoinhibition of the anteroventral subdivision of BST results in an augmented HPA profile that enhances memory consolidation in a glucocorticoid-dependent manner (Lingg et al., 2020). Further, while previous reports, including our prior work, indicate posttraining increases in CORT are sufficient to enhance memory strength for IA training, the increase in CORT produced by posttraining rPL-BST photoinhibition observed here did not produce similar effects for the shock-context. Indeed, avoidance for the shock-context was similar for all groups regardless of viral manipulation. Our lab has previously demonstrated BST modulation of HPA-related activity functions, in part, to integrate multiple HPA-inhibitory influences stemming from mPFC and the hippocampal formation (HF) (Radley & Sawchenko 2011)

that may account for this discrepancy. Specifically, BST receives HPA-related negative feedback information from mPFC (Prelimbic Cortex) and the ventral subiculum, among other sources. Dual lesions of the mPFC and ventral subiculum result in additive enhancements of HPA responding following stress, as compared to lesions of one area alone (Radley & Sawchenko 2011), and this additive enhancement is similar in magnitude as to that observed following a single lesion of avBST. As such, removal of a single source of glutamatergic input to BST may not be sufficient to generate the endogenous level of CORT necessary to modulate consolidation processes in a manner that results in memory strengthening.

Comparison with previous work

Our finding that the rPL-BST pathway can prevent generalization to contexts that share similar features, or are temporally linked, is reminiscent of a recent study showing the IL-BST pathway constrains fear responding to a partially reinforced CS (Glover et al., 2020). Despite targeting memory retrieval in their study, these results appear largely consistent with that demonstrated here. Although much work has demonstrated functional differences between infralimbic and prelimbic regions in mediating threat learning and retention (Corcoran & Quirk 2007; Sangha, Diehl, Bergstrom & Drew 2020; Capuzzo & Floresco 2020; Sierra-Mercado, Padilla-Coreano, Quirk 2011; Alexandra Kredlow et al., 2022), an intriguing possibility here is that projections to the BST from rPL and IL are mobilized in concert to mediate potentially diverging components of an organism's response to threat to ultimately promote a similar outcome (i.e. restraining fear-related behavior to less threat-predictive stimuli). One example here may be the differential

recruitment of neuroendocrine or pre-autonomic effector nuclei in the PVH that has been shown to be associated with PL and IL, respectively (Radley, Arias & Sawchenko 2006). Specifically, lesions of PL prior to stress produce augment HPA responses whereas pre-stress lesions of IL do not (IL). Rather, pre-stress lesions of IL produce a robust recruitment of pre-autonomic neuronal activity in PVH (Radley, Arias & Sawchenko 2006). As both prefrontal regions are connected with PVH via the BST (Radley, Gosselink, Sawchenko 2006; Herman, Ostrander, Mueller, Figueiredo 2005; Hurley, Herbet, Moga, Saper 1991; Glover et al., 2020), global prefrontal innervation of BST may be recruited during exposure to threat to differentially mediate the neuroendocrine and autonomic processes downstream via PVH. Indeed, optogenetic excitation of the IL has previously been shown to reduce component measurements of autonomic reactivity, including mean arterial pressure and heart rate (Wallace, Schaeuble, Pace, Schackmuth, Hentges, Chicco, & Myers 2021). Further studies should explore the exact nature of prefrontal circuits in mediating neuroendocrine and autonomic activity and the relation to fear discrimination as abnormal responding in each of these components are highlighted in cases of psychiatric disease (including PTSD).

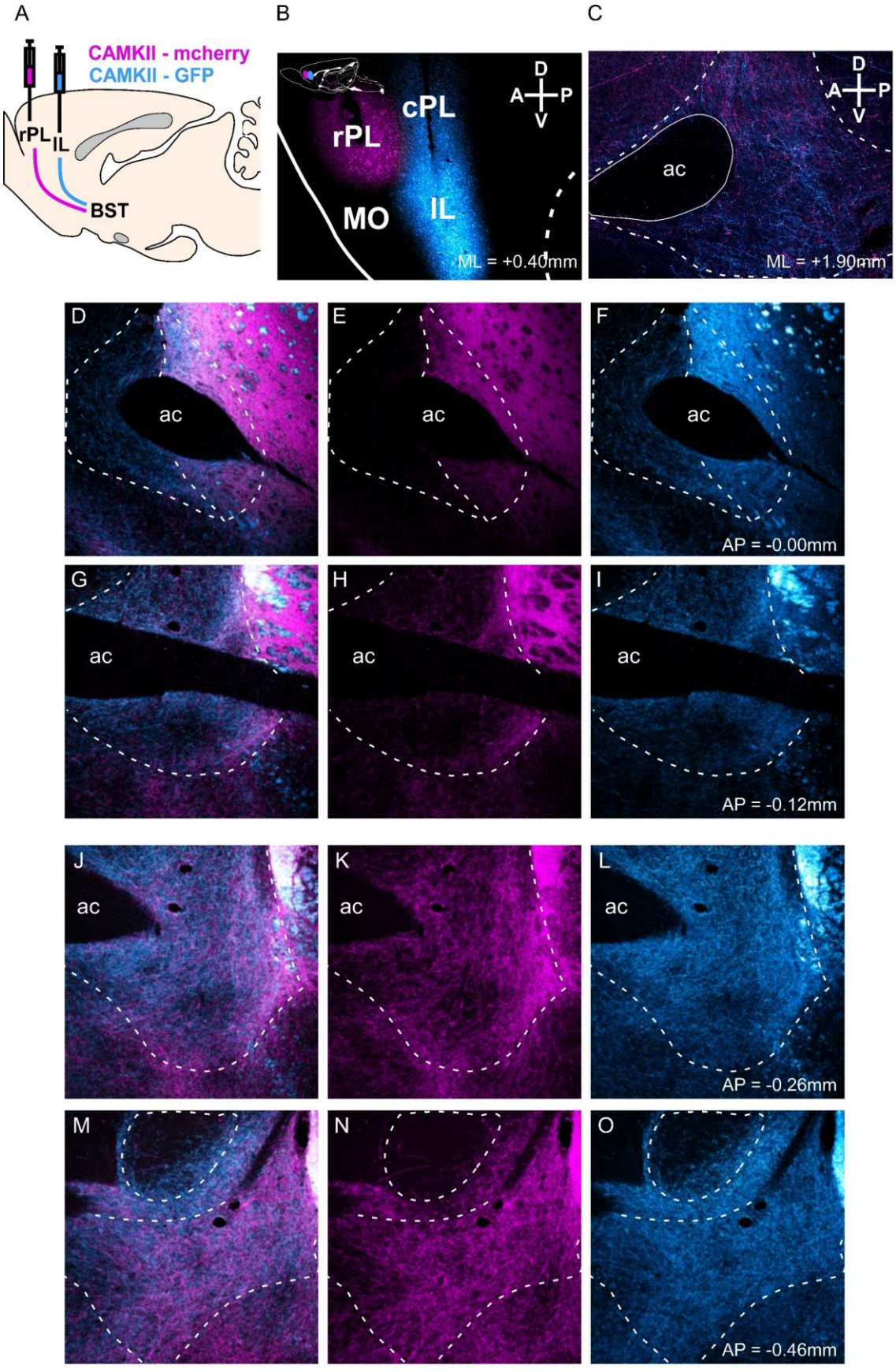
A
B
C
CAMKII - mcherry
CAMKII - GFP
rPL
IL
BST
cPL
rPL
MO
IL
D
A
P
V
ML = +0.40mm
ac
ML = +1.90mm
D
E
F
AP = -0.00mm
G
H
I
AP = -0.12mm
J
K
L
AP = -0.26mm
M
N
O
AP = -0.46mm

Figure 3.1 – Anatomic characterization of prefrontal projections across BST. ***A-C***: Illustration depicting viral strategy for targeting rPL and IL prefrontal subfields (***B***) Sagittal image depicting CAMKII-mCherry (magenta) and CAMKII-GFP (cyan) injections in rPL and IL. (***C***), Example sagittal image of BST. (***D***, ***G***, ***J***, ***M***) Coronal images depicting overlay of rPL-mCherry and IL-GFP expression in BST at sequential levels of BST (AP:0.00; -0.12; -0.26; -0.46mm). (***E***, ***H***, ***K***, ***N***) Isolated fluorescent expression for rPL-BST at all levels of BST. (***F***, ***I***, ***L***, ***O***) Isolated fluorescent expression for IL-BST at all levels of BST.

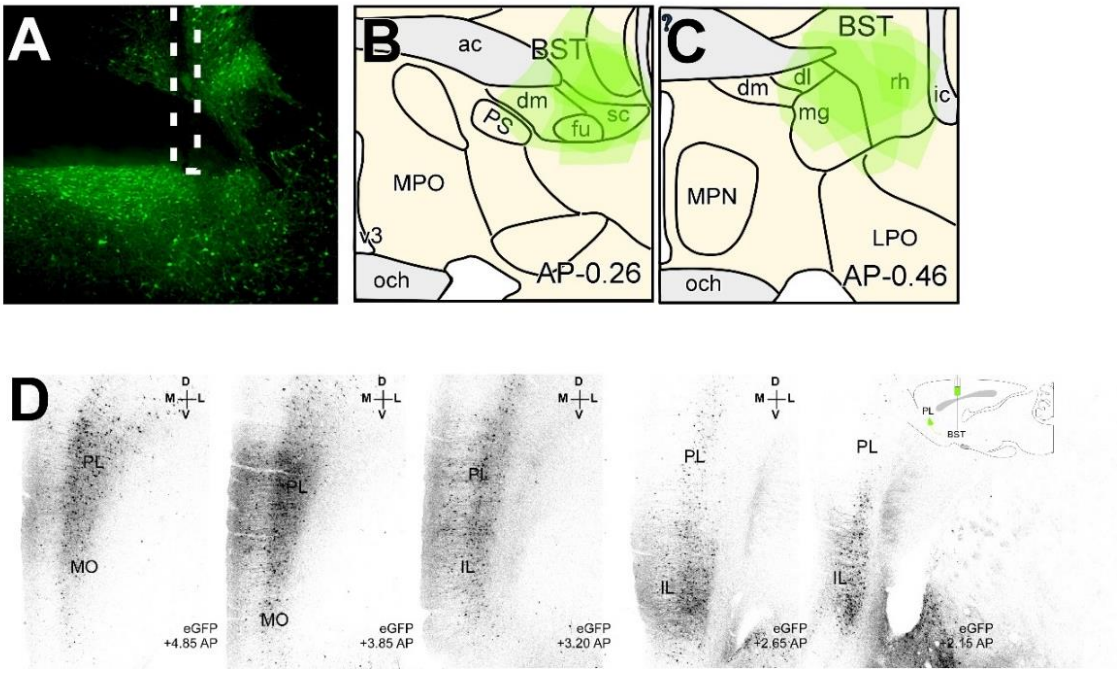

Figure 3.2 – Characterization of prefrontal - BST projection neurons using retrograde AAV tracing. ***A****:* Representative micrograph of AAV2-retro-GFP injection in BST. ***B****-****C****:* Depiction of injection sites in BST. **D**: Coronal images of fluorescent expression (pseudo-colored: black and white) across the prefrontal cortex starting at the most rostral (*left)* and extending to caudal regions (*right*).

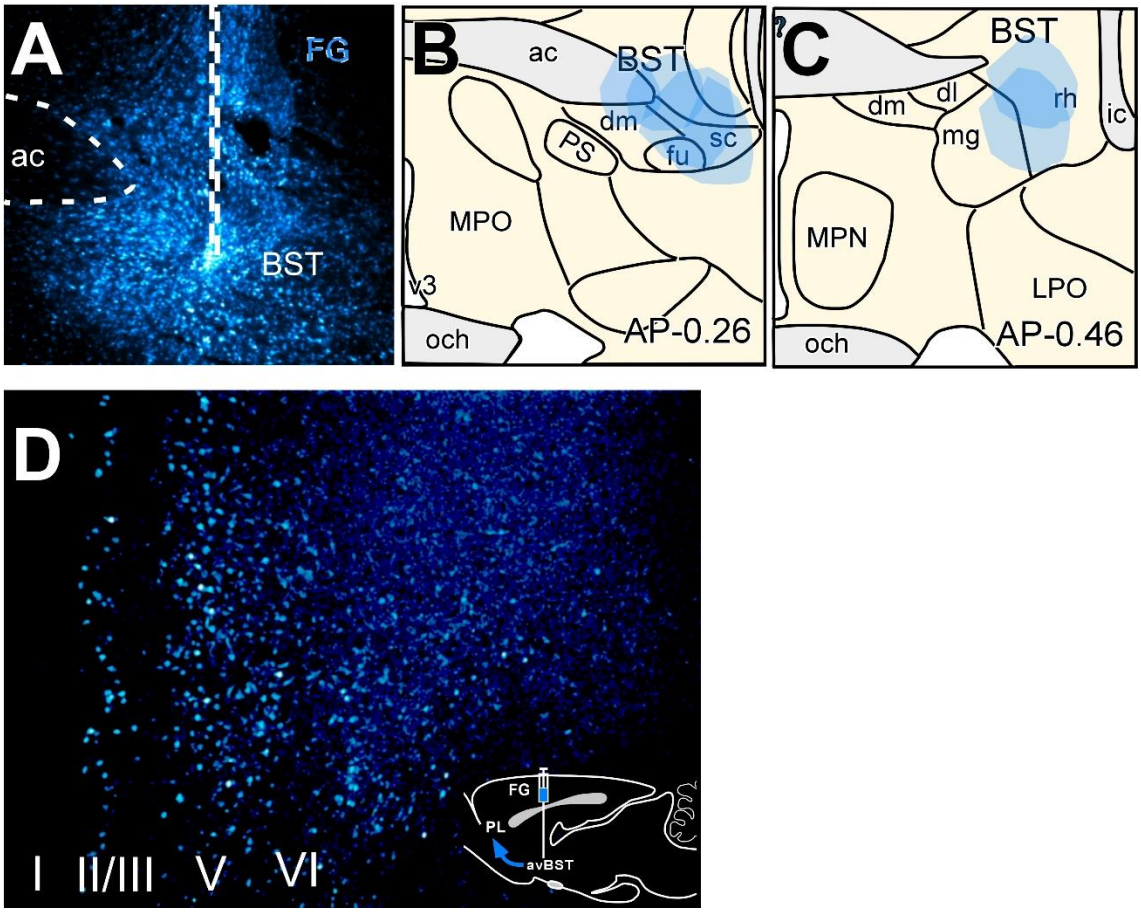

Figure 3.3 – Validation of AAV-retro-GFP approach using conventional tracer Fluorogold.
A*:* Representative micrograph of Fluorogold (FG) injection in BST. ***B***-***C***: Illustration of FG injection sites in BST across n= 6. ***D***: Example coronal image of FG expression in rPL (~AP:3.86mm).

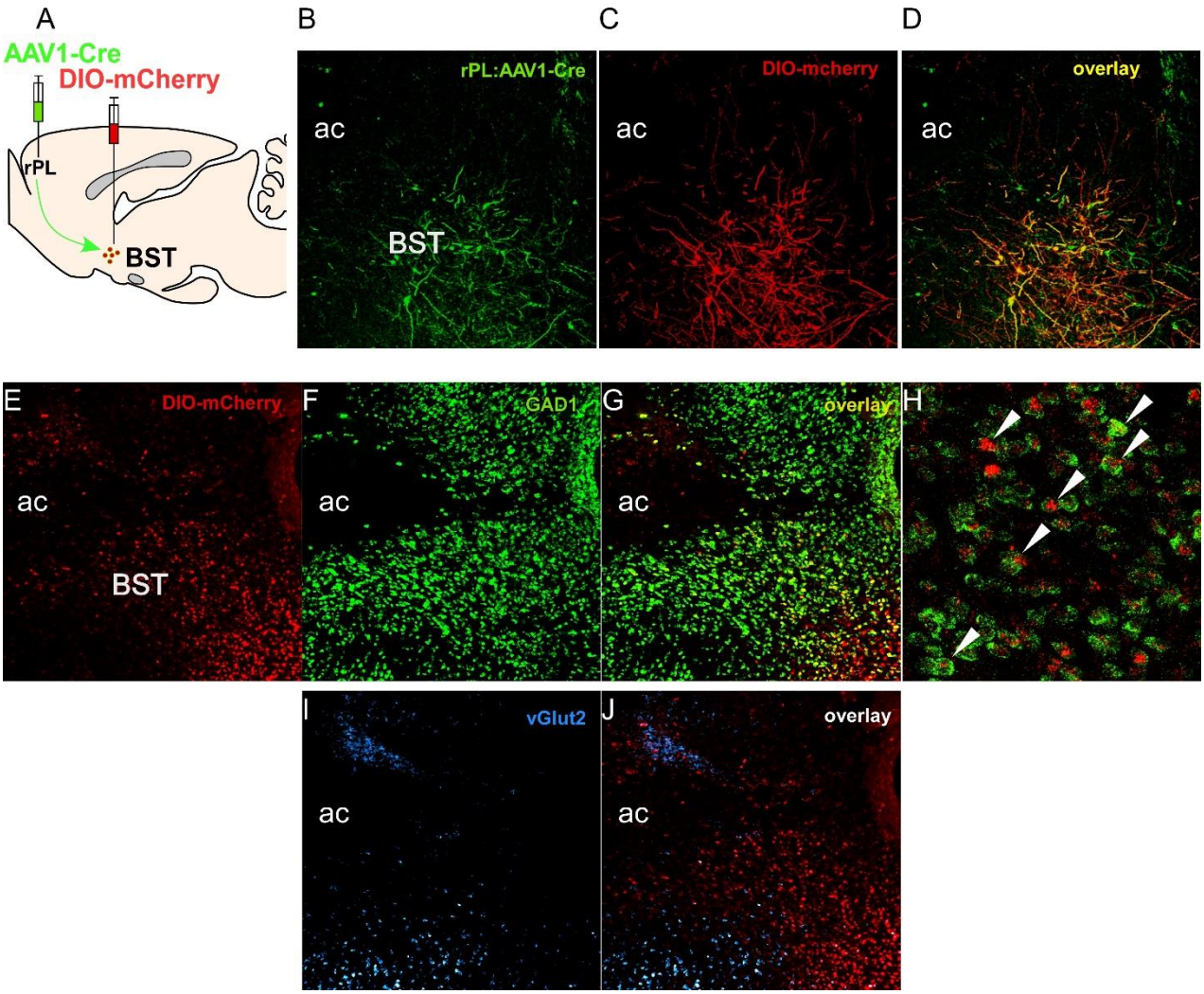

Figure 3.4 - Trans-Neuronal characterization of BST cell types receiving input from rPL. ***A***: Illustration depicting viral strategy. ***B-D***: Coronal images of fluorescent expression in BST with AAV1-Cre-GFP (***B***) DIO-mCherry (***C****)* and overlay (***D***). ***E-H****:* RNAscope *in situ* hybridization for mCherry-RNA (***E***), GAD1-RNA (***F***), and overlay (***G***) at 20x magnification. (***H****)* 100x magnification of overlay of mCherry-RNA and GAD1-RNA illustrating BST neurons receiving input from rPL are GAD1+. ***I-J****:* vGlut2-RNA(***I***) and overlay (***J***) of mCherry/vGlut2 indicate minimal overlap and lack of vGlut2 presence in BST.

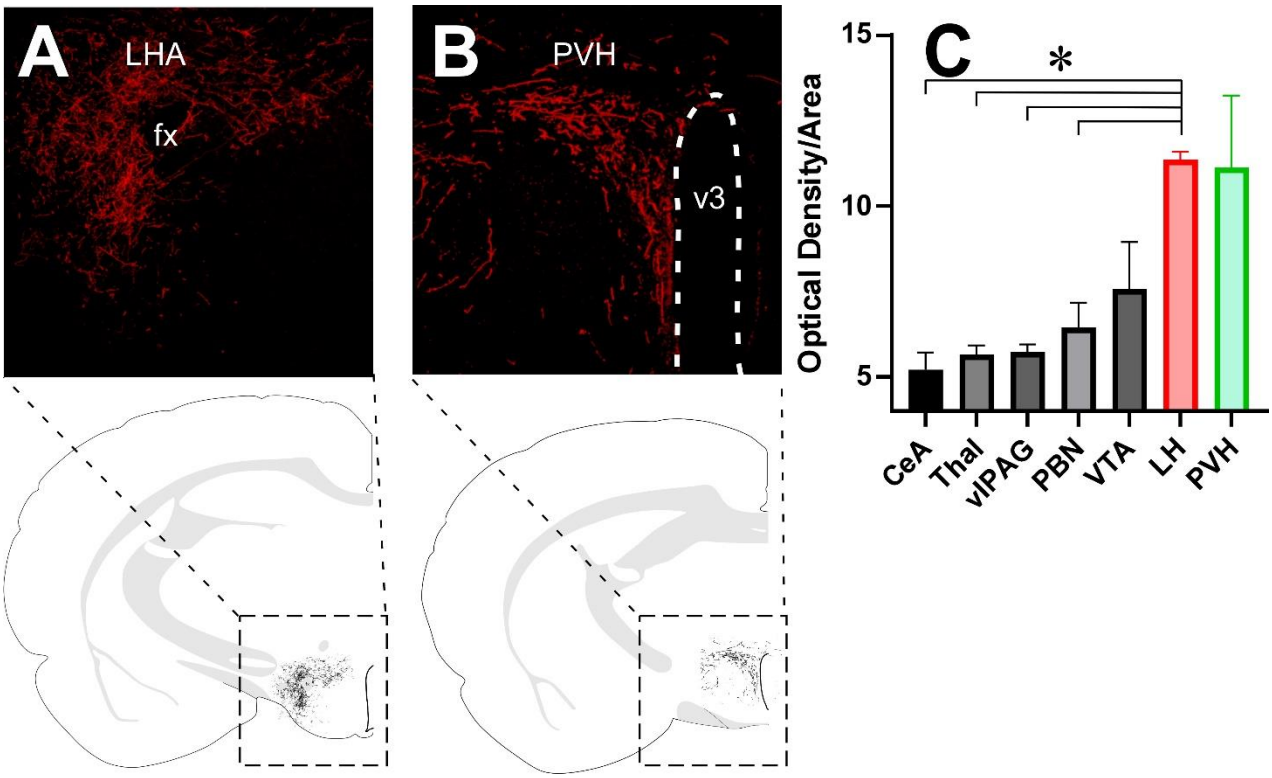

Figure 3.5 - Trans-Neuronal targeting of rPL-BST reveal predominant downstream targets. ***A***: Representative fluorescent imaging of the lateral hypothalamic area (LHA) following injection of AAV1-cre in rPL and DIO-mCherry in BST (top), with approximate location of fiber expression overlayed on atlas image (bottom). ***B***: Coronal image of fluorescent expression in PVH (top) with approximate atlas location (bottom). ***C***: Quantification of optical density for brain wide downstream targeting of rPL-BST revealed the majority of disynaptic connections for rPL-BST are either LHA or PVH. (N = 3) (*, $p<0.05$).

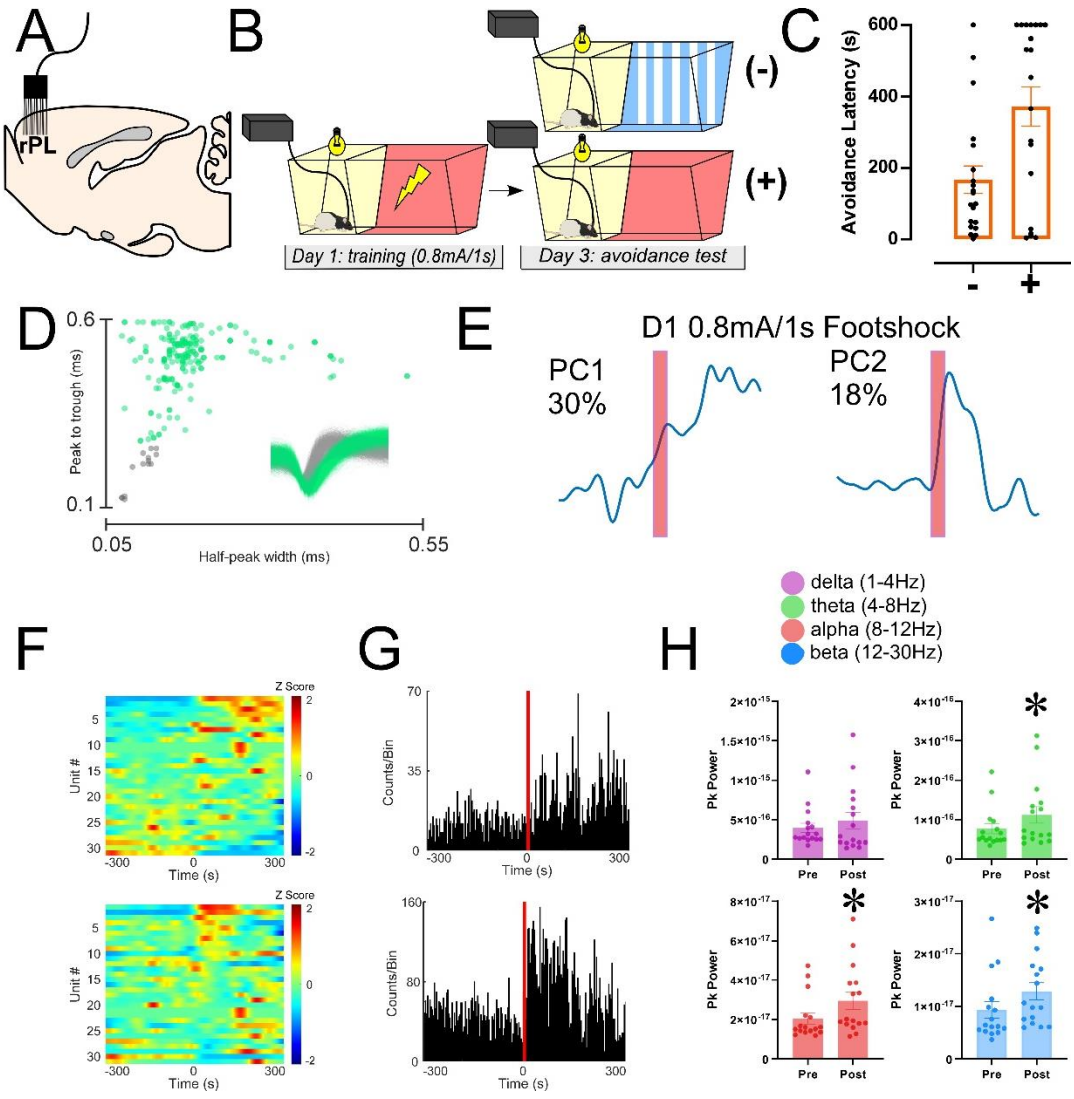

Figure 3.6 – Electrophysiological characterization of rPL activity during IA training. Depiction of electrode implantation (***A***) and behavioral procedures (***B***). Differential avoidance latencies based on context (i.e. -: context modified, +: original training) (***C***) in a non-surgerized sample of rats. Avoidance for (-) was significantly less than avoidance for (+) (*, $p < 0.05$). *D*, rPL neuronal waveform characteristics, Half-peak width (ms) and Peak-to-trough (ms) were used to remove putative interneurons (gray circles). ***E****:* PC analysis revealed two predominant components following footshock, with the PC2 reflective of shock responsivity. ***F***: Raster plots of rPL neuronal activity ordered by PC1 (top) and PC2 (bottom) coefficient values. ***G***: Representative single-unit activity for PC1 (top) and PC2(bottom). ***H***: Field potential power spectral density comparison for post-footshock, as compared to pre-footshock. Increases in peak PSD values were observed in theta (green), alpha (red), and beta (blue) oscillatory bands post-footshock, as

compared to pre-footshock (*, $p<0.05$). N = 4 animals implanted with electrode. FP analyses (N=16, electrodes averaged across N=4 animals).

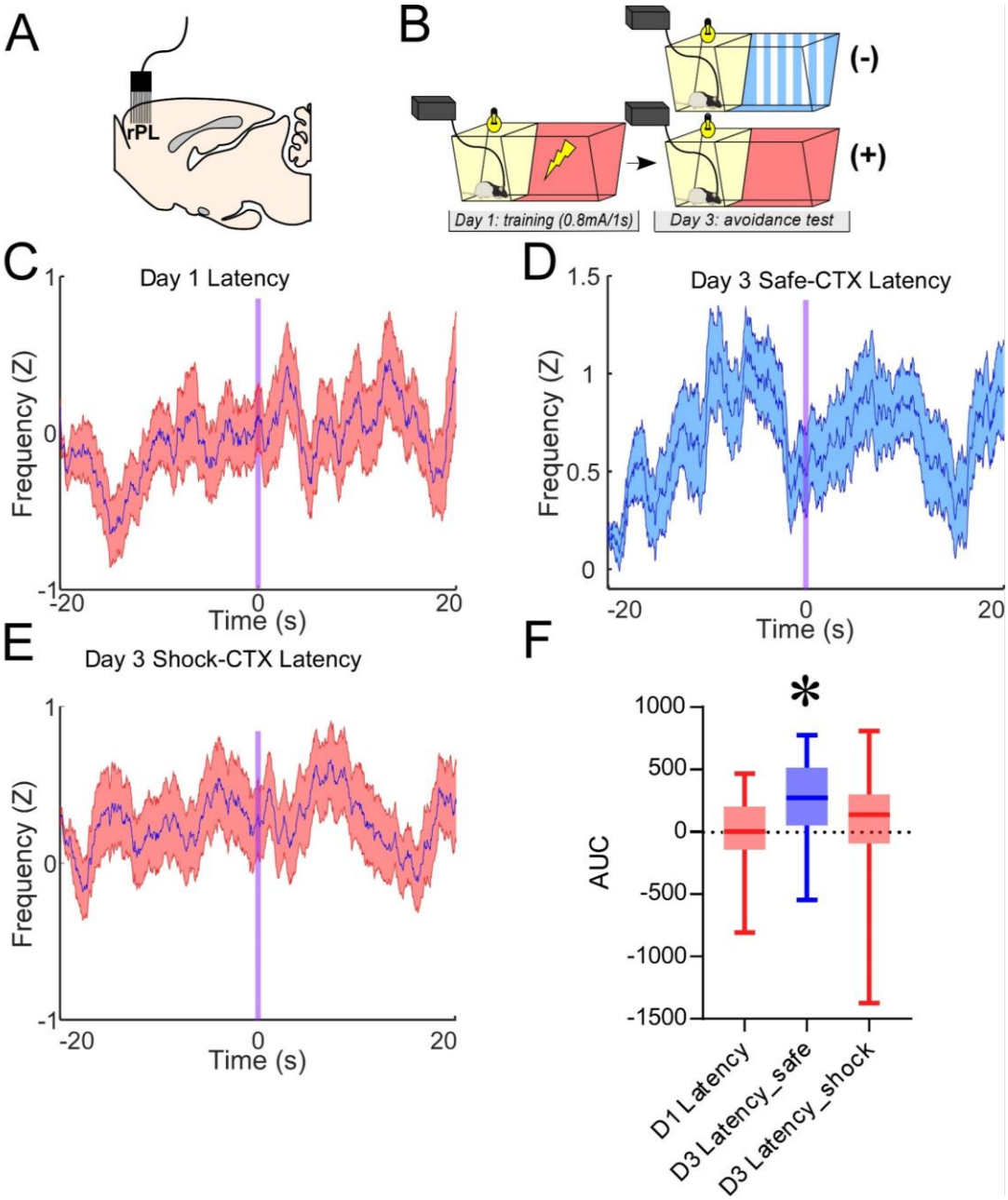

Figure 3.7 - Neurophysiological characterization of rPL activity around latency to enter darkened chamber on D1-D3. ***A***: Illustration of electrode implantation location and ***B***: behavioral procedures for IA paradigm. ***C***: Z-scored activity for all single units on Day 1 aligned to latency to enter. *D*, rPL activity surrounding latency to enter the adjacent darkened area in the contextually modified "safe" chamber on D3. ***E***: rPL activity aligned to latency to enter darkened area of the original training context on D3. Area under the curve analysis for the period prior to latency, as compared across days indicated an increased AUC for D3 Safe-CTX in the 10s prior to latency, as compared to Day 1, and trending increase as compared to D3-ShCTX (*, $p<0.05$).

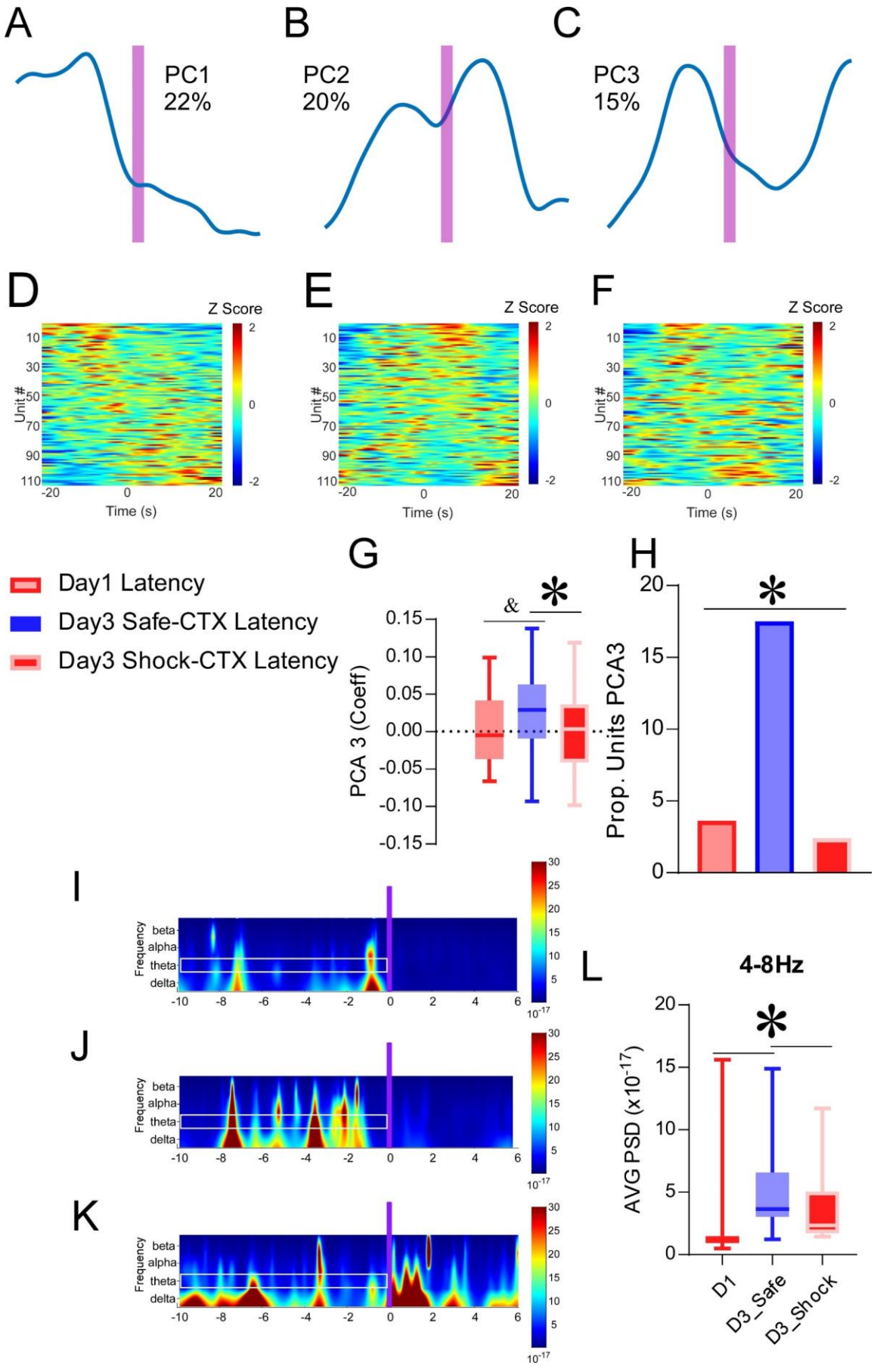
A
PC1
22%
B
PC2
20%
C
PC3
15%
D
Z Score
Unit #
Time (s)
E
Z Score
Unit #
Time (s)
F
Z Score
Unit #
Time (s)
Day1 Latency
Day3 Safe-CTX Latency
Day3 Shock-CTX Latency
G
PCA 3 (Coeff)
&
*
H
Prop. Units PCA3
*
I
J
K
Frequency
beta
alpha
theta
delta
L
4-8Hz
AVG PSD (x10^-17)
*
D1
D3_Safe
D3_Shock

Figure 3.8 – Further electrophysiological characterization of rPL activity aligned to latency to enter darkened adjacent area. ***A***-***C***: PC components for rPL neural activity aligned to latency across D1-D3 revealed three predominant components. ***D***-***F****:* Raster plots for rPL activity ordered by PC1(D), PC2(E), or PC3(F). ***G***: PC3 coefficient values were increased for Day 3 Safe-CTX as compared to D3 Shock-CTX ($p<0.05$) and D1 ($p<0.1$). *H*, Chi-square test of independence indicated a significantly greater proportion of units loading on the upper 25% if PC3 coefficient values for D3 SafeCTX ($p<0.05$). ***I***-***K***: Time frequency Morelet wavelets for D1 (***I***), D3 Safe-CTX (***J***), and D3 Shock-CTX (***K***). ***L***: Field potential analyses for latency to enter revealed increased average rPL theta (4-8Hz) (frequency analyzed indicated by white rectangle) PSD values in the 10s period prior to latency in D3 Safe CTX as compared to D1 ($p<0.05$) and D3 Shock-CTX ($p<0.05$), no other oscillatory band displayed a similar pattern prior to latency.

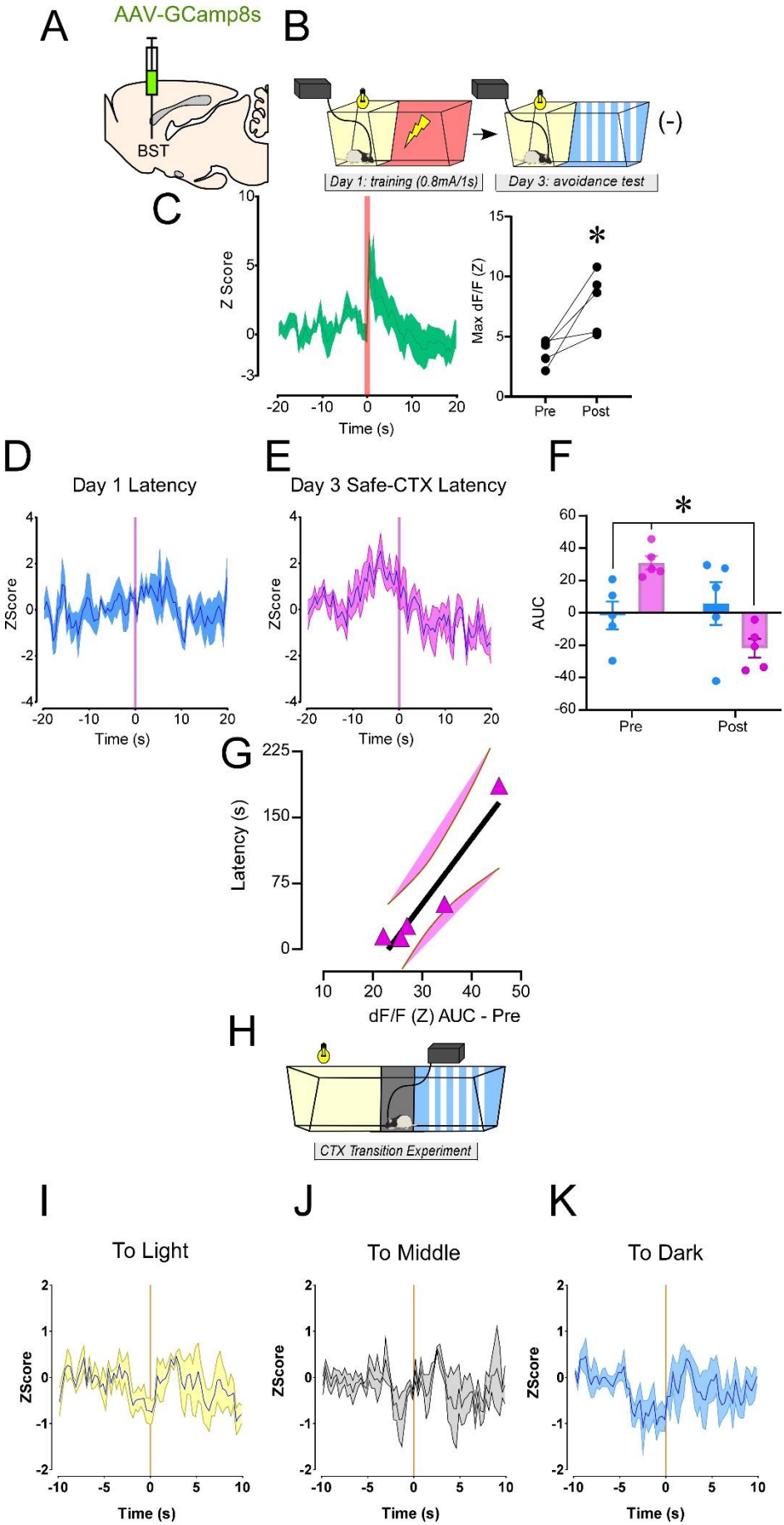
A
AAV-GCamp8s
BST
B
(-)
Day 1: training (0.8mA/1s)
Day 3: avoidance test
C
Z Score
Time (s)
Max dF/F (Z)
Pre
Post
D
Day 1 Latency
ZScore
Time (s)
E
Day 3 Safe-CTX Latency
ZScore
Time (s)
F
AUC
Pre
Post
G
Latency (s)
dF/F (Z) AUC - Pre
H
CTX Transition Experiment
I
To Light
ZScore
Time (s)
J
To Middle
ZScore
Time (s)
K
To Dark
ZScore
Time (s)

Figure 3.9 – Calcium imaging of BST during IA training and testing. ***A***: Viral strategy for calcium imaging of BST, rats received microinjection of AAV-GCamp8s in BST, and fiber optic placement in BST. ***B****:* Illustration of behavioral procedures, rats were trained in one context and then tested for avoidance in a contextually modified chamber. ***C***: Peri-event histogram of BST activity (Z-Score dF/F) immediately following shock(left) and (right) area under the curve analysis for pre vs post max Z-Score dF/F values. Peak values were significantly greater post-shock as compared to pre-shock (*, $p<0.05$). ***D***: BST activity on D1 aligned to latency to enter adjacent darkened area. **E**: BST activity on D3 aligned to latency to enter adjacent darkened area of contextually modified chamber. ***F***: AUC values for D1 (blue) and D3 (purple) prior to and post latency to enter. D1 latency values were no different between pre and post levels. D3 pre-AUC values were significantly increased as compared to D1 and D3 post-latency to enter (*, $p <0.05$). ***G***: Scatter plot of pre latency AUC values for D3 and total avoidance time revealed a significant association between variables ($p<0.05$). ***H***: Illustration of additional context transition experiment and (***H***-***K****)* associated peri-event plots of Z-Scored dF/F values for entrance into a lit (***I***), middle (***J***), and darkened-contextually distinct (***K***) chamber revealed no differences BST activity as a function of context transitions. ***A***-***F***, N = 5; ***H***-***J***, N = 4.

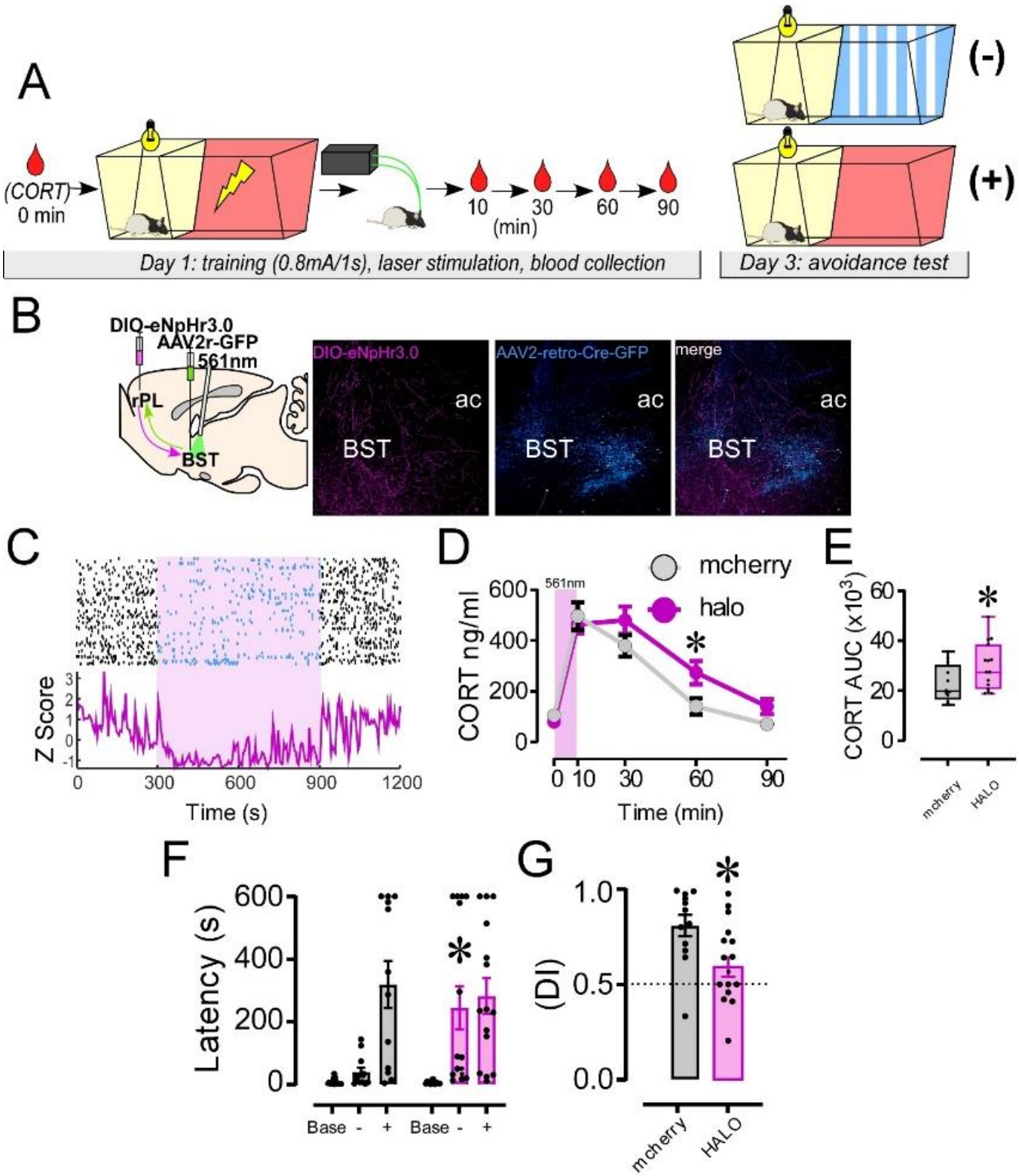
A
(CORT)
0 min
10
30
60
90
(min)
(-)
(+)
Day 1: training (0.8mA/1s), laser stimulation, blood collection
Day 3: avoidance test
B
DIO-eNpHr3.0
AAV2r-GFP
561nm
rPL
BST
DIO-eNpHr3.0
AAV2-retro-Cre-GFP
merge
ac
BST
C
Z Score
Time (s)
D
561nm
mcherry
halo
CORT ng/ml
Time (min)
E
CORT AUC (x10^3)
mcherry
HALO
F
Latency (s)
Base - + Base - +
G
(DI)
mcherry
HALO

Figure 3.10 – Posttraining photoinhibition of rPL-BST *A*: Illustration of optogenetic and behavioral manipulations in the IA task. ***B***: Illustration of viral strategy for targeting rPL-BST projection (left), and representative images of viral expression of rPL fibers in BST (right). ***C***: Electrophysiological verification of opsin functionality in BST, 561nm laser stimulation (purple box) was applied for 10 minutes. (**C**-Top) Randomized raster of unit activity prior to, during, and post laser stimulation for illustration. (**C**-Bottom) Z-Scored unit activity across the entire recording session. **D**: Corticosterone responses during D1 prior to (T0) and post-footshock (T10,30,60,90min) revealed an overall significant increase across time ($p<0.05$), and a specific increase at T60 ($p<0.05$) in CORT for rPL-BST^{Halo} expressing animals. **E**: integrated area under the curve (AUC) values for experimental animals revealed a significant increase for rPL-BST^{Halo}, as compared to rPL-BST^{mCherry} ($p<0.05$). ***F***: Avoidance latencies across D1 (base) and D3 (-, +) revealed a significant increase in avoidance for rPL-BST^{Halo} animals on D3 for (-) context (i.e., Contextually modified safe chamber) ($p<0.05$). Avoidance for D3 (+) context was no different between groups. ***G***: Discrimination index (DI) values (i.e. (+)/ {(-) +(+)}) revealed significant decreases in rPL-BST^{Halo}, as compared to rPL-BST^{mCherry} ($p<0.05$). N = 15; Halo, N = 11; mCherry.

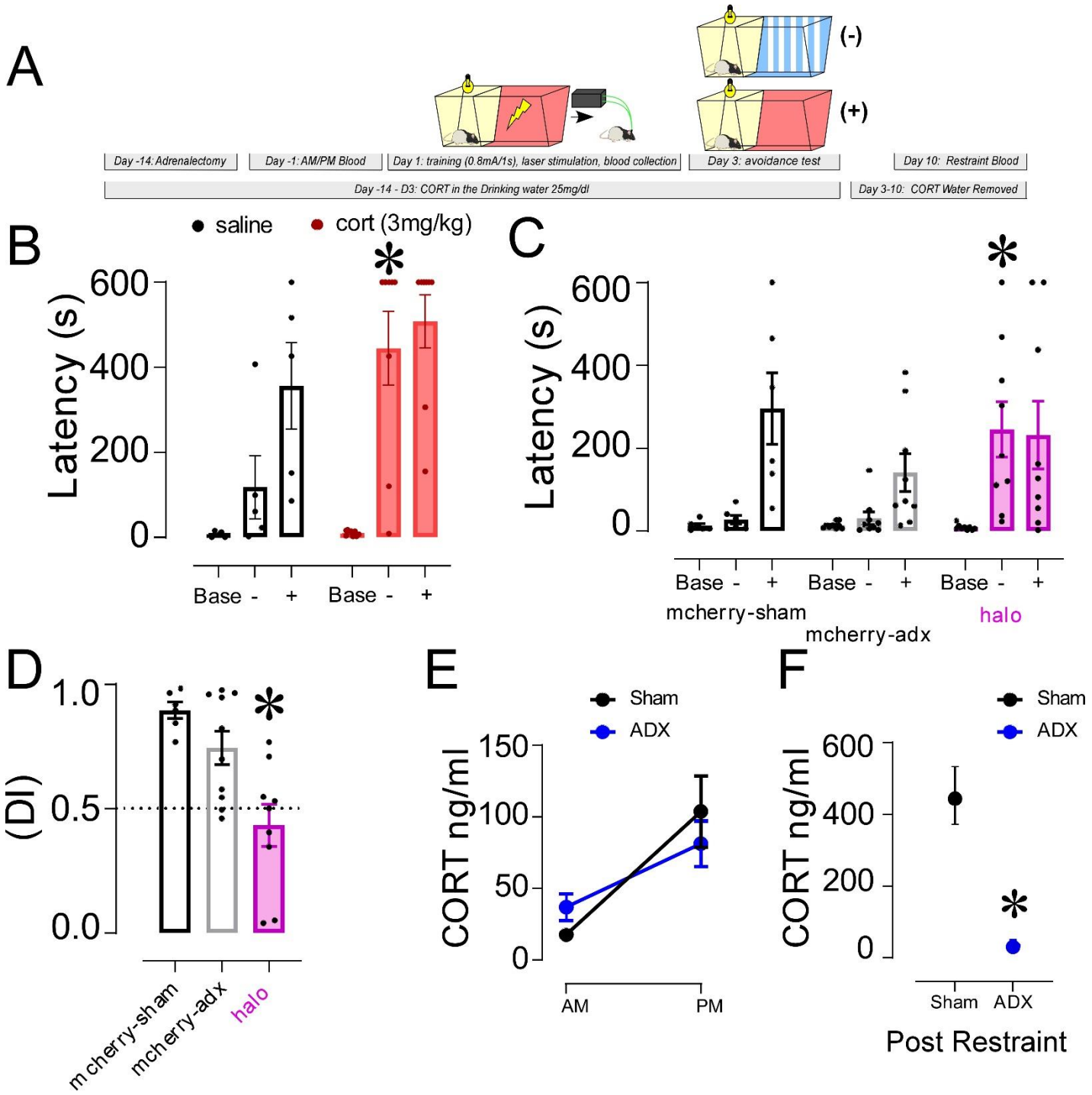

Figure 3.11 – Posttraining rPL-BST photoinhibition following adrenalectomy. ***A***: Schematic diagram depicting surgical and behavioral procedures. ADX was performed 14 days prior to experimentation, and animals received CORT in the drinking water (25mg/dL) from D-14 to D3. CORT in the drinking water was then removed from D3 to

D10 to assess restraint-induced mobilization of CORT. ***B***: Avoidance latencies across D1(base) to D3 (- & +) for animals that received either post-training injection of saline or CORT (3mg/kg i.p), avoidance for D3- was increased for animals that received CORT injections ($p<0.05$). ***C***: Avoidance latencies across D1 (base) to D3 (- & +) for rPL-BST$^{mCherry\text{-}Sham}$, rPL-BST$^{mCherry\text{-}ADX}$, and rPL-BST$^{Halo\text{-}ADX}$. Avoidance latencies for D3(-) were increased in rPL-BST^{Halo} animals as compared to both control groups ($p<0.05$). ***D***: Discrimination index values were decreased in rPL-BST^{Halo} animals, as compared to both control groups ($p<0.05$). *E*, Radioimmunoassay for AM (0700Hr) and PM (1700Hr) CORT values, blood collection occurred prior to training (D-1) and indicated no differences in AM or PM values for ADX animals, as compared to Sham animals ($p>0.05$). ***F***: following completion of training and testing ADX animals had CORT in the drinking water removed for 7 days to subsequently test restraint-induced values of CORT. Following a 30 min restraint test Sham rats displayed substantially higher values of CORT than ADX rats ($p<0.05$). N = 6 rPL-BST$^{mCherry\text{-}Sham}$, N = 9 rPL-BST$^{mCherry\text{-}ADX}$, N = 9 rPL-BST$^{Halo\text{-}ADX}$.

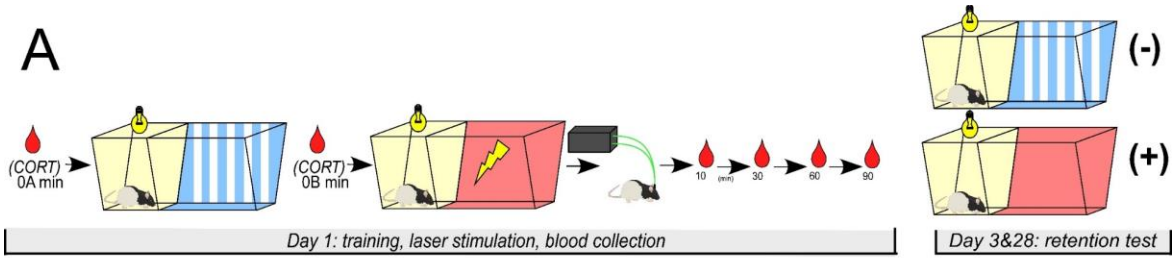
A
(CORT)
0A min
(CORT)
0B min
10
30
60
90
(-)
(+)
Day 1: training, laser stimulation, blood collection
Day 3&28: retention test

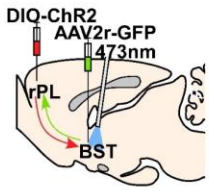
B
DIO-ChR2
AAV2r-GFP
473nm
rPL
BST

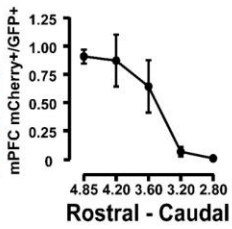
C
mPFC mCherry+/GFP+
1.25
1.00
0.75
0.50
0.25
0
4.85 4.20 3.60 3.20 2.80
Rostral - Caudal

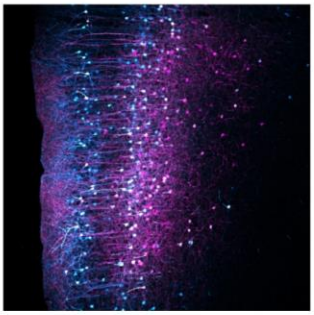
D

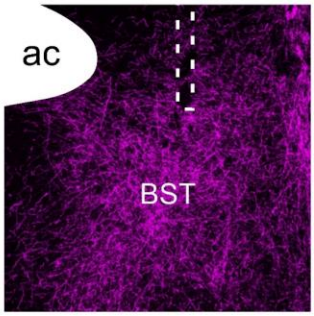
E
ac
BST

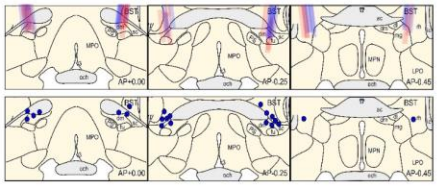
F

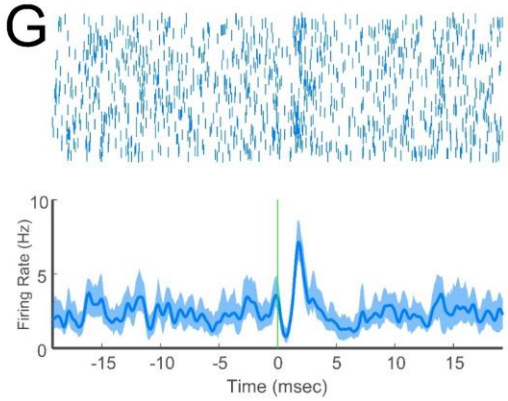
G
Firing Rate (Hz)
10
5
0
-15
-10
-5
0
5
10
15
Time (msec)

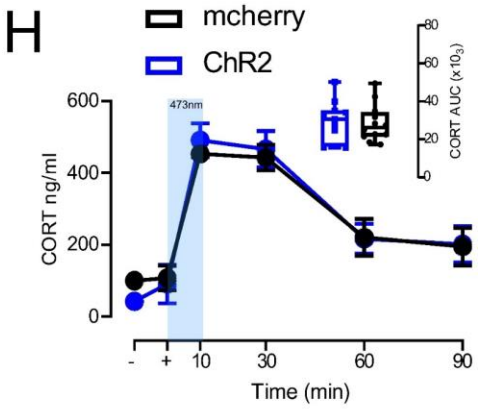
H
mcherry
ChR2
473nm
CORT ng/ml
600
400
200
0
CORT AUC (x10³)
80
60
40
20
0
-
+
10
30
60
90
Time (min)

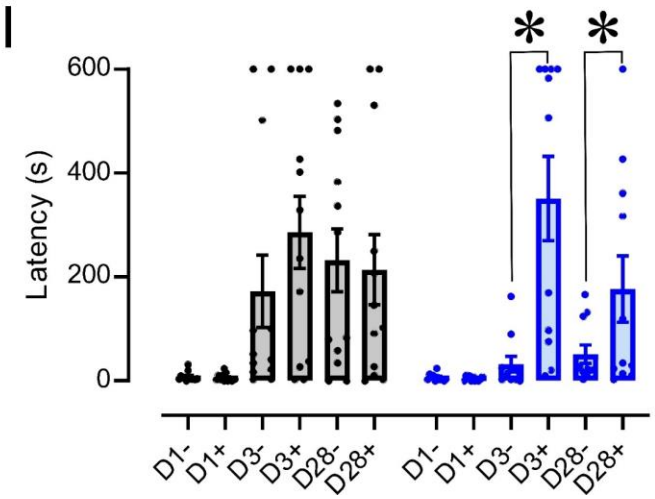
I
Latency (s)
600
400
200
0
*
*
D1-
D1+
D3-
D3+
D28-
D28+
D1-
D1+
D3-
D3+
D28-
D28+

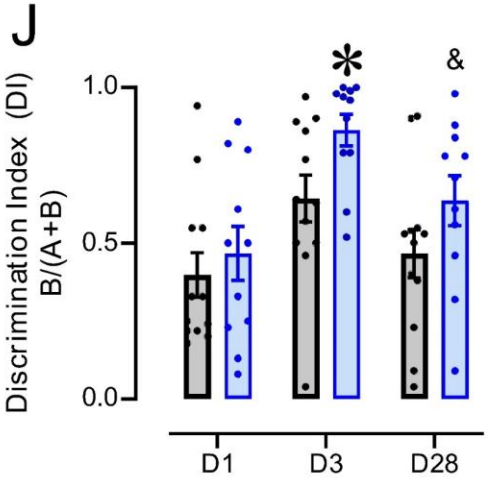
J
Discrimination Index (DI)
B/(A+B)
1.0
0.5
0.0
*
&
D1
D3
D28

Figure 3.12 – Posttraining photoexcitation of rPL-BST prevents context generalization produced by context pre-exposure. ***A***: Illustration of behavioral and optogenetic procedures. ***B***: Depiction of viral strategy for pathway-specific targeting of rPL-BST. ***C***: Characterization of viral overlap across the rostro-caudal extent of mPFC for DIO-mCherry/ChR2 (microinjection in rPL; AP coordinates ~3.85mm relative to bregma) and AAV2-retro-Cre-GFP (microinjection in BST; AP coordinates ~ -0.20mm relative to bregma) (overlap: mCherry+/GFP+). Proportion of overlap was greater at rostral levels of mPFC, as compared to caudal levels. ***D***-***E***: Representative images of viral expression in rPL (***D***) and BST (***E***). *F*, Illustration of optic fiber placements in BST (top) and AAV-retro-Cre-GFP injections in BST (bottom). ***G***: Electrophysiological verification of ChR2 opsin functionality in BST, 473nm laser stim (20Hz, 5ms pulse width) evoked short latency increases in BST neurons (green line, 473nm laser pulse). **H**: Pre- and posttraining CORT responses were no different between rPL-BST^{mCherry} and rPL-BST^{ChR2}. **I**: Avoidance latency values across D1 – D3 – D28 for pre-exposed neutral chamber (-) and training chamber (+). Results indicated rPL-BST^{mCherry} rats had similar latencies between chambers on D3 and D28 ($p>0.10$), whereas rPL-BST^{ChR2} rats displayed significantly higher avoidance latencies for (+) as compared to (-) on both D3 and D28 (*, $p<0.05$). **J**: Discrimination index values were increased on D3 for rPL-BST^{ChR2} rats, as compared to rPL-BST^{mCherry} but not on D28 (*, $p<0.05$; &, $p>0.10$) N = 12 rPL-BST^{mCherry}, N=11 rPL-BST^{ChR2}.

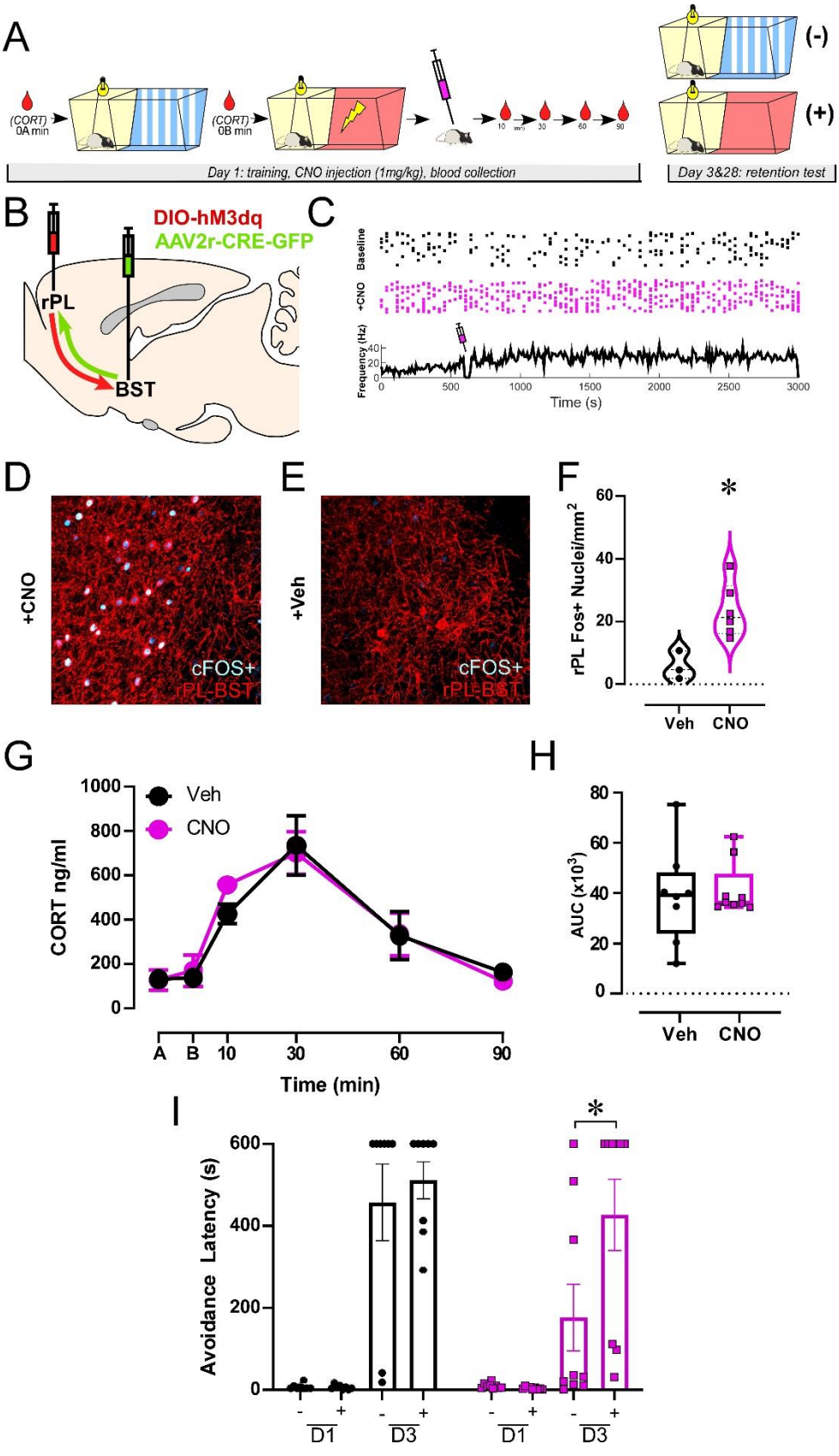
A
(CORT)
0A min
(CORT)
0B min
10
30
60
90
(-)
(+)
Day 1: training, CNO injection (1mg/kg), blood collection
Day 3&28: retention test
B
DIO-hM3dq
AAV2r-CRE-GFP
rPL
BST
C
Baseline
+CNO
Frequency (Hz)
Time (s)
D
+CNO
cFOS+
rPL-BST
E
+Veh
cFOS+
rPL-BST
F
rPL Fos+ Nuclei/mm2
Veh
CNO
G
CORT ng/ml
Veh
CNO
Time (min)
H
AUC (x10³)
Veh
CNO
I
Avoidance Latency (s)
D1
D3
D1
D3

Figure 3.13 –rPL-BST Chemogenetic excitation prevents context generalization at D3. ***A***: Behavioral strategy for rPL-BST chemogenetic excitation with hM3dq. CNO (1mg/kg, i.p) injection was administered immediately after training. ***B***: Illustration of intersectional chemogenetic approach. ***C***: Electrophysiological characterization of chemogenetic functionality, recording in BST revealed single unit increases as a result of CNO injection that persisted for at least 50min following injection. ***D***-***E***: Representation histochemical staining for cFos in rPL following injection of CNO or vehicle in a subset of rats with hM3dq expression in rPL-BST pathway. CNO (left), vehicle (middle), quantification of cFos+ nuclei in rPL (right). ***G***: RIA for CORT prior to and following training on D1 revealed no significant differences across time as a function of CNO injection. ***H***: Quantification of CORT area under the curve revealed no significant differences in CORT. ***I***: Avoidance latencies for Vehicle and CNO injected animals on D1 and D3. CNO injected animals displayed reduced avoidance to context (-) on D3, as compared to (-) avoidance for Veh injected animals ($p<0.05$). Avoidance difference between (-) and (+) for CNO injected animals revealed significantly lower avoidance for (-) as compared to (+) (*, $p<0.05$). *D-F*, N = 3 rPL-BST$^{hM3dq\text{-}Veh}$, N = 6 rPL-BST$^{hM3dq\text{-}CNO}$. *G-I*, N = 9 rPL-BST$^{hM3dq\text{-}Veh}$, N = 9, rPL-BST$^{hM3dq\text{-}CNO}$.

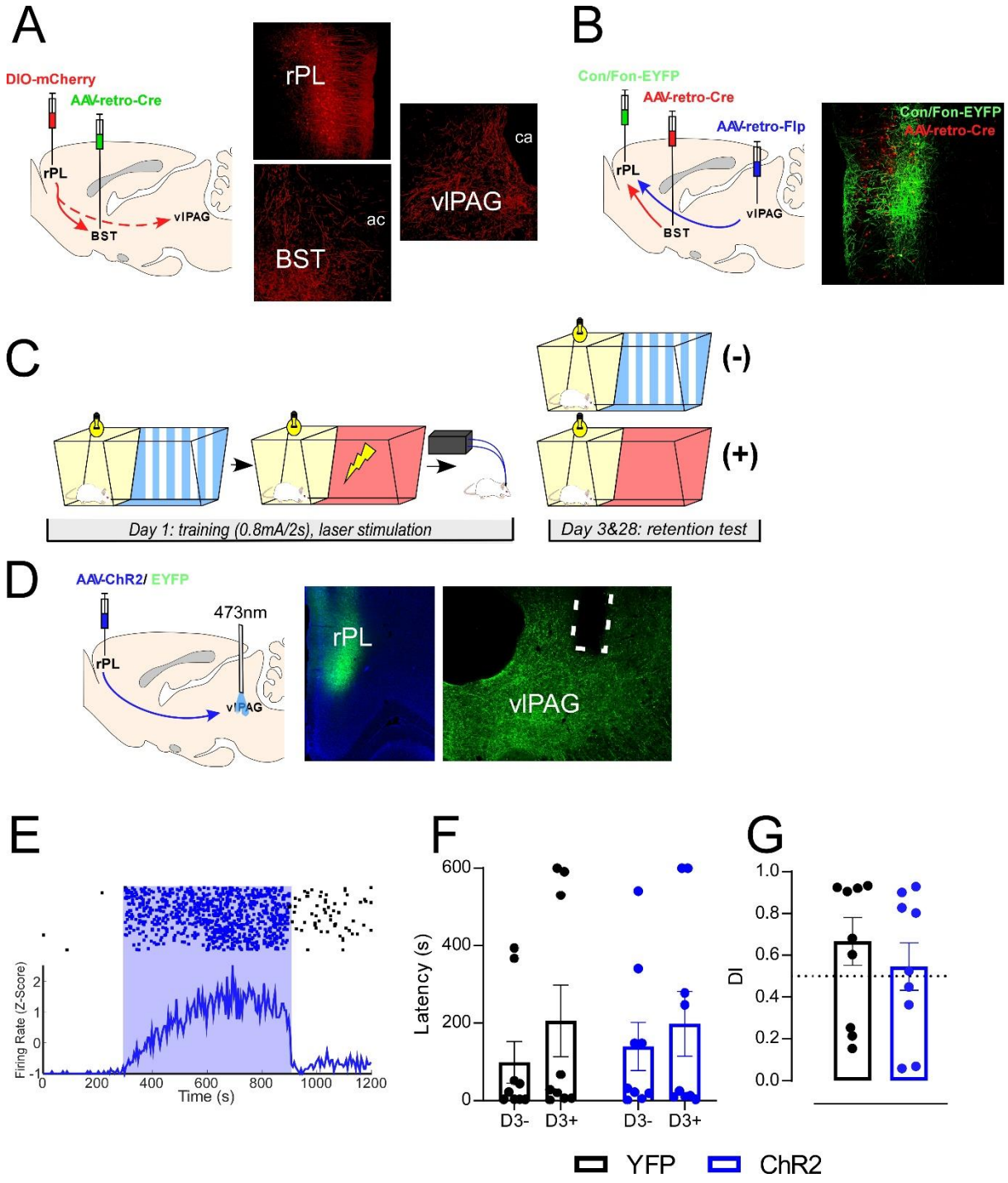

Figure 3.14 – Characterization of rPL-vlPAG circuit that collateralizes with BST but does not influence IA generalization. ***A***: Dual-viral targeting of the rPL-BST pathway revealed some collateralization with vlPAG, (left) Illustration of viral strategy (right) representative images of viral expression in rPL, BST, and vlPAG. ***B***: triple-intersection viral strategy revealed a subset of rPL neurons that project to both BST and vlPAG. (left) illustration of viral strategy. Dual projection rPL neuronal ensembles were labeled by microinjecting a retrogradely transported Cre virus in BST, a separate retrogradely

transported Flp virus in vlPAG, and a CreON/FlpON-EYFP virus in rPL. Red cells are rPL-BST projecting nuclei, Green are dual projecting (i.e., BST & vlPAG) rPL nuclei. ***C***: illustration of pre-exposure model. ***D***: illustration of viral strategy for targeting rPL-vlPAG (left) and representative images of rPL (middle) and vlPAG (right) viral expression. ***E***: Electrophysiological characterization of rPL-vlPAG ChR2 opsin functionality, 473nm stimulation of ChR2 expressing rPL fibers in vlPAG resulted in increased activity coincident with laser stimulation. ***F***: Avoidance latencies on D3 for YFP and CHR2 expressing rats revealed no differences in latencies for either (-) or (+) chambers. ***G***: Discrimination index values were no different between groups. N = 9 rPL-YFP, N = 9, rPL-ChR2.

CHAPTER IV:

Discussion and conclusions

Introduction

Adaptively responding to environmental threats requires the coordinated mobilization of multiple physiological systems. The BST acts crucially to mediate behavioral and neuroendocrine components of an organism's response to psychological stress as an interface between limbic forebrain regions and downstream effector regions.

Summary of Findings

The studies described in this thesis were undertaken with the goal of testing the hypotheses that 1) the BST mediates the contribution of HPA signaling during memory consolidation and 2) that the prefrontal cortex coordinates HPA responding and facilitates context disambiguation through an interaction with the BST. Chapter 2 outlined the studies demonstrating support for the first hypothesis. Optogenetic inhibition of avBST, or avBST-PVH projections immediately following training on an inhibitory avoidance task augmented HPA-component indices including ACTH, and CORT, and electrophysiological activity in PVH neurons. This enhanced HPA responding was associated with an increased retention for the shock-associated context 48hrs later suggesting an enhancement of memory consolidation processes that contributed to a greater "memory" for the training event. Blockade of footshock-induced increases in CORT using metyrapone, a 11-β-hydroxylase inhibitor, was sufficient to prevent the

enhanced CORT response, and retention provided by posttraining avBST photoinhibition suggesting increases in CORT release were necessary for the facilitatory effects of our optogenetic manipulation.

Follow-up excitatory manipulations of avBST revealed posttraining photoexcitation of avBST, or projections to the vlPAG, could reduce memory consolidation independent of any alterations in HPA responding. We further confirmed photoexcitation of avBST-PVH was unable to carry out these effects suggesting a dissociation between glucocorticoid-dependent and independent effects carried out by avBST during memory consolidation. The vlPAG is known to mediate both conditioned (McNally & Johansen 2011; Wright & McDannald 2019; Arico et al., 2017; Amat et al., 1998) and unconditioned (Assareh, Sarrami, Carrive, McNally 2016) fear responses via ascending and descending neural circuits, respectively (Cameron, Khan, Westlund & Willis 1995; Cameron, Khan, Westlund, Cliffer, & Willis 1995). In conditioned fear, vlPAG neurons are recruited via the disinhibition provided by GABAergic inputs from the central amygdala targeting vlPAG interneurons (Tovote et al., 2016; Carrive, Leung, Harris, Paxinos 1997), to promote freezing during retention (discussed in more detail below).

Chapter 3 provided support for the hypothesis that prefrontal cortical projections to BST are capable of restraining CORT responses following an aversive event, and that this activity was necessary to prevent generalization to a novel context. We further demonstrated these effects were not dependent upon one another, and that rPL-BST photoinhibition produced generalized behavioral avoidance regardless of adrenocortical status. We also demonstrated here that rPL and BST activity were largely explained by patterns of shock responsivity during training, and selectivity during avoidance testing.

Specifically, we observed a mobilization of rPL and BST activity immediately prior to latency to enter an adjacent darkened area of a novel context, suggesting these regions are recruited during retention to disambiguate environmental features predictive of threat likelihood, or similarly to prevent inappropriate avoidance. Importantly, a greater level of BST activity, as determined by AUC values prior to latency was required to initiate latency to enter the safe chamber the longer the avoidance period went on, suggesting a greater level of activity in BST is necessary to overcome increased levels of avoidance. Posttraining photo or chemogenetic excitation of the rPL-BST pathway was also sufficient to encourage discrimination between a neutral pre-exposed chamber and a shock-associated chamber as well, further indicating posttraining activity could modulate long-term behavioral expression of generalization. Aligning neural activity with optogenetic manipulations, our results suggest that during training mobilization of rPL and BST is required to learn and/or consolidate information from the IA experience and disrupting the rPL-BST pathway prevents this potentially encouraging an overall “abstracted” or schematic representation of the event that lacks specific details necessary for future discrimination. Further, these regions are mobilized during retention to prevent avoidance in a novel chamber, and potentially a greater mobilization of this circuit is necessary to overcome excessive levels of avoidance.

Consideration of BST as an upstream regulator of memory consolidation

Much of the work describing the posttraining effects of glucocorticoids highlight an involvement with the BLA (de Quervain, Schwabe, & Roozendaal; McGaugh 2000).

Evidence suggests that glucocorticoids, released in response to an emotionally arousing event, converge on the BLA to interact with noradrenergic signaling and modulate memory consolidation processes across a diverse network that involves projections to the mPFC (Roozendaal et al., 2009), hippocampus (Roozendaal, Griffith, Burandav, Dominique & McGaugh 2003), among others (Roozendaal, Williams & McGaugh 1999). However, this work largely suggests the BLA acts *downstream* of the release of glucocorticoids to integrate stress hormone release across a presumptive consolidation network. Importantly, little regard has been directed to the central circuits that mediate glucocorticoid responding and the consideration that these structures may act *upstream* of glucocorticoid actions within the BLA. Our results position the avBST as a component of a neuroendocrine regulatory network that acts as an upstream initiator of memory consolidation processes that ultimately rely on the BLA.

That avBST receives particularly dense excitatory input from regions of the basolateral complex should be noted (Dong, Petrovich & Swanson 2001; Petrovich, Risold & Swanson 1996), as this might suggest that the BLA initiates memory consolidation processes via indirect modulation of the HPA axis by way of the BST. However, the extant literature examining the BLA on neuroendocrine release suggests this is unlikely. Specifically, lesions of the BLA do not directly impact HPA responding to a threat (Feldman et al., 1994), but rather selectively impair long-term consolidation processes that rely on the integration of glucocorticoids (McGaugh, McIntyre, & Power 2002). As such, it is possible that the projections from the BLA to avBST serve a posttraining modulatory role for integrating the actions of glucocorticoids at the level of the BST, rather than acting as an initiator of HPA related modulation of memory

consolidation as is demonstrated by the avBST here. Indeed, support for the BLA as integrating peripheral hormone signaling within the BST has been reported. Posttraining intra-BLA microinjections of NE, or systemic injections of epinephrine enhance inhibitory avoidance learning (Liang, Juler & McGaugh 1986; Liang & McGaugh, 1983a; 1983b),), and this enhancement is blocked by surgical transection of the major fiber path the BLA utilizes to communicate with avBST (i.e., the stria terminalis). Further, a similar effect is demonstrated following posttraining administration of a glucocorticoid receptor agonist. Specifically, posttraining systemic injection of dexamethasone enhanced memory for inhibitory avoidance training, and this effect was also blocked by surgical transection of the stria terminalis (Roozendaal & McGaugh 1996). Importantly in that study, lesions of the stria terminalis did not significantly affect retention in animals that were not treated with dexamethasone suggesting this fiber tract does not contribute to the mobilization of HPA responding as an enhanced glucocorticoid response following such a manipulation would be expected to enhance inhibitory avoidance learning, such as that demonstrated here. Taken together with our results here, the data suggest that activity within the avBST is recruited to set the level, or “gain” of glucocorticoid mediated memory consolidation, and that posttraining actions of glucocorticoids may depend on a functional interaction between the BLA and structures connected via the stria terminalis-namely the bed nucleus, among others.

Generalization and the HPA axis

Photoinhibition of the rPL – BST pathway promoted generalization of fear to a novel context without altering avoidance to the original training context. Surprisingly, we did not observe this effect was dependent on increased HPA responding despite observing increase in CORT following pathway inactivation, and additional experiments indicated posttraining injections of CORT produce generalized avoidance as well. In comparison, photoinhibition of avBST, or avBST-PVH projections, increased HPA component indices and increased avoidance to the original training context; an effect that was dependent upon increases in CORT. As previously mentioned, an explanation for these seemingly contrasting effects may be that the involvement of BST during memory consolidation is to integrate signals from multiple HPA-inhibitory regions, and that removal of a single HPA-inhibitory component is insufficient to alter HPA responses to the level required to modulate consolidation processes. From this standpoint, it may be that while removal of the rPL-BST pathway activity following IA learning disrupts consolidation of specific features that contribute to alterations in memory specificity, the augmented CORT response observed under pathway inactivation represented a partial recruitment of the HPA axis.

Thus, while our results clearly position the rPL-BST pathway as critical for preventing future generalization regardless of adrenocortical activation, this partial recruitment of the HPA axis following pathway inactivation represents a unique alteration that requires further elaboration from the standpoint of its functional significance. Much of the work on glucocorticoids promoting memory generalization emphasize that high levels

of CORT release are necessary. Specifically, under low-intensity threat levels, glucocorticoids tend to facilitate consolidation resulting in enhanced memory for the core aversive event and do not alter generalization (Kaouane et al., 2012). At high-intensity threat levels, however, glucocorticoids begin to enhance generalization to irrelevant predictors of threat (dos Santos Corrêa et al., 2019). These high levels of glucocorticoids result in morphological, and functional alterations in mPFC (Anderson et al., 2016; 2020), hippocampus (Starkman et al., 1992; Sheline et al., 1996; McEwen & Magarinos 1997; McEwen 1999), and amygdala (Vyas et al., 2002a; Vyas et al., 2002b; Vyas et al., 2006).

As such, under high stress conditions it is possible that multiple HPA-inhibitory circuits show diminished recruitment that results in a sufficiently high glucocorticoid release to facilitate the morphological and function alterations necessary to promote rapid recruitment of defensive behavior regardless of threat likelihood in the future (i.e., manifestation of generalized fear behavior). Indeed, chronic stress, an experimental paradigm in rodents that results in excessive mobilization of the HPA axis in response to acute threats, alters rPL-BST morphological characteristics including reduced spine densities (Radley, Anderson, Hamilton, Alcock & Romig-Martin 2013) suggesting the capacity for further recruitment of the rPL-BST projection following chronic stress, or excessive glucocorticoid release, is diminished. As the rPL-BST pathway is capable of restraining context generalization on its own, the net effect of enhanced glucocorticoid responding would be to bias behavioral responses toward generalization regardless of threat through diminished functional recruitment of the rPL-BST pathway. That our monitoring of BST activity during retention suggest a greater recruitment of BST activity is necessary to overcome increased levels of avoidance in an ostensibly “safe” chamber

align well with the notion that a diminished functional recruitment of this region during avoidance testing might contribute to excessive or inappropriate avoidance.

In addition, our results do not support the notion that rPL-BST pathway inactivation represents an impairment, *per se*. We observed no change in avoidance to the original training context in any manipulation involving this pathway. This lack of decrement, or enhancement, suggests the animals learned the training context at similar levels to that of our controls. It may be expected that a more specific impairment in consolidation would involve reduced levels of avoidance in both contexts, or at least the original training context, similar to that observed following pathway activation of the avBST-vlPAG projection. Accordingly, this “abstracted” representation (i.e., consistent across distinct environments) may be the product of an inability to attend to the specific details that inform an accurate memory while still attending to the overall schema of the aversive event (i.e., organization of footshock and general features of environment into associative category) (Lashley & Wade 1948). Much of the work on cases of PTSD, or other stress-related disorders (Miles & Maren 2019), might suggest a similar mechanism that relates to an impairment in encoding peri-traumatic cues and/or contexts. This idea that generalization represents an impairment in encoding these peri-traumatic cues or contexts might be thought of as an indication of maladaptive behavior. Alternatively, generalized behavior represents an ethologically valid approach for promoting survival in situations of ambiguity, or uncertainty (Asok, Kandel & Rayman 2019). And so, a shift toward generalized behavioral responses may not be reflective of an impairment but rather bias of organismal responses to prioritize risk assessment or caution when exposed to a novel challenge.

Consideration of the vlPAG within the context of memory consolidation

It is generally accepted that the vlPAG is a critical component of the fear circuitry responsible for directly responding to threats (i.e., freezing or immobility) (Carrive 1993; Deng, Xaio & Wang 2016; Fanselow, DeCola, De Oca, Landeira-Fernandez 1995; Kim et al., 2013a). Thus, the vlPAG maintains a role as an output region, directly interfacing with pre-motor effectors within medullary regions to differentially influence threat-related behavior (Cameron, Khan, Westlund & Willis 1995a; Tovote et al., 2016). This predominantly descending circuitry is contrasted with an ascending feature that is proposed to be related to processing, or relay, of affective information to limbic-forebrain regions (Cole & McNally 2009). Indeed, ascending vlPAG projections signal threat probability via an interaction with the central amygdala (Wright & McDannald 2019; Walker, Wright, Jhou & McDannald 2020), and nociceptive signals to the basal forebrain (Yu et al., 2021), along with a projection to the posterior paraventricular thalamus (pPVT) (Cameron, Khan, Westlund, Cliffer & Willis 1995b; Boorman, Brown, Keay 2021) that is broadly involved in affective processing (Yeh, Ozawa & Johansen 2021). As such, activation of an avBST-vlPAG projection following stress exposure may disrupt ascending vlPAG activity signaling affective components of the IA learning event. Consistent with our histochemical procedures outlining the avBST-vlPAG projection is largely GABAergic, we observed reduced activity following optogenetic excitation of the ChR2 expressing

avBST fibers in vlPAG, suggesting post-training activation of the avBST-vlPAG circuit may diminish recruitment of vlPAG during consolidation.

However, the specific post-synaptic targets of the avBST-vlPAG pathway were not addressed here, and prior work has demonstrated BST projections to the vlPAG target a heterogenous population of neuronal subtypes. Specifically, at rostral levels of vlPAG, similar regions BST addressed here target a GABAergic subtype that is largely involved in intra-vlPAG signaling-that is within vlPAG (Hao et al., 2019). Chemogenetic inhibition of this more rostrally oriented projection results in increased cFos immunoreactivity within the vlPAG (Bruzsik et al., 2021), consistent with an inhibitory population that largely targets intra-vlPAG GABAergic interneurons to disinhibit vlPAG output neurons. Conversely, our prior optogenetic targeting of avBST-vlPAG demonstrated behavioral effects consistent with interfacing amongst vlPAG output neurons; a largely glutamatergic subtype residing that may predominate in more caudal regions (Tovote et al., 2016). Specifically, avBST-vlPAG photoexcitation during tail-suspension, or shock-probe defensive burying reduced immobility (Johnson et al., 2016; 2019); a behavior proposed to be exclusively mediated by glutamatergic vlPAG output neurons targeting pre-motor effectors within the magnocellular nucleus of the medulla (Tovote et al., 2016). Moreover, chemogenetic excitation of glutamatergic vlPAG neurons produces higher indices of anxiety-related behavior (Taylor et al., 2019), bidirectionally control the formation of fear memories (Frontera et al., 2020), and microinjections of glutamate into the vlPAG increase markers of sympatho-adrenal activation (Alikhani et al., 2021). As such, activation of a GABAergic avBST cell population targeting glutamatergic pre-autonomic effectors within the vlPAG may contribute to reduced sympatho-adrenal drive and thus

impair IA memory consolidation, as seen here. This would be consistent with prior observations that disruption of sympatho-adrenal activation following IA learning significantly impairs memory (Nielson, Czech, & Laubmeier 1999). Further work will be necessary to elaborate upon these effects, however, as injections of excitatory amino acids in the vlPAG have also been shown to induce behavioral quiescence and hypotension (Bandler, Keay, Floyd & Price 2000) which suggest a complex interplay between vlPAG^{vGlut} and vlPAG^{GABA}, particularly as it relates to input from BST populations that may target both.

That our results targeting avBST-vlPAG produced reduced IA memory consolidation overall, whereas rPL-BST activation promoted a selective enhancement in discrimination while sparing memory for the original aversive context suggest the consolidation network rPL-BST mobilizes to influence future discrimination does not likely involve the vlPAG. This observation is further supported by our data demonstrating that posttraining rPL-vlPAG activation did not influence discrimination. Regardless, our prior and current anatomical characterization of the rPL-BST pathway indicate that rPL is di-synaptically connected to the vlPAG via the BST (Johnson et al., 2019), and that rPL maintains dual-projecting nuclei that directly target both avBST and vlPAG, along with differential sub-BST regions that target vlPAG suggest a complex interaction between these three regions that is not yet reconciled. It may be that rPL differentially recruits BST during the initial learning or consolidation of an aversive event, and vlPAG more specifically during the expression of fear discrimination, as reported by others (Rozeske et al., 2018). Further, as BST receives input from a variety of limbic-forebrain regions the subset of avBST neurons projecting to vlPAG may be exclusively recruited by other

upstream regions (i.e., amygdala, hippocampus, PVT) to diminish consolidation and this projection may not be functionally related to the rPL-BST pathway during memory consolidation. Prior work from our laboratory has also demonstrated that a rPL-avBST-vlPAG circuit is recruited to mediate acute behavioral responses to stress suggesting perhaps a more direct relevance in stress-coping behaviors rather than an associative capacity (Johnson et al., 2016; 2019).

Broader network circuitry underlying rPL-BST enhancement of discrimination

While largely speculative, our anatomical characterization of the downstream network rPL-BST is associated with may offer some insight into the mechanisms by which discrimination is altered following posttraining photoperturbation of rPL-BST. Prior characterization of BST projections throughout the brain reveals a distributed network that involves multiple regions (Dong & Swanson 2004b; Dong, Petrovich, Watts, & Swanson 2001). Our trans-neuronal targeting reveals a substantially more restricted network of downstream regions that are contacted by the rPL-BST pathway. We have previously discussed the vlPAG, and generally accept that this projection may not be involved in mediating discrimination as produce herein. Moreover, di-synaptic targeting of vlPAG via the rPL-BST pathway indicated vlPAG was not one of the main targets (**FIG 3.5**). Outside of the vlPAG, however, and relatively exclusive in the extent with which it was targeted, the hypothalamus was of note (**FIG 3.5**). In particular, we noted significantly greater fluorescent density values for the LH and PVH as compared to several other regions. We expected to find a significant targeting of the PVH, based on our prior work (Johnson et

al., 2019; Radley, Gosselink, Sawchenko 2006) and results demonstrating modulation of the HPA axis following optogenetic inhibition of the rPL-BST pathway. However, despite prior work outlining the importance of the BST-LH pathway in mediating aversive states (Giardino et al., 2018; Jennings et al., 2013b; Rossi & Stuber 2018), and the anatomical characterization of the BST-LH network implicating a robust interaction between these regions we were surprised by the extent with which the LH was targeted. Interestingly, a recent report suggested BST neuronal populations that project to the LH are non-overlapping with those that project to the vlPAG (Hao et al., 2019)

The LH is a region containing a rich diversity of peptidergic neuronal subtypes, including hypocretin (HCRT), leptin (lep), and melanin-concentrating hormone (MCH) (Giardino et al., 2018) containing neurons. LH^{HCRT} has been demonstrated to convey aversive signals (Giardino et al., 2018), and this neuronal population has been reported to receive input from regions of BST containing CRF+ neurons to drive avoidance that would be largely opposite to the pattern of behavioral results demonstrated here. However, the LH^{MCH} population has been recently demonstrated to be critical for prevention of excessive cued-fear behavior (Concetti et al., 2020). More generally, LH^{MCH} neurons are proposed to a modulator of memory storage, specifically as it relates to the stabilization of vigilance/arousal states (Burdakov & Peleg-Raibstein 2020; Adamantidis & de Lecea, 2009). LH^{MCH} neurons target a distributed network of circuits involved in memory processing (e.g., hippocampus) and arousal (e.g., locus coeruleus, raphe nuclei and spinal cord) (Bittencourt et al., 1992; Bittencourt 2011). Of interest to our work with rPL-BST is the LH^{MCH} innervation of the hippocampus, as the hippocampus is critical for mediating context generalization (Seo et al., 2021; Keiser et al., 2017; Wiltgen et al.,

2010). rPL and BST do not directly target the hippocampus, although the rPL maintains connectivity with the entorhinal cortex (Vertes 2004; Hoover & Vertes 2011), presumably as a means of influencing hippocampal activity. As such, our experiments demonstrating increased generalization following rPL-BST photoinhibition represent an interesting problem for describing how this may occur without directly interfacing with the hippocampus. Although more anatomical work is necessary to outline whether the rPL-BST-LH network specifically involves MCH-expressing neurons in the LH, an intriguing possibility with regard to our behavioral results is that inactivation of the rPL-BST projection alters LH^{MCH} neuronal responses during fear learning and consolidation, and this disrupts context processing in the hippocampus by way of a direct LH^{MCH}-Hipp circuit. That LH^{MCH} neurons also directly interact with noradrenergic signaling in the LC (Adamantidis & de Lecea 2009) suggest the possibility for increasing emotional arousal in a manner that might differentially alter fear discrimination and offers a site through which rPL-BST may modulate central noradrenergic signaling in parallel with the mediation of neuroendocrine signaling provided by the targeting of PVH. As the regions of BST investigated here only sparsely target the LC (Dong, Petrovich, Watts & Swanson 2001; Dong & Swanson 2004b), this may implicate a broader network organization that rPL-BST may be predominantly biased toward neuroendocrine and central noradrenergic modulation by way of parallel downstream circuitry involving the PVH and LH, respectively. Overall, a broader network characterization of these circuits will be necessary in the future to more fully appreciate the complexity with which circuit perturbation is altering fear-related memory processing.

Methodological concerns

Electrophysiological properties

Alterations in retention for inhibitory avoidance learning were limited to 20Hz photoexcitation parameters. The use of this stimulation frequency was based on the consensus that 20Hz stimulation allows for excitatory neuronal responses that fall within physiologically relevant frequencies. We have successfully used this stimulation frequency to elicit acute changes in behavioral responses (Johnson et al., 2016; 2019), and associated HPA reactivity, consistent with what others have shown deploying similar stimulation parameters in these regions (Jennings et al., 2013a; Kim et al., 2013a; Henckens et al., 2018). Moreover, we generally observed stimulatory effects that are opposite in sign from that of our photoinhibition experiments or produced no relevant change in retention when applied to specific circuits, suggesting these effects are consistent with a gain-of-function mechanism. Our rPL recording data also demonstrate that following footshock rPL is broadly mobilized, across multiple frequency domains, suggesting prefrontal activity during the post-footshock period is not necessarily specific to a certain frequency. Calcium imaging in BST also support the notion that this region is broadly mobilized following footshock, although calcium imaging does not reflect frequency specific alterations in activity and so further work would be needed to characterize whether frequency dependent alterations were associated with post-footshock BST activity.

However, our *in vivo* recording of rPL data also suggest the presence of frequency specific signaling during retention that is associated with a novel chamber, and consistent with the demonstration that specific frequency parameters are associated with successful disambiguation of threat-related information (Likhtik et al., 2104). In particular, rPL theta band oscillatory power was increased in the 10s prior to latency to enter the adjacent darkened area of the safe chamber suggesting activity within this oscillatory band is critical for preventing inappropriate avoidance, and/or distinguishing the novel chamber from the original training chamber.

Our approach to optogenetic and/or chemogenetic intervention involved “off-line” manipulations during the posttraining period in order to avoid disrupting signaling during these “on-line” periods where the animal is actively engaged in an acquisition or retention specific manner. A critical component here is the use of a delayed stimulation experiment that does not impact retention. In this way, our data from Chp 2 suggest a critical period immediately following the training event is susceptible to intervention, and this does not extend to periods 3hrs after training. That increases in rPL, and BST, activity was associated with avoidance to a novel chamber 2 days following training would suggest these regions are mobilized during retention, however, our data are unable to clarify whether posttraining alterations in rPL or BST activity influence the mobilization of these regions during avoidance testing. A critical endeavor will be examining how regions are mobilized during learning to modulate posttraining consolidation mechanisms, and whether these same neuronal populations are engaged during retention, and if so, what role they play in this capacity.

Additionally, although optogenetic stimulation of soma, or projections is not identical to producing endogenous rhythms, the potential importance of studying specific frequency parameters may underlie the difficulty in producing behavioral or neuroendocrine effects in some experiments here. Specifically, whereas photostimulation of rPL-BST, or avBST-vlPAG were able to modulate inhibitory avoidance learning, rPL-vlPAG and avBST-PVH were not and more generally we were consistently unable to observe *decreases* in HPA responding regardless of circuit manipulation. It may be that HPA reactivity following an acute stressor is unable to be reduced further than a set level of stress hormone responding, as might be determined by recruitment of other stress-neurocircuitry. Alternatively, 20Hz stimulation of PVH projecting BST neurons may not be relevant for modulating HPA activity. Further, whereas the rPL-vlPAG circuit is a putatively glutamatergic projection, avBST-PVH is a GABAergic pathway and the influence of stimulating inhibitory populations within certain frequencies is not well understood, particularly in regions that co-express a variety of neuropeptides. Indeed, it has been reported that channelrhodopsin stimulation at higher frequencies may also encourage responses consistent with the release of neuropeptides (Arrigo & Saper 2014; Jego et al., 2013; Qiu et al., 2016; Adamantidis et al., 2007), that may have contrasting effects to the primary neurotransmitter released.

GABAergic neurons of the BST can be segregated based on membrane and firing properties (Hammack et al., 2007; Rodriguez-Sierra et al., 2013). Of note, a population of low-threshold bursting cells (i.e., Type II) are observed in lateral BST regions similar to those regions examined here. Type II neurons in lateral BST regions have been demonstrated to co-express peptidergic markers for CRF, enkephalin (ENK), and protein

kinase C – delta (PKCδ) (Beyeler and Dabrowska 2020). Although other peptidergic markers are present in this region, electrophysiological properties of these populations have yet to be clarified. Regardless, type II BST cells display burst firing up to 120Hz (Rodriguez-Sierra et al., 2013) within a single burst. Similarly, whereas baseline firing rats of the anteroventral BST are reported to be relatively low (i.e., <4Hz) (Rodriguez-Sierra et al., 2013), recruitment of these regions during context fear expression results in increases in activity up to 30Hz (Haufler et al., 2013). As such, these results demonstrate BST can reliably fire at 20Hz, or greater, consistent with our optogenetic manipulations here. However, this wide range of firing capabilities likely underlies our difficulty producing specific neuroendocrine outcomes using ChR2 stimulation. That avBST projections to the vlPAG do not overlap with avBST projections to PVH (Johnson et al., 2019), and ChR2 stimulation of avBST-vlPAG reduced IA memory consolidation while avBST-PVH ChR2 stimulation did not also suggest the potential that BST projections may be differentially recruited based on frequency parameters. Further studies will need careful consideration of stimulation parameters to elucidate whether specific frequencies can modulate distinct neuronal circuit capacities.

Conclusions

The data reported herein contribute to our overall understanding of BST functioning, particularly as it relates to the modulation of hormonal and behavioral indices associated with threat memory consolidation and generalization. The BST is a critical hub for integration of affective signaling during exposure to a threat and involves dynamically

responding to the presence of danger to determine the degree with which danger is remembered, and through an interaction with prefrontal cortical regions whether that danger may extend to novel situations. In line with these findings, there is abundant evidence that dysfunctional threat processing in regions such as the prefrontal cortex and BST may contribute to the development of stress-related psychiatric diseases characterized by alterations in consolidation and generalization. However, due to the complexity with which these neural circuits mobilize cell-type and pathway specific processes, along with neuroendocrine-dependent and -independent mechanisms during threat learning, it will be imperative for increasingly targeted interrogation of BST and related circuitry to inform the potential for developing therapeutic interventions in cases of psychiatric illness.

REFERENCES

Adamantidis, A. R., Zhang, F., Aravanis, A. M., Deisseroth, K., & De Lecea, L. (2007). Neural substrates of awakening probed with optogenetic control of hypocretin neurons. Nature, 450(7168), 420-424.

Adamantidis, A., & de Lecea, L. (2009). A role for Melanin-Concentrating Hormone in learning and memory. Peptides, 30(11), 2066-2070.

Adolphs, R. (2013). The biology of fear. Current biology, 23(2), R79-R93.

Ahima R, Harlan R (1990) Charting of type II glucocorticoid receptor-like immunoreactivity in the rat central nervous system. Neuroscience 39:579-604.

Ahima R, Krozowsi Z, Harlan R (1991) Type I corticosteroid receptor-like immunoreactivity in the rat CNS: distribution and regulation by corticosteroids. The Journal of Comparative Neurology 313:522-538

Akana SF, Chu A, Soriano L, Dallman MF (2001) Corticosterone exerts site-specific and state-dependent effects in prefrontal cortex and amygdala on regulation of adrenocorticotropic hormone, insulin and fat depots. J Neuroendocrinology 13:625-637.

Akirav, I., & Richter-Levin, G. (1999). Biphasic modulation of hippocampal plasticity by behavioral stress and basolateral amygdala stimulation in the rat. Journal of Neuroscience, 19(23), 10530-10535.

Akirav, I., & Richter-Levin, G. (2002). Mechanisms of amygdala modulation of hippocampal plasticity. Journal of Neuroscience, 22(22), 9912-9921.

Alberini, C. M., & LeDoux, J. E. (2013). Memory reconsolidation. Current Biology, 23(17), R746-R750.

Alexandra Kredlow, M., Fenster, R. J., Laurent, E. S., Ressler, K. J., & Phelps, E. A. (2022). Prefrontal cortex, amygdala, and threat processing: implications for PTSD. Neuropsychopharmacology, 47(1), 247-259.

Alheid, G. F., & Heimer, L. (1988). New perspectives in basal forebrain organization of special relevance for neuropsychiatric disorders: the striatopallidal, amygdaloid, and corticopetal components of substantia innominata. Neuroscience, 27(1), 1-39.

Alikhani, V., Mohebbati, R., Hosseini, M., Khajavirad, A., & Shafei, M. N. (2021). Role of the glutamatergic system of ventrolateral periaqueductal gray (vlPAG) in the cardiovascular responses in normal and hemorrhagic conditions in rats. Iranian Journal of Basic Medical Sciences, 24(5), 586.

Amat J, Matus-Amat P, Watkins LR, Maier SF (1998) Escapable and inescapable stress differentially and selectively alter extracellular levels of 5-HT in the ventral hippocampus and dorsal periaqueductal gray of the rat. Brain Research 797:12-22.

Amat J, Baratta MV, Paul E, Bland ST, Watkins LR, Maier SF (2005) Medial prefrontal cortex determines how stressor controllability affects behavior and dorsal raphe nucleus. Nature Neuroscience 8:365-371.

Andalman AS, Burns VM, Lovett-Barron M, Broxton M, Poole B, Yang SJ, Grosenick L, Lerner TN, Chen R, Benster T (2019) Neuronal dynamics regulating brain and behavioral state transitions. Cell 177:970-985. e920.

Anderson, R. M., Birnie, A. K., Koblesky, N. K., Romig-Martin, S. A., & Radley, J. J. (2014). Adrenocortical status predicts the degree of age-related deficits in prefrontal structural plasticity and working memory. Journal of Neuroscience, 34(25), 8387-8397.

Anderson, R. M., Glanz, R. M., Johnson, S. B., Miller, M. M., Romig-Martin, S. A., & Radley, J. J. (2016). Prolonged corticosterone exposure induces dendritic spine remodeling and attrition in the rat medial prefrontal cortex. Journal of Comparative Neurology, 524(18), 3729-3746.

Anderson, R. M., Johnson, S. B., Lingg, R. T., Hinz, D. C., Romig-Martin, S. A., & Radley, J. J. (2020). Evidence for similar prefrontal structural and functional alterations in male and female rats following chronic stress or glucocorticoid exposure. Cerebral Cortex, 30(1), 353-370.

Antoni FA (1986) Hypothalamic control of adrenocorticotropin secretion: advances since the discovery of 41-residue corticotropin-releasing factor. Endocrine Reviews 7:351-378.

Antoniadis, E. A., & McDonald, R. J. (2006). Fornix, medial prefrontal cortex, nucleus accumbens, and mediodorsal thalamic nucleus: roles in a fear-based context discrimination task. Neurobiology of Learning and Memory, 85(1), 71-85.

Aravanis AM, Wang L-P, Zhang F, Meltzer LA, Mogri MZ, Schneider MB, Deisseroth K (2007) An optical neural interface: in vivo control of rodent motor cortex with integrated fiberoptic and optogenetic technology. Journal of Neural Engineering 4:S143.

Arico, C., Bagley, E. E., Carrive, P., Assareh, N., & McNally, G. P. (2017). Effects of chemogenetic excitation or inhibition of the ventrolateral periaqueductal gray on the acquisition and extinction of Pavlovian fear conditioning. Neurobiology of Learning and Memory, 144, 186-197.

Arrigoni, E., & Saper, C. B. (2014). What optogenetic stimulation is telling us (and failing to tell us) about fast neurotransmitters and neuromodulators in brain circuits for wake–sleep regulation. Current Opinion in Neurobiology, 29, 165-171.

Aronsson, M., Fuxe, K., Dong, Y., Agnati, L. F., Okret, S., & Gustafsson, J. A. (1988). Localization of glucocorticoid receptor mRNA in the male rat brain by in situ hybridization. Proceedings of the National Academy of Sciences, 85(23), 9331-9335.

Asok, A., Draper, A., Hoffman, A. F., Schulkin, J., Lupica, C. R., & Rosen, J. B. (2018). Optogenetic silencing of a corticotropin-releasing factor pathway from the central amygdala to the bed nucleus of the stria terminalis disrupts sustained fear. Molecular psychiatry, 23(4), 914-922.

Asok, A., Kandel, E. R., & Rayman, J. B. (2019). The neurobiology of fear generalization. Frontiers in behavioral neuroscience, 329.

Assareh N, Sarrami M, Carrive P, McNally GP (2016) The Organization of Defensive Behavior Elicited by Optogenetic Excitation of Rat Lateral or Ventrolateral Periaqueductal Gray. Behavioral Neuroscience 130:406-414.

Assareh, N., Bagley, E. E., Carrive, P., & McNally, G. P. (2017). Brief optogenetic inhibition of rat lateral or ventrolateral periaqueductal gray augments the acquisition of Pavlovian fear conditioning. Behavioral Neuroscience, 131(6), 454.

Aston-Jones, G., & Cohen, J. D. (2005). An integrative theory of locus coeruleus-norepinephrine function: adaptive gain and optimal performance. Annual Review Neuroscience, 28, 403-450.

Atucha, E., & Roozendaal, B. (2015). The inhibitory avoidance discrimination task to investigate accuracy of memory. Frontiers in Behavioral Neuroscience, 9, 60.

Atucha, E., Vukojevic, V., Fornari, R. V., Ronzoni, G., Demougin, P., Peter, F., ... & Roozendaal, B. (2017). Noradrenergic activation of the basolateral amygdala maintains hippocampus-dependent accuracy of remote memory. Proceedings of the National Academy of Sciences, 114(34), 9176-9181.

Bahtiyar, S., Karaca, K. G., Henckens, M. J., & Roozendaal, B. (2020). Norepinephrine and glucocorticoid effects on the brain mechanisms underlying memory accuracy and generalization. Molecular and Cellular Neuroscience, 108, 103537.

Bains JS, Wamsteeker Cusulin JI, Inoue W (2015) Stress-related synaptic plasticity in the hypothalamus. Nat Rev Neurosci 16:377-388.

Baldi, E., Lorenzini, C. A., & Bucherelli, C. (2004). Footshock intensity and generalization in contextual and auditory-cued fear conditioning in the rat. Neurobiology of learning and memory, 81(3), 162-166.

Bandler R, Carrive P, Zhang SP (1991) Integration of somatic and autonomic reactions within the midbrain periaqueductal grey: viscerotopic, somatotopic and functional organization. In: Progress in brain research, pp 269-305: Elsevier.

Bandler R, Keay KA, Floyd N, Price J (2000) Central circuits mediating patterned autonomic activity during active vs. passive emotional coping. Brain Res Bull 53:95-104.

Barsegyan, A., Mackenzie, S. M., Kurose, B. D., McGaugh, J. L., & Roozendaal, B. (2010). Glucocorticoids in the prefrontal cortex enhance memory consolidation and impair working memory by a common neural mechanism. Proceedings of the National Academy of Sciences, 107(38), 16655-16660.

Barsegyan, A., McGaugh, J. L., & Roozendaal, B. (2014). Noradrenergic activation of the basolateral amygdala modulates the consolidation of object-in-context recognition memory. Frontiers in Behavioral Neuroscience, 8, 160.

Barsegyan, A., Mirone, G., Ronzoni, G., Guo, C., Song, Q., van Kuppeveld, D., ... & Roozendaal, B. (2019). Glucocorticoid enhancement of recognition memory via basolateral amygdala-driven facilitation of prelimbic cortex interactions. Proceedings of the National Academy of Sciences, 116(14), 7077-7082.

Baxter LR, Jr., Schwartz JM, Phelps ME, Mazziotta JC, Guze BH, Selin CE, Gerner RH, Sumida RM (1989) Reduction of prefrontal cortex glucose metabolism common to three types of depression. Arch Gen Psychiatry 46:243-250.

Bechara A, Damasio H, Damasio AR (2000) Emotion, decision making and the orbitofrontal cortex. Cereb Cortex 10:295-307.

Behbehani MM (1995) Functional characteristics of the midbrain periaqueductal gray. Progress in Neurobiology 46:575-605.

Bevilaqua, L., Ardenghi, P., Schröder, N., Bromberg, E., Schmitz, P. K., Schaeffer, E., Quevedo, J., Bianchin, M., Walz, R., Medina, J. & Izquierdo, I. (1997). Drugs acting upon the cyclic adenosine monophosphate/protein kinase A signalling pathway modulate memory consolidation when given late after training into rat hippocampus but not amygdala. Behavioural Pharmacology, 8(4), 331-338.

Beyeler, A., & Dabrowska, J. (2020). Neuronal diversity of the amygdala and the bed nucleus of the stria terminalis. In Handbook of behavioral neuroscience (Vol. 26, pp. 63-100). Elsevier.

Bigham J. (1894). Memory. The Psychological Review;1:453-461.

Bittencourt, J. C., Presse, F., Arias, C., Peto, C., Vaughan, J., Nahon, J. L., ... & Sawchenko, P. E. (1992). The melanin-concentrating hormone system of the rat brain: an immuno-and hybridization histochemical characterization. Journal of Comparative Neurology, 319(2), 218-245.

Bittencourt, J. C. (2011). Anatomical organization of the melanin-concentrating hormone peptide family in the mammalian brain. General and Comparative Endocrinology, 172(2), 185-197.

Bjorni, M., Rovero, N. G., Yang, E. R., Holmes, A., & Halladay, L. R. (2020). Phasic signaling in the bed nucleus of the stria terminalis during fear learning predicts within-and across-session cued fear expression. Learning & Memory, 27(3), 83-90.

Bland, S. T., Schmid, M. J., Der-Avakian, A., Watkins, L. R., Spencer, R. L., & Maier, S. F. (2005). Expression of c-fos and BDNF mRNA in subregions of the prefrontal cortex of male and female rats after acute uncontrollable stress. Brain Research, 1051(1-2), 90-99.

Bohus B, Benus RF, Fokkema DS, Koolhaas JM, Nyakas C, van Oortmerssen GA, Prins AJ, de Ruiter AJ, Scheurink AJ, Steffens AB (1987) Neuroendocrine states and behavioral and physiological stress responses. Progress in Brain Research 72:57-70.

Bohus, B. (1994). Humoral modulation of learning and memory processes: physiological significance of brain and peripheral mechanisms. In The Memory System of the Brain; Vol. 4 (pp. 337-364). World scientific.

Bodnoff, S. R., Humphreys, A. G., Lehman, J. C., Diamond, D. M., Rose, G. M., & Meaney, M. J. (1995). Enduring effects of chronic corticosterone treatment on spatial learning, synaptic plasticity, and hippocampal neuropathology in young and mid-aged rats. Journal of Neuroscience, 15(1), 61-69.

Boorman, D. C., Brown, R., & Keay, K. A. (2021). Periaqueductal gray inputs to the paraventricular nucleus of the thalamus: Columnar topography and glucocorticoid (in) sensitivity. Brain Research, 1750, 147171.

Boyden ES, Zhang F, Bamberg E, Nagel G, Deisseroth K (2005) Millisecond-timescale, genetically targeted optical control of neural activity. Nature Neuroscience 8:1263-1268.

Brake W, Flores G, Francis D, Meaney M, Srivastava L, Gratton A (2000) Enhanced nucleus accumbens dopamine and plasma corticosterone stress responses in adult rats with neonatal excitotoxic lesions to the medial prefrontal cortex. Neuroscience 96:687-695.

Brandao ML, Zanoveli JM, Ruiz-Martinez RC, Oliveira LC, Landeira-Fernandez J (2008) Different patterns of freezing behavior organized in the periaqueductal gray of rats: Association with different types of anxiety. Behavioural Brain Research 188:1-13.

Brown MR, Rivier C, Vale W (1984) Central Nervous-System Regulation of Adrenocorticotropin Secretion - Role of Somatostatins. Endocrinology 114:1546-1549.

Bruno, C. A., O'Brien, C., Bryant, S., Mejaes, J. I., Estrin, D. J., Pizzano, C., & Barker, D. J. (2021). pMAT: An open-source software suite for the analysis of fiber photometry data. Pharmacology Biochemistry and Behavior, 201, 173093.

Bruzsik, B., Biro, L., Zelena, D., Sipos, E., Szebik, H., Sarosdi, K. R., ... & Toth, M. (2021). Somatostatin neurons of the bed nucleus of stria terminalis enhance associative fear memory consolidation in mice. Journal of Neuroscience, 41(9), 1982-1995.

Buchanan, T. W., & Lovallo, W. R. (2001). Enhanced memory for emotional material following stress-level cortisol treatment in humans. Psychoneuroendocrinology, 26(3), 307-317.

Burdakov, D., & Peleg-Raibstein, D. (2020). The hypothalamus as a primary coordinator of memory updating. Physiology & Behavior, 223, 112988.

Cahill, L., & McGaugh, J. L. (1998). Mechanisms of emotional arousal and lasting declarative memory. Trends in neurosciences, 21(7), 294-299.

Cahill, L., Gorski, L., & Le, K. (2003). Enhanced human memory consolidation with post-learning stress: Interaction with the degree of arousal at encoding. Learning & Memory, 10(4), 270-274.

Cai, D. J., Aharoni, D., Shuman, T., Shobe, J., Biane, J., Song, W., ... & Silva, A. J. (2016). A shared neural ensemble links distinct contextual memories encoded close in time. Nature, 534(7605), 115-118.

Cameron AA, Khan IA, Westlund KN, Willis WD (1995a) The efferent projections of the periaqueductal gray in the rat: a Phaseolus vulgaris-leucoagglutinin study. II. Descending projections. Journal of Comparative Neurology 351:585-601.

Cameron AA, Khan IA, Westlund KN, Cliffer KD, Willis WD (1995b) The efferent projections of the periaqueductal gray in the rat: a Phaseolus vulgarisleucoagglutinin study. I. Ascending projections. Journal of Comparative Neurology 351:568-584.

Cannon WB (1929) Organization for physiological homeostasis. Physiological Reviews 9:399-431.

Canteras, N. S., Simerly, R. B., & Swanson, L. W. (1995). Organization of projections from the medial nucleus of the amygdala: a PHAL study in the rat. Journal of Comparative Neurology, 360(2), 213-245.

Capuzzo, G., & Floresco, S. B. (2020). Prelimbic and infralimbic prefrontal regulation of active and inhibitory avoidance and reward-seeking. Journal of Neuroscience, 40(24), 4773-4787.

Carrive P (1993) The periaqueductal gray and defensive behavior: functional representation and neuronal organization. Behavioural Brain Research 58:27-47.

Carrive P, Leung P, Harris J, Paxinos G (1997) Conditioned fear to context is associated with increased fos expression in the caudal ventrolateral region of the midbrain periaqueductal gray. Neuroscience 78:165-177.

Casada JH, Dafny N (1991) Restraint and Stimulation of Bed Nucleus of the Stria Terminalis Produce Similar Stress-Like Behaviors. Brain Research Bulletin 27:207-212.

Cecchi M, Khoshbouei H, Javors M, Morilak DA (2002) Modulatory effects of norepinephrine in the lateral bed nucleus of the stria terminalis on behavioral and neuroendocrine responses to acute stress. Neuroscience 112:13-21.

Chao, H. M., Choo, P. H., & McEwen, B. S. (1989). Glucocorticoid and mineralocorticoid receptor mRNA expression in rat brain. Neuroendocrinology, 50(4), 365-371.
Chan R, Sawchenko P (1994) Spatially and temporally differentiated patterns of c-fos expression in brainstem catecholamilriergic cell groups induced by cardiovascular challenges in the rat. Journal of Comparative Neurology 348:433-460.
Chang YC, Gottlieb DI (1988) Characterization of the proteins purified with monoclonal antibodies to glutamic acid decarboxylase. Journal of Neuroscience 8:2123-2130.
Chen, D. Y., Bambah-Mukku, D., Pollonini, G., & Alberini, C. M. (2012). Glucocorticoid receptors recruit the CaMKIIα-BDNF-CREB pathways to mediate memory consolidation. Nature Neuroscience, 15(12), 1707-1714.
Chen, Y., Rex, C. S., Rice, C. J., Dubé, C. M., Gall, C. M., Lynch, G., & Baram, T. Z. (2010). Correlated memory defects and hippocampal dendritic spine loss after acute stress involve corticotropin-releasing hormone signaling. Proceedings of the National Academy of Sciences, 107(29), 13123-13128.
Chiba T, Kayahara T, Nakano K (2001) Efferent projections of infralimbic and prelimbic areas of the medial prefrontal cortex in the Japanese monkey, Macaca fuscata. Brain Res 888:83-101.
Choi DC, Furay AR, Evanson NK, Ostrander MM, Ulrich-Lai YM, Herman JP (2007) Bed nucleus of the stria terminalis subregions differentially regulate hypothalamicpituitary-adrenal axis activity: Implications for the integration of limbic inputs. Journal of Neuroscience 27:2025-2034.
Choi DC, Evanson NK, Furay AR, Ulrich-Lai YM, Ostrander MM, Herman JP (2008) The anteroventral bed nucleus of the stria terminalis differentially regulates hypothalamic-pituitary-adrenocortical axis responses to acute and chronic stress. Endocrinology 149:818-826.
Chow BY, Han X, Dobry AS, Qian X, Chuong AS, Li M, Henninger MA, Belfort GM, Lin Y, Monahan PE, Boyden ES (2010) High-performance genetically targetable optical neural silencing by light-driven proton pumps. Nature 463:98-102.
Ciocchi, S., Herry, C., Grenier, F., Wolff, S. B., Letzkus, J. J., Vlachos, I., ... & Lüthi, A. (2010). Encoding of conditioned fear in central amygdala inhibitory circuits. Nature, 468(7321), 277-282.
Clark, R. E., & Sutherland, R. J. (2013). The neurobiology of remote memory in the experimental animal. Neurobiology of learning and memory, 106, 292-293.
Cole, S., & McNally, G. P. (2009). Complementary roles for amygdala and periaqueductal gray in temporal-difference fear learning. Learning & Memory, 16(1), 1-7.
Concetti, C., Bracey, E. F., Peleg-Raibstein, D., & Burdakov, D. (2020). Control of fear extinction by hypothalamic melanin-concentrating hormone–expressing neurons. Proceedings of the National Academy of Sciences, 117(36), 22514-22521.
Corcoran KA, Quirk GJ (2007) Activity in prelimbic cortex is necessary for the expression of learned, but not innate, fears. J Neurosci 27:840-844.
Cordero, M. I., Merino, J. J., & Sandi, C. (1998). Correlational relationship between shock intensity and corticosterone secretion on the establishment and subsequent expression of contextual fear conditioning. Behavioral neuroscience, 112(4), 885.
Cordero, M. I., & Sandi, C. (1998). A role for brain glucocorticoid receptors in contextual fear conditioning: dependence upon training intensity. Brain research, 786(1-2), 11-17.

Crane, J. W., Ebner, K., & Day, T. A. (2003). Medial prefrontal cortex suppression of the hypothalamic–pituitary–adrenal axis response to a physical stressor, systemic delivery of interleukin-1β. European Journal of Neuroscience, 17(7), 1473-1481.

Crestani CC, Alves FH, Correa FM, Guimaraes FS, Joca SR (2010) Acute reversible inactivation of the bed nucleus of stria terminalis induces antidepressant-like effect in the rat forced swimming test. Behav Brain Funct 6:30.

Crestani CC, Alves FH, Gomes FV, Resstel LB, Correa FM, Herman JP (2013) Mechanisms in the bed nucleus of the stria terminalis involved in control of autonomic and neuroendocrine functions: a review. Current Neuropharmacology 11:141-159.

Csaki A, Kocsis K, Halasz B, Kiss J (2000) Localization of glutamatergic/aspartatergic neurons projecting to the hypothalamic paraventricular nucleus studied by retrograde transport of [3H]D-aspartate autoradiography. Neuroscience 101:637-655.

Cullen, P. K., Gilman, T. L., Winiecki, P., Riccio, D. C., & Jasnow, A. M. (2015). Activity of the anterior cingulate cortex and ventral hippocampus underlie increases in contextual fear generalization. Neurobiology of Learning and Memory, 124, 19-27.

Cullinan WE, Herman JP, Watson SJ (1993) Ventral subicular interaction with the hypothalamic paraventricular nucleus: evidence for a relay in the bed nucleus of the stria terminalis. The Journal of Comparative Neurology 332:1-20.

Cullinan WE, Herman JP, Battaglia DF, Akil H, Watson SJ (1995a) Pattern and time course of immediate early gene expression in rat brain following acute stress. Neuroscience 64:477-505.

Cullinan WE, Herman JP, Battaglia DF, Akil H, Watson S (1995b) Pattern and time course of immediate early gene expression in rat brain following acute stress. Neuroscience 64:477-505.

Cullinan, W. E., Ziegler, D. R., & Herman, J. P. (2008). Functional role of local GABAergic influences on the HPA axis. Brain Structure and Function, 213(1), 63-72.

Dallman MF, Yates FE (1969) Dynamic asymmetries in the corticosteroid feedback path and distribution-metabolism-binding elements of the adrenocortical system. Annals of the New York Academy of Sciences 156:696-721.

Dallman M, Jones M (1973) Corticosteroid feedback control of ACTH secretion: effect of stress-induced corticosterone secretion on subsequent stress responses in the rat. Endocrinology 92:1367-1375.

Dallman, M. F., Viau, V. G., Bhatnagar, S., Gomez, F., Laugero, K., & Bell, M. E. (2002). Corticotropin-releasing factor, corticosteroids, stress, and sugar: energy balance, the brain, and behavior. In Hormones, brain and behavior (pp. 571-631). Academic Press.

Dallman MF (2005) Fast glucocorticoid actions on brain: back to the future. Front Neuroendocrinol 26:103-108.

Daniel SE, Rainnie DG (2016) Stress Modulation of Opposing Circuits in the Bed Nucleus of the Stria Terminalis. Neuropsychopharmacol 41:103-125.

Davis M, Walker DL, Miles L, Grillon C (2010) Phasic vs Sustained Fear in Rats and Humans: Role of the Extended Amygdala in Fear vs Anxiety. Neuropsychopharmacol 35:105-135.

Day TA (2005) Defining stress as a prelude to mapping its neurocircuitry: No help fromallostasis. Prog Neuro-Psychoph 29:1195-1200.
de Boer S, Koopmans S, Slangen J, Van der Gugten J (1990) Plasma catecholamine, corticosterone and glucose responses to repeated stress in rats: effect of interstressor interval length. Physiology & behavior 47:1117-1124.
de Bundel, D., Zussy, C., Espallergues, J., Gerfen, C. R., Girault, J. A., & Valjent, E. (2016). Dopamine D2 receptors gate generalization of conditioned threat responses through mTORC1 signaling in the extended amygdala. Molecular psychiatry, 21(11), 1545-1553.
de Kloet ER, Oitzl MS, Joëls M (1999) Stress and cognition: are corticosteroids good or bad guys? Trends in Neurosciences 22:422-426.
de Kloet, E. R., Joëls, M., & Holsboer, F. (2005). Stress and the brain: from adaptation to disease. Nature reviews neuroscience, 6(6), 463-475.
de Olmos, J. S., Beltramino, C. A., & Alheid, G. (2004). Amygdala and extended amygdala of the rat: a cytoarchitectonical, fibroarchitectonical, and chemoarchitectonical survey. In The rat nervous system (pp. 509-603). Academic Press.
de Quervain, D., Schwabe, L., & Roozendaal, B. (2017). Stress, glucocorticoids and memory: implications for treating fear-related disorders. Nature Reviews Neuroscience, 18(1), 7-19.
Deng H, Xiao X, Wang Z (2016) Periaqueductal gray neuronal activities underlie different aspects of defensive behaviors. J Neurosci 36:7580-7588.
Dewar, M. T., Cowan, N., & Della Sala, S. (2007). Forgetting due to retroactive interference: A fusion of Müller and Pilzecker's (1900) early insights into everyday forgetting and recent research on anterograde amnesia. Cortex, 43(5), 616-634.
Diamond, D. M., Bennett, M. C., Fleshner, M., & Rose, G. M. (1992). Inverted-U relationship between the level of peripheral corticosterone and the magnitude of hippocampal primed burst potentiation. Hippocampus, 2(4), 421-430.
Diamond, D. M., & Rose, G. M. (1994). Stress impairs LTP and hippocampal-dependent memory. Stress.
Diehl MM, Bravo-Rivera C, Rodriguez-Romaguera J, Pagan-Rivera PA, Burgos-Robles A, Roman-Ortiz C, Quirk GJ (2018) Active avoidance requires inhibitory signaling in the rodent prelimbic prefrontal cortex. Elife 7.143
Diehl, M. M., Iravedra-Garcia, J. M., Morán-Sierra, J., Rojas-Bowe, G., Gonzalez-Diaz, F. N., Valentín-Valentín, V. P., & Quirk, G. J. (2020). Divergent projections of the prelimbic cortex bidirectionally regulate active avoidance. Elife, 9, e59281.
Diorio D, Viau V, Meaney MJ (1993) The role of the medial prefrontal cortex (cingulate gyrus) in the regulation of hypothalamic-pituitary-adrenal responses to stress. J Neurosci 13:3839-3847.
Donley, M. P., Schulkin, J., & Rosen, J. B. (2005). Glucocorticoid receptor antagonism in the basolateral amygdala and ventral hippocampus interferes with long-term memory of contextual fear. Behavioural brain research, 164(2), 197-205.
Dong, H.W., Petrovich, G. D., & Swanson, L. W. (2001). Topography of projections from amygdala to bed nuclei of the stria terminalis. Brain research reviews, 38(1-2), 192-246.

Dong HW, Petrovich GD, Watts AG, Swanson LW (2001) Basic organization of projections from the oval and fusiform nuclei of the bed nuclei of the stria terminalis in adult rat brain. Journal of Comparative Neurology 436:430-455.
Dong HW, Swanson LW (2004a) Projections from bed nuclei of the stria terminalis, posterior division: implications for cerebral hemisphere regulation of defensive and reproductive behaviors. The Journal of Comparative Neurology 471:396-433.
Dong, H. W., & Swanson, L. W. (2004b). Organization of axonal projections from the anterolateral area of the bed nuclei of the stria terminalis. Journal of Comparative Neurology, 468(2), 277-298.
Dong HW, Swanson LW (2006a) Projections from bed nuclei of the stria terminalis, anteromedial area: cerebral hemisphere integration of neuroendocrine, autonomic, and behavioral aspects of energy balance. The Journal of Comparative Neurology 494:142-178.
Dong HW, Swanson LW (2006b) Projections from bed nuclei of the stria terminalis, dorsomedial nucleus: Implications for cerebral hemisphere integration of neuroendocrine, autonomic, and drinking responses. The Journal of Comparative Neurology 494:75-107.
dos Santos Corrêa, M., dos Santos Vaz, B., Grisanti, G. D. V., de Paiva, J. P. Q., Tiba, P. A., & Fornari, R. V. (2019). Relationship between footshock intensity, post-training corticosterone release and contextual fear memory specificity over time. Psychoneuroendocrinology, 110, 104447.
Drevets WC, Price JL, Simpson JR, Jr., Todd RD, Reich T, Vannier M, Raichle ME (1997) Subgenual prefrontal cortex abnormalities in mood disorders. Nature 386:824-827.
Duncan, C. P. (1949). The retroactive effect of electroshock on learning. Journal of comparative and physiological psychology, 42(1), 32.
Dunn JD (1987a) Plasma corticosterone responses to electrical stimulation of the bed nucleus of the stria terminalis. Brain Res 407:327-331.
Dunn JD (1987b) Differential plasma corticosterone responses to electrical stimulation of the medial and lateral septal nuclei. Neuroendocrinology 46:406-411.
Dunn, J. D., & Orr, S. E. (1984). Differential plasma corticosterone responses to hippocampal stimulation. Experimental Brain Research, 54(1), 1-6.
Dunn, J. D., & Whitener, J. (1986). Plasma corticosterone responses to electrical stimulation of the amygdaloid complex: cytoarchitectural specificity. Neuroendocrinology, 42(3), 211-217.
Dunsmoor, J. E., & Paz, R. (2015). Fear generalization and anxiety: behavioral and neural mechanisms. Biological psychiatry, 78(5), 336-343.
Duvarci, S., & Paré, D. (2007). Glucocorticoids enhance the excitability of principal basolateral amygdala neurons. Journal of Neuroscience, 27(16), 4482-4491.
Duvarci, S., Bauer, E. P., & Paré, D. (2009). The bed nucleus of the stria terminalis mediates inter-individual variations in anxiety and fear. Journal of Neuroscience, 29(33), 10357-10361.
Dymond, S., Dunsmoor, J. E., Vervliet, B., Roche, B., & Hermans, D. (2015). Fear generalization in humans: systematic review and implications for anxiety disorder research. Behavior therapy, 46(5), 561-582.
Ely DL (1981) Hypertension, social rank, and aortic arteriosclerosis in CBA/J mice. Physiology & behavior 26:655-661.

Elzinga, B. M., Schmahl, C. G., Vermetten, E., van Dyck, R., & Bremner, J. D. (2003). Higher cortisol levels following exposure to traumatic reminders in abuse-related PTSD. Neuropsychopharmacology, 28(9), 1656-1665.

Emmons, E. B., De Corte, B. J., Kim, Y., Parker, K. L., Matell, M. S., & Narayanan, N. S. (2017). Rodent medial frontal control of temporal processing in the dorsomedial striatum. Journal of Neuroscience, 37(36), 8718-8733.

Ericsson A, Kovacs KJ, Sawchenko PE (1994) A Functional Anatomical Analysis of Central Pathways Subserving the Effects of Interleukin-1 on Stress-Related Neuroendocrine Neurons. J Neurosci 14:897-913.

Erlander MG, Tillakaratne NJ, Feldblum S, Patel N, Tobin AJ (1991) Two genes encode distinct glutamate decarboxylases. Neuron 7:91-100.

Fanselow MS (1980) Conditional and unconditional components of post-shock freezing. The Pavlovian Journal of Biological Science: Official Journal of the Pavlovian 15:177-182.

Fanselow MS, DeCola JP, De Oca BM, Landeira-Fernandez J (1995) Ventral and dorsolateral regions of the midbrain periaqueductal gray (PAG) control different stages of defensive behavior: Dorsolateral PAG lesions enhance the defensive freezing produced by massed and immediate shock. Aggressive Behavior 21:63-77.

Fanselow, M. S., & Dong, H. W. (2010). Are the dorsal and ventral hippocampus functionally distinct structures?. Neuron, 65(1), 7-19.

Feldman, S., Conforti, N., & Saphier, D. (1990). The preoptic area and bed nucleus of the stria terminalis are involved in the effects of the amygdala on adrenocortical secretion. Neuroscience, 37(3), 775-779.

Feldman, S., Conforti, N., Itzik, A., & Weidenfeld, J. (1994). Differential effect of amygdaloid lesions on CRF-41, ACTH and corticosterone responses following neural stimuli. Brain research, 658(1-2), 21-26.

Ferraguti F, Zoli M, Aronsson M, Agnati LF, Goldstein M, Filer D, Fuxe K (1990) Distribution of glutamic acid decarboxylase messenger RNA-containing nerve cell populations of the male rat brain. Journal of chemical neuroanatomy 3:377-396.

Ferry, B., Roozendaal, B., & McGaugh, J. L. (1999). Role of norepinephrine in mediating stress hormone regulation of long-term memory storage: a critical involvement of the amygdala. Biological Psychiatry, 46(9), 1140-1152.

Fetterly, T. L., Basu, A., Nabit, B. P., Awad, E., Williford, K. M., Centanni, S. W., ... & Winder, D. G. (2019). α2A-adrenergic receptor activation decreases parabrachial nucleus excitatory drive onto BNST CRF neurons and reduces their activity in vivo. Journal of Neuroscience, 39(3), 472-484.

Figueiredo HF, Bruestle A, Bodie B, Dolgas CM, Herman JP (2003) The medial prefrontal cortex differentially regulates stress-induced c-fos expression in the forebrain depending on type of stressor. Eur J Neurosci 18:2357-2364.

Fink, G. (2011). Stress controversies: post-traumatic stress disorder, hippocampal volume, gastroduodenal ulceration. Journal of Neuroendocrinology, 23(2), 107-117.

Finsterwald, C., & Alberini, C. M. (2014). Stress and glucocorticoid receptor-dependent mechanisms in long-term memory: from adaptive responses to psychopathologies. Neurobiology of learning and memory, 112, 17-29.

Flood, J. F., Vidal, D., Bennett, E. L., Orme, A. E., Vasquez, S., & Jarvik, M. E. (1978). Memory facilitating and anti-amnesic effects of corticosteroids. Pharmacology Biochemistry and Behavior, 8(1), 81-87.

Floyd NS, Keay KA, Arias CM, Sawchenko PE, Bandler R (1996) Projections from the ventrolateral periaqueductal gray to endocrine regulatory subdivisions of the paraventricular nucleus of the hypothalamus in the rat. Neuroscience Letters 220:105-108.

Floyd NS, Price JL, Ferry AT, Keay KA, Bandler R (2000) Orbitomedial prefrontal cortical projections to distinct longitudinal columns of the periaqueductal gray in the rat. Journal of Comparative Neurology 422:556-578.

Fox AS, Oler JA, Tromp do PM, Fudge JL, Kalin NH (2015) Extending the amygdala in theories of threat processing. Trends Neurosci 38:319-329.

Fox, A. S., Shelton, S. E., Oakes, T. R., Converse, A. K., Davidson, R. J., & Kalin, N. H. (2010). Orbitofrontal cortex lesions alter anxiety-related activity in the primate bed nucleus of stria terminalis. Journal of Neuroscience, 30(20), 7023-7027.

Frontera, J. L., Baba Aissa, H., Sala, R. W., Mailhes-Hamon, C., Georgescu, I. A., Léna, C., & Popa, D. (2020). Bidirectional control of fear memories by cerebellar neurons projecting to the ventrolateral periaqueductal grey. Nature Communications, 11(1), 1-17.

Frysztak, R. J., & Neafsey, E. J. (1994). The effect of medial frontal cortex lesions on cardiovascular conditioned emotional responses in the rat. Brain Research, 643(1-2), 181-193.

Gallagher, B. B., Flanigin, H. F., King, D. W., & Littleton, W. H. (1987). The effect of electrical stimulation of medial temporal lobe structures in epileptic patients upon ACTH, prolactin, and growth hormone. Neurology, 37(2), 299-299.

García-López, M., Abellán, A., Legaz, I., Rubenstein, J. L., Puelles, L., & Medina, L. (2008). Histogenetic compartments of the mouse centromedial and extended amygdala based on gene expression patterns during development. Journal of Comparative Neurology, 506(1), 46-74.

Giardino, W. J., Eban-Rothschild, A., Christoffel, D. J., Li, S. B., Malenka, R. C., & de Lecea, L. (2018). Parallel circuits from the bed nuclei of stria terminalis to the lateral hypothalamus drive opposing emotional states. Nature Neuroscience, 21(8), 1084-1095.

Giardino, W. J., & Pomrenze, M. B. (2021). Extended amygdala neuropeptide circuitry of emotional arousal: waking up on the wrong side of the bed nuclei of stria terminalis. Frontiers in behavioral neuroscience, 6.

Gilmartin MR, Balderston NL, Helmstetter FJ (2014) Prefrontal cortical regulation of fear learning. Trends Neurosci 37:455-464.

Ginsberg AB, Campeau S, Day HE, Spencer RL (2003) Acute glucocorticoid pretreatment suppresses stress-induced hypothalamic-pituitary-adrenal axis hormone secretion and expression of corticotropin-releasing hormone hnRNA but does not affect cfos mRNA or fos protein expression in the paraventricular nucleus of the hypothalamus. J Neuroendocrinol 15:1075-1083.

Glangetas C, Massi L, Fois GR, Jalabert M, Girard D, Diana M, Yonehara K, Roska B, Xu C, Luthi A, Caille S, Georges F (2017) NMDA-receptor-dependent plasticity in the bed nucleus of the stria terminalis triggers long-term anxiolysis. Nat Commun 8:14456.

Glover, L. R., McFadden, K. M., Bjorni, M., Smith, S. R., Rovero, N. G., Oreizi-Esfahani, S., ... & Holmes, A. (2020). A prefrontal-bed nucleus of the stria terminalis circuit limits fear to uncertain threat. ELife, 9, e60812.

Goel N, Bale TL (2009) Examining the intersection of sex and stress in modelling neuropsychiatric disorders. J Neuroendocrinol 21:415-420.

Goel N, Workman JL, Lee TT, Innala L, Viau V (2014) Sex differences in the HPA axis. Compr Physiol 4:1121-1155.

Gold, P. E., & Van Buskirk, R. B. (1975). Facilitation of time-dependent memory processes with posttrial epinephrine injections. Behavioral biology, 13(2), 145-153.

Gold, P. E., & van Buskirk, R. (1978). Posttraining brain norepinephrine concentrations: correlation with retention performance of avoidance training and with peripheral epinephrine modulation of memory processing. Behavioral Biology, 23(4), 509-520.

Goode, T. D., & Maren, S. (2017). Role of the bed nucleus of the stria terminalis in aversive learning and memory. Learning & Memory, 24(9), 480-491.

Goode, T. D., Ressler, R. L., Acca, G. M., Miles, O. W., & Maren, S. (2019). Bed nucleus of the stria terminalis regulates fear to unpredictable threat signals. Elife, 8, e46525.

Goode, T. D., Acca, G. M., & Maren, S. (2020). Threat imminence dictates the role of the bed nucleus of the stria terminalis in contextual fear. Neurobiology of learning and memory, 167, 107116.

Gourley, S. L., Swanson, A. M., Jacobs, A. M., Howell, J. L., Mo, M., DiLeone, R. J., ... & Taylor, J. R. (2012). Action control is mediated by prefrontal BDNF and glucocorticoid receptor binding. Proceedings of the National Academy of Sciences, 109(50), 20714-20719.

Gray TS, Carney ME, Magnuson DJ (1989) Direct projections from the central amygdaloid nucleus to the hypothalamic paraventricular nucleus: possible role in stress induced adrenocorticotropin release. Neuroendocrinology 50:433-446.

Gray TS, Piechowski RA, Yracheta JM, Rittenhouse PA, Bethea CL, Van de Kar LD (1993) Ibotenic acid lesions in the bed nucleus of the stria terminalis attenuate conditioned stress-induced increases in prolactin, ACTH and corticosterone. Neuroendocrinology 57:517-524.

Grosso, A., Santoni, G., Manassero, E., Renna, A., & Sacchetti, B. (2018). A neuronal basis for fear discrimination in the lateral amygdala. Nature communications, 9(1), 1-12.

Gungor, N. Z., & Paré, D. (2016). Functional heterogeneity in the bed nucleus of the stria terminalisfunctional heterogeneity in the bed nucleus of the stria terminalis. Journal of Neuroscience, 36(31), 8038-8049.

Hägglöf B, Blom L, Dahlquist G, Lönnberg G, Sahlin B (1991) The Swedish childhood diabetes study: indications of severe psychological stress as a risk factor for type 1 (insulin-dependent) diabetes mellitus in childhood. Diabetologia 34:579-583.

Hall RE, Marr HB (1975) Influence of electrical stimulation of posterior orbital cortex upon plasma cortisol levels in unanesthetized sub-human primate. Brain research.
Hamani C, Diwan M, Macedo CE, Brandao ML, Shumake J, Gonzalez-Lima F, Raymond R, Lozano AM, Fletcher PJ, Nobrega JN (2010) Antidepressant-like effects of medial prefrontal cortex deep brain stimulation in rats. Biol Psychiatry 67:117-124.
Hammack SE, Mania I, Rainnie DG (2007) Differential expression of intrinsic membrane currents in defined cell types of the anterolateral bed nucleus of the stria terminalis. Journal of Neurophysiology 98:638-656.
Hammack, S. E., Todd, T. P., Kocho-Schellenberg, M., & Bouton, M. E. (2015). Role of the bed nucleus of the stria terminalis in the acquisition of contextual fear at long or short context-shock intervals. Behavioral neuroscience, 129(5), 673.
Hammen C (2005) Stress and depression. Annu Rev Clin Psychol 1:293-319.
Han X, Boyden ES (2007) Multiple-color optical activation, silencing, and desynchronization of neural activity, with single-spike temporal resolution. PloS one 2:e299.
Hao, S., Yang, H., Wang, X., He, Y., Xu, H., Wu, X., ... & Wang, H. (2019). The lateral hypothalamic and BNST GABAergic projections to the anterior ventrolateral periaqueductal gray regulate feeding. Cell Reports, 28(3), 616-624.
Hatfield, T., & McGaugh, J. L. (1999). Norepinephrine infused into the basolateral amygdala posttraining enhances retention in a spatial water maze task. Neurobiology of learning and memory, 71(2), 232-239.
Haufler D, Nagy FZ, Pare D (2013) Neuronal correlates of fear conditioning in the bed nucleus of the stria terminalis. Learning & Memory 20:633-641.
Heimer, L., & Alheid, G. F. (1991). Piecing together the puzzle of basal forebrain anatomy. The basal forebrain, 1-42.
Henckens, M. J. A. G., Printz, Y., Shamgar, U., et al. (2017). CRF receptor type 2 neurons in the posterior bed nucleus of the stria terminalis critically contribute to stress recovery. Molecular Psychiatry, 22(12), 1691-1700.
Henry JP (1992) Biological basis of the stress response. Integrative physiological and behavioral science : the official journal of the Pavlovian Society 27:66-83.
Henry JP, Stephens PM (1977) Stress, Health and the social environment: a sociobiological approach to medicine. Berlin: Springer.
Henry JP, Liu Y-Y, Nadra WE, Qian C-g, Mormede P, Lemaire V, Ely D, Hendley ED (1993) Psychosocial stress can induce chronic hypertension in normotensive strains of rats. Hypertension 21:714-723.
Herman JP, Cullinan WE, Watson SJ (1994a) Involvement of the bed nucleus of the stria terminalis in tonic regulation of paraventricular hypothalamic CRH and AVP mRNA expression. J Neuroendocrinol 6:433-442.
Herman JP, Cullinan WE, Watson SJ (1994b) Involvement of the Bed Nucleus of the Stria Terminalis in Tonic Regulation of Paraventricular Hypothalamic Crh and Avp Messenger-Rna Expression. J Neuroendocrinol 6:433-442.
Herman JP, Adams D, Prewitt C (1995) Regulatory changes in neuroendocrine stressintegrative circuitry produced by a variable stress paradigm. Neuroendocrinology 61:180-190.
Herman JP, Cullinan WE (1997) Neurocircuitry of stress: central control of the hypothalamo–pituitary–adrenocortical axis. Trends in Neurosciences 20:78-84.

Herman, J. P., Dolgas, C. M., & Carlson, S. L. (1998). Ventral subiculum regulates hypothalamo–pituitary–adrenocortical and behavioural responses to cognitive stressors. Neuroscience, 86(2), 449-459.

Herman JP, Figueiredo H, Mueller NK, Ulrich-Lai Y, Ostrander MM, Choi DC, Cullinan WE (2003) Central mechanisms of stress integration: hierarchical circuitry controlling hypothalamo–pituitary–adrenocortical responsiveness. Frontiers in neuroendocrinology 24:151-180.

Herman, J. P., Ostrander, M. M., Mueller, N. K., & Figueiredo, H. (2005). Limbic system mechanisms of stress regulation: hypothalamo-pituitary-adrenocortical axis. Progress in Neuro-Psychopharmacology and Biological Psychiatry, 29(8), 1201-1213.

Hill MN, McLaughlin RJ, Pan B, Fitzgerald ML, Roberts CJ, Lee TT, Karatsoreos IN, Mackie K, Viau V, Pickel VM, McEwen BS, Liu QS, Gorzalka BB, Hillard CJ (2011) Recruitment of prefrontal cortical endocannabinoid signaling by glucocorticoids contributes to termination of the stress response. J Neurosci 31:10506-10515.

Holstege G (2014) The periaqueductal gray controls brainstem emotional motor systems including respiration. In: Progress in Brain Research, pp 379-405: Elsevier.

Hoover, W. B., & Vertes, R. P. (2011). Projections of the medial orbital and ventral orbital cortex in the rat. Journal of Comparative Neurology, 519(18), 3766-3801.

Huff ML, Miller RL, Deisseroth K, Moorman DE, LaLumiere RT (2013) Posttraining optogenetic manipulations of basolateral amygdala activity modulate consolidation of inhibitory avoidance memory in rats. Proceedings of the National Academy of Sciences of the United States of America 110:3597-3602.

Huff, N. C., Wright-Hardesty, K. J., Higgins, E. A., Matus-Amat, P., & Rudy, J. W. (2005). Context pre-exposure obscures amygdala modulation of contextual-fear conditioning. Learning & memory, 12(5), 456-460.

Hulsey, D. R., Riley, J. R., Loerwald, K. W., Rennaker II, R. L., Kilgard, M. P., & Hays, S. A. (2017). Parametric characterization of neural activity in the locus coeruleus in response to vagus nerve stimulation. Experimental Neurology, 289, 21-30.

Hui, G. K., Figueroa, I. R., Poytress, B. S., Roozendaal, B., McGaugh, J. L., & Weinberger, N. M. (2004). Memory enhancement of classical fear conditioning by post-training injections of corticosterone in rats. Neurobiology of Learning and Memory, 81(1), 67-74.

Hurley KM, Herbert H, Moga MM, Saper CB (1991) Efferent projections of the infralimbic cortex of the rat. The Journal of Comparative Neurology 308:249-276.

Ikegaya, Y., Saito, H., & Abe, K. (1995). Requirement of basolateral amygdala neuron activity for the induction of long-term potentiation in the dentate gyrus in vivo. Brain research, 671(2), 351-354.

Izquierdo, I., da Cunha, C., Rosat, R., Jerusalinsky, D., Ferreira, M. B. C., & Medina, J. H. (1992). Neurotransmitter receptors involved in post-training memory processing by the amygdala, medial septum, and hippocampus of the rat. Behavioral and neural biology, 58(1), 16-26.

Jacobson, L., & Sapolsky, R. (1991). The role of the hippocampus in feedback regulation of the hypothalamic-pituitary-adrenocortical axis. Endocrine reviews, 12(2), 118-134.

Jankord, R., & Herman, J. P. (2008). Limbic regulation of hypothalamo-pituitary-adrenocortical function during acute and chronic stress. Annals of the New York Academy of Sciences, 1148(1), 64-73.
Jego, S., Glasgow, S. D., Herrera, C. G., Ekstrand, M., Reed, S. J., Boyce, R., ... & Adamantidis, A. R. (2013). Optogenetic identification of a rapid eye movement sleep modulatory circuit in the hypothalamus. Nature Neuroscience, 16(11), 1637-1643.
Jennings JH, Sparta DR, Stamatakis AM, Ung RL, Pleil KE, Kash TL, Stuber GD (2013a) Distinct extended amygdala circuits for divergent motivational states. Nature 496:224-228.
Jennings, J. H., Rizzi, G., Stamatakis, A. M., Ung, R. L., & Stuber, G. D. (2013b). The inhibitory circuit architecture of the lateral hypothalamus orchestrates feeding. Science, 341(6153), 1517-1521.
Joëls, M., & De Kloet, E. R. (1992). Coordinative mineralocorticoid and glucocorticoid receptor-mediated control of responses to serotonin in rat hippocampus. Neuroendocrinology, 55(3), 344-350.
Joëls, M., & Krugers, H. J. (2007). LTP after stress: up or down?. Neural Plasticity, 2007.
Joëls, M., Fernandez, G., & Roozendaal, B. (2011). Stress and emotional memory: a matter of timing. Trends in Cognitive Sciences, 15(6), 280-288.
Johansen, J. P., Tarpley, J. W., LeDoux, J. E., & Blair, H. T. (2010). Neural substrates for expectation-modulated fear learning in the amygdala and periaqueductal gray. Nature Neuroscience, 13(8), 979-986.
Johnson SB, Emmons EB, Anderson RM, Glanz RM, Romig-Martin SA, Narayanan NS, LaLumiere RT, Radley JJ (2016) A Basal Forebrain Site Coordinates the Modulation of Endocrine and Behavioral Stress Responses via Divergent Neural Pathways. J Neurosci 36:8687-8699.
Johnson SB, Emmons EB, Lingg RT, Anderson RM, Romig-Martin SA, LaLumiere RT, Narayanan NS, Viau V, Radley JJ (2019) Prefrontal–bed nucleus circuit modulation of a passive coping response set. J Neurosci 39:1405-1419.
Johnston, J. B. (1923). Further Contributions to the Study to the Evolution of the Forebrain, Journal of Comparative Neurology, 35(5), 337.
Jones M, Hillhouse E, Burden J (1976) Effect of various putative neurotransmitters on the secretion of corticotrophin-releasing hormone from the rat hypothalamus in vitro–a model of the neurotransmitters involved. Journal of Endocrinology 69:1-10.
Kaouane, N., Porte, Y., Vallée, M., Brayda-Bruno, L., Mons, N., Calandreau, L., ... & Desmedt, A. (2012). Glucocorticoids can induce PTSD-like memory impairments in mice. Science, 335(6075), 1510-1513.
Keay KA, Bandler R (2001) Parallel circuits mediating distinct emotional coping reactions to different types of stress. Neurosci Biobehav R 25:669-678.
Keller-Wood ME, Dallman MF (1984) Corticosteroid inhibition of ACTH secretion. Endocrine Reviews 5:1-24.
Keller-Wood M (2015) Hypothalamic-Pituitary--Adrenal Axis-Feedback Control. Compr Physiol 5:1161-1182.

Keiser, A. A., Turnbull, L. M., Darian, M. A., Feldman, D. E., Song, I., & Tronson, N. C. (2017). Sex differences in context fear generalization and recruitment of hippocampus and amygdala during retrieval. Neuropsychopharmacology, 42(2), 397-407.

Kim EJ, Horovitz O, Pellman BA, Tan LM, Li Q, Richter-Levin G, Kim JJ (2013a) Dorsal periaqueductal gray-amygdala pathway conveys both innate and learned fear responses in rats. Proceedings of the National Academy of Sciences 110:14795-14800.

*Kim, J. S., Han, S. Y., & Iremonger, K. J. (2019). Stress experience and hormone feedback tune distinct components of hypothalamic CRH neuron activity. Nature communications, 10(1), 1-15.

Kim SY, Adhikari A, Lee SY, Marshel JH, Kim CK, Mallory CS, Lo M, Pak S, Mattis J, Lim BK, Malenka RC, Warden MR, Neve R, Tye KM, Deisseroth K (2013b) Diverging neural pathways assemble a behavioural state from separable features in anxiety. Nature 496:219-223.

Kitamura, T., Ogawa, S. K., Roy, D. S., Okuyama, T., Morrissey, M. D., Smith, L. M., ... & Tonegawa, S. (2017). Engrams and circuits crucial for systems consolidation of a memory. Science, 356(6333), 73-78.

Kivimäki, M., Virtanen, M., Elovainio, M., Kouvonen, A., Väänänen, A., & Vahtera, J. (2006). Work stress in the etiology of coronary heart disease—a meta-analysis. Scandinavian Journal of Work, Environment & Health, 431-442.

Kolodziejczyk, M. H., & Fendt, M. (2020). Corticosterone treatment and incubation time after contextual fear conditioning synergistically induce fear memory generalization in neuropeptide S receptor-deficient mice. Frontiers in Neuroscience, 14, 128.

Kovács, G. L., Telegdy, G., & Lissák, K. (1977). Dose-dependent action of corticosteroids on brain serotonin content and passive avoidance behavior. Hormones and Behavior, 8(2), 155-165.

Krantz DS, McCeney MK (2002) Effects of psychological and social factors on organic disease: a critical assessment of research on coronary heart disease. Annual Review of Psychology 53:341-369.

Krettek JE, Price JL (1977) The cortical projections of the mediodorsal nucleus and adjacent thalamic nuclei in the rat. The Journal of Comparative Neurology 171:157-191.

Kudo T, Uchigashima M, Miyazaki T, Konno K, Yamasaki M, Yanagawa Y, Minami M, Watanabe M (2012) Three Types of Neurochemical Projection from the Bed Nucleus of the Stria Terminalis to the Ventral Tegmental Area in Adult Mice. J Neurosci 32:18035-18046.

LaLumiere, R. T., Buen, T. V., & McGaugh, J. L. (2003). Post-training intra-basolateral amygdala infusions of norepinephrine enhance consolidation of memory for contextual fear conditioning. Journal of Neuroscience, 23(17), 6754-6758.

LaLumiere, R. T., McGaugh, J. L., & McIntyre, C. K. (2017). Emotional modulation of learning and memory: pharmacological implications. Pharmacological Reviews, 69(3), 236-255.

Lashley, K. S. (1917). The Effects of Strychnine and Caffeine Upon the Rate of Learning. Psychobiology, 1(2), 141.

Lashley, K. S., & Wade, M. (1946). The Pavlovian theory of generalization. Psychological Review, 53(2), 72.
Latané, B., & Schachter, S. (1962). Adernalin and avoidance learning. Journal of Comparative and Physiological Psychology, 55(3), 369.
Layton, B., & Krikorian, R. (2002). Memory mechanisms in posttraumatic stress disorder. The Journal of neuropsychiatry and clinical neurosciences, 14(3), 254-261.
Lebow MA, Chen A (2016) Overshadowed by the amygdala: the bed nucleus of the stria terminalis emerges as key to psychiatric disorders. Mol Psychiatry. 21(4), 450-463.
Ledoux JE, Iwata J, Cicchetti P, Reis DJ (1988) Different Projections of the Central Amygdaloid Nucleus Mediate Autonomic and Behavioral-Correlates of Lehmann, H., Lacanilao, S., & Sutherland, R. J. (2007). Complete or partial hippocampal damage produces equivalent retrograde amnesia for remote contextual fear memories. European Journal of Neuroscience, 25(5), 1278-1286.Conditioned Fear. J Neurosci 8:2517-2529.
Lehmann, H., Lacanilao, S., & Sutherland, R. J. (2007). Complete or partial hippocampal damage produces equivalent retrograde amnesia for remote contextual fear memories. European Journal of Neuroscience, 25(5), 1278-1286.
Lesuis, S. L., Timmermans, W., Lucassen, P. J., Hoogenraad, C. C., & Krugers, H. J. (2020). Glucocorticoid and β-adrenergic regulation of hippocampal dendritic spines. Journal of Neuroendocrinology, 32(1), e12811.
Lesuis, S. L., Brosens, N., Immerzeel, N., van der Loo, R. J., Mitrić, M., Bielefeld, P., ... & Krugers, H. J. (2021). Glucocorticoids promote fear generalization by increasing the size of a dentate gyrus engram cell population. Biological psychiatry, 90(7), 494-504.
Li H-Y, Sawchenko P (1998) Hypothalamic effector neurons and extended circuitries activated in “neurogenic” stress: a comparison of footshock effects exerted acutely, chronically, and in animals with controlled glucocorticoid levels. Journal of Comparative Neurology 393:244-266.
Li, X., Rubio, F. J., Zeric, T., Bossert, J. M., Kambhampati, S., Cates, H. M., ... & Shaham, Y. (2015). Incubation of methamphetamine craving is associated with selective increases in expression of Bdnf and trkb, glutamate receptors, and epigenetic enzymes in cue-activated fos-expressing dorsal striatal neurons. Journal of Neuroscience, 35(21), 8232-8244.
Liang, K. C., & McGaugh, J. L. (1983a). Lesions of the stria terminalis attenuate the amnestic effect of amygdaloid stimulation on avoidance responses. Brain research, 274(2), 309-318.
Liang, K. C., & McGaugh, J. L. (1983b). Lesions of the stria terminalis attenuate the enhancing effect of post-training epinephrine on retention of an inhibitory avoidance response. Behavioural brain research, 9(1), 49-58.
Liang, K. C., Juler, R. G., & McGaugh, J. L. (1986). Modulating effects of posttraining epinephrine on memory: involvement of the amygdala noradrenergic system. Brain Research, 368(1), 125-133.
Liang, Chen & Huang (1995). The role of amygdala norepinephrine in memory formation: involvement in the memory enhancing effect of peripheral epinephrine." The Chinese journal of physiology 38, 2: 81-91.

Liang, K.C., Chen, H.C., & Chen, D.Y. (2001) Posttraining infusion of norepinephrine and corticotropin releasing factor into the bed nucleus of the stria terminalis enhanced retention in an inhibitory avoidance task. The Chinese Journal of Physiology 44: 33-43.

Liberzon, I., & Sripada, C. S. (2007). The functional neuroanatomy of PTSD: a critical review. Progress in Brain Research, 167, 151-169.

Likhtik, E., Stujenske, J. M., Topiwala, M. A., Harris, A. Z., & Gordon, J. A. (2014). Prefrontal entrainment of amygdala activity signals safety in learned fear and innate anxiety. Nature neuroscience, 17(1), 106-113.

Lingg, R. T., Johnson, S. B., Emmons, E. B., Anderson, R. M., Romig-Martin, S. A., Narayanan, N. S., ... & Radley, J. J. (2020). Bed nuclei of the stria terminalis modulate memory consolidation via glucocorticoid-dependent and-independent circuits. Proceedings of the National Academy of Sciences, 117(14), 8104-8114.

Liu, T. L., Chen, D. Y., & Liang, K. C. (2009). Post-training infusion of glutamate into the bed nucleus of the stria terminalis enhanced inhibitory avoidance memory: An effect involving norepinephrine. Neurobiology of Learning and Memory, 91(4), 456-465.

Liu, T. L., & Liang, K. C. (2009). Posttraining infusion of cholinergic drugs into the ventral subiculum modulated memory in an inhibitory avoidance task: Interaction with the bed nucleus of the stria terminalis. Neurobiology of learning and memory, 91(3), 235-242.

Loewy AD, McKellar S (1980) The neuroanatomical basis of central cardiovascular control. Fed Proc 39:2495-2503.

Lupien, S. J., & McEwen, B. S. (1997). The acute effects of corticosteroids on cognition: integration of animal and human model studies. Brain research reviews, 24(1), 1-27.

Lynch, J., Cullen, P. K., Jasnow, A. M., & Riccio, D. C. (2013). Sex differences in the generalization of fear as a function of retention intervals. Learning & memory, 20(11), 628-632.

Makino, S., Gold, P. W., & Schulkin, J. (1994). Corticosterone effects on corticotropin-releasing hormone mRNA in the central nucleus of the amygdala and the parvocellular region of the paraventricular nucleus of the hypothalamus. Brain Research, 640(1-2), 105-112.

Marcinkiewcz, C. A., Mazzone, C. M., D'Agostino, G., Halladay, L. R., Hardaway, J. A., DiBerto, J. F., ... & Kash, T. L. (2016). Serotonin engages an anxiety and fear-promoting circuit in the extended amygdala. Nature, 537(7618), 97-101.

Maren, S. (2001). Neurobiology of Pavlovian fear conditioning. Annual review of neuroscience, 24(1), 897-931.

Martínez-Rivera, F. J., Pérez-Torres, J., Velázquez-Díaz, C. D., Sánchez-Navarro, M. J., Huertas-Pérez, C. I., Diehl, M. M., ... & Quirk, G. J. (2022). A novel insular/orbital-prelimbic circuit that prevents persistent avoidance in a rodent model of compulsive behavior. Biological Psychiatry.

Mason, J. W. (1958). Plasma 17-hydroxycorticosteroid levels during electrical stimulation of the amygdaloid complex in conscious monkeys. American Journal of Physiology-Legacy Content, 196(1), 44-48.

Mason JW (1972) Corticosteroid response to chair restraint in the monkey. American Journal of Physiology-Legacy Content 222:1291-1294.
Mason JW (1975) A historical view of the stress field. Journal of Human Stress 1:22-36.
Mason JW, Maher JT, Hartley LH, Mougey EH, Perlow MJ, Jones LG (1976) Selectivity of corticosteroid and catecholamine responses to various natural stimuli. New York: Springer.
Mason, J. W., Giller, E. L., Kosten, T. R., Ostroff, R. B., & Podd, L. (1986). Urinary free-cortisol levels in posttraumatic stress disorder patients. Journal of Nervous and Mental Disease 174:145-149.
Matheson, G. K., Branch, B. J., & Taylor, A. N. (1971). Effects of amygdaloid stimulation on pituitary-adrenal activity in conscious cats. Brain Research, 32(1), 151-167.
Mazure CM (1998) Life stressors as risk factors in depression. Clinical Psychology: Science and Practice 5:291-313.
McDonald, A. J. (1998). Cortical pathways to the mammalian amygdala. Progress in neurobiology, 55(3), 257-332.
McDonald, A. J., Shammah-Lagnado, S. J., Shi, C., & Davis, M. (1999). Cortical afferents to the extended amygdala. Annals of the New York Academy of Sciences, 877(1), 309-338.
McEwen, B. S., Weiss, J. M., & Schwartz, L. S. (1968). Selective retention of corticosterone by limbic structures in rat brain. Nature, 220(5170), 911-912.
McEwen BS, de Kloet R, Wallach G (1976) Interactions in vivo and in vitro of corticoids and progesterone with cell nuclei and soluble macromolecules from rat brain regions and pituitary. Brain Research 105:129-136.
McEwen, B. S., De Kloet, E. R., & Rostene, W. (1986). Adrenal steroid receptors and actions in the nervous system. Physiological Reviews, 66(4), 1121-1188.
McEwen, B. S., & Sapolsky, R. M. (1995). Stress and cognitive function. Current Opinion in Neurobiology, 5(2), 205-216.
McEwen, B. S., & Magarinos, A. M. (1997). Stress effects on morphology and function of the hippocampus. Annals of the New York Academy of Sciences, 821, 271-284.
McEwen, B. S. (1999). Stress and hippocampal plasticity. Annual Review of Neuroscience, 22(1), 105-122.
McGaugh, J. L. (1966). Time-Dependent Processes in Memory Storage: Recent studies of learning and memory indicate that memory storage involves time-dependent processes. Science, 153(3742), 1351-1358.
McGaugh, J.L. and M.J. Herz, Memory Consolidation. 1972, San Francisco: Albion Pub. Co. viii, 204.
McGaugh, J. L. (1999). The perseveration-consolidation hypothesis: Mueller and Pilzecker, 1900. Brain research bulletin.
McGaugh, J. L. (2000). Memory--a century of consolidation. Science, 287(5451), 248-251.
McGaugh, J. L., McIntyre, C. K., & Power, A. E. (2002). Amygdala modulation of memory consolidation: interaction with other brain systems. Neurobiology of Learning and Memory, 78(3), 539-552.
McGaugh JL, Roozendaal B (2002) Role of adrenal stress hormones in forming lasting memories in the brain. Current Opinion in Neurobiology 12:205-210.

McGaugh, J. L. (2003). Memory and emotion: The making of lasting memories. Columbia University Press.
McGaugh, J. L. (2013). Making lasting memories: Remembering the significant. Proceedings of the National Academy of Sciences, 110(Supplement 2), 10402-10407.
McIntyre, C. K., & Roozendaal, B. (2007). 13 Adrenal Stress Hormones and Enhanced Memory for Emotionally Arousing Experiences. Neural plasticity and memory: from genes to brain imaging, 265.
McNally, G. P., Johansen, J. P., & Blair, H. T. (2011). Placing prediction into the fear circuit. Trends in Neurosciences, 34(6), 283-292.
Meaney MJ, Aitken DH (1985) [3H]Dexamethasone binding in rat frontal cortex. Brain Res 328:176-180.
Medina, A. C., Charles, J. R., Espinoza-González, V., Sánchez-Resendis, O., Prado-Alcalá, R. A., Roozendaal, B., & Quirarte, G. L. (2007). Glucocorticoid administration into the dorsal stratium facilitates memory consolidation of inhibitory avoidance training but not of the context or footshock components. Learning & Memory, 14(10), 673-677.
Miller EK, Cohen JD (2001) An integrative theory of prefrontal cortex function. Annu Rev Neurosci 24:167-202.
Miles, O. W., & Maren, S. (2019). Role of the bed nucleus of the stria terminalis in PTSD: insights from preclinical models. Frontiers in Behavioral Neuroscience, 13, 68
Miyashita, T., & Williams, C. L. (2006). Epinephrine administration increases neural impulses propagated along the vagus nerve: Role of peripheral β-adrenergic receptors. Neurobiology of Learning and Memory, 85(2), 116-124.
Monroe SM, Simons AD (1991) Diathesis-stress theories in the context of life stress research: implications for the depressive disorders. Psychological bulletin 110:406.
Morgan MA, LeDoux JE (1995) Differential contribution of dorsal and ventral medial prefrontal cortex to the acquisition and extinction of conditioned fear in rats. Behav Neurosci 109:681-688.
Müller, G. E., & Pilzecker, A. (1900). Experimentelle beiträge zur lehre vom gedächtniss (Vol. 1). JA Barth.
Mugnaini E, Oertel W (1985) Handbook of chemical neuroanatomy, Vol 4, GABA and neuropeptides in the CNS, part I.
Myers B, McKlveen JM, Herman JP (2014) Glucocorticoid actions on synapses, circuits, and behavior: implications for the energetics of stress. Front Neuroendocrinol 35:180-196.
Nadel, L., Winocur, G., Ryan, L., & Moscovitch, M. (2007). Systems consolidation and hippocampus: two views. Debates in Neuroscience, 1(2), 55-66.
Nielson, K. A., Czech, D. A., & Laubmeier, K. K. (1999). Chronic administration of propranolol impairs inhibitory avoidance retention in mice. Neurobiology of Learning and Memory, 71(2), 248-257.
Oitzl, M. S., & de Kloet, E. R. (1992). Selective corticosteroid antagonists modulate specific aspects of spatial orientation learning. Behavioral neuroscience, 106(1), 62.

Okuda, S., Roozendaal, B., & McGaugh, J. L. (2004). Glucocorticoid effects on object recognition memory require training-associated emotional arousal. Proceedings of the National Academy of Sciences, 101(3), 853-858.
O'Reilly, R. C., & Rudy, J. W. (2001). Conjunctive representations in learning and memory: principles of cortical and hippocampal function. Psychological review, 108(2), 311.
Paxinos, G., & Watson, C. (2006). The rat brain in stereotaxic coordinates. (Elsevier Academic, Amsterdam).
Pedraza, L. K., Sierra, R. O., Boos, F. Z., Haubrich, J., Quillfeldt, J. A., & de Oliveira Alvares, L. (2016). The dynamic nature of systems consolidation: Stress during learning as a switch guiding the rate of the hippocampal dependency and memory quality. Hippocampus, 26(3), 362-371.
Pelletier, J. G., Likhtik, E., Filali, M., & Paré, D. (2005). Lasting increases in basolateral amygdala activity after emotional arousal: implications for facilitated consolidation of emotional memories. Learning & Memory, 12(2), 96-102.
Plotsky PM, Otto S, Sutton S (1987) Neurotransmitter modulation of corticotropin releasing factor secretion into the hypophysial-portal circulation. Life Sciences 41:1311-1317.
Pomrenze, M. B., Millan, E. Z., Hopf, F. W., Keiflin, R., Maiya, R., Blasio, A., ... & Messing, R. O. (2015). A transgenic rat for investigating the anatomy and function of corticotrophin releasing factor circuits. Frontiers in Neuroscience, 9, 487.
Pomrenze, M. B., Fetterly, T. L., Winder, D. G., & Messing, R. O. (2017). The corticotropin releasing factor receptor 1 in alcohol use disorder: still a valid drug target?. Alcoholism: Clinical and Experimental Research, 41(12), 1986-1999.
Pomrenze, M. B., Giovanetti, S. M., Maiya, R., Gordon, A. G., Kreeger, L. J., & Messing, R. O. (2019). Dissecting the roles of GABA and neuropeptides from rat central amygdala CRF neurons in anxiety and fear learning. Cell Reports, 29(1), 13-21.
Porter RW (1954) The central nervous system and stress-induced eosinopenia. Recent Progress in Hormone Research.
Poulin JF, Arbour D, Laforest S, Drolet G (2009) Neuroanatomical characterization of endogenous opioids in the bed nucleus of the stria terminalis. Prog Neuropsychopharmacol Biol Psychiatry 33:1356-1365.
Poulos, A. M., Mehta, N., Lu, B., Amir, D., Livingston, B., Santarelli, A., ... & Fanselow, M. S. (2016). Conditioning-and time-dependent increases in context fear and generalization. Learning & Memory, 23(7), 379-385.
Prewitt CM, Herman JP (1998) Anatomical interactions between the central amygdaloid nucleus and the hypothalamic paraventricular nucleus of the rat: a dual tracttracing analysis. Journal of Chemical Neuroanatomy 15:173-186.
Qiu, J., Nestor, C. C., Zhang, C., Padilla, S. L., Palmiter, R. D., Kelly, M. J., & Rønnekleiv, O. K. (2016). High-frequency stimulation-induced peptide release synchronizes arcuate kisspeptin neurons and excites GnRH neurons. Elife, 5, e16246.
Quirarte, G. L., Roozendaal, B., & McGaugh, J. L. (1997). Glucocorticoid enhancement of memory storage involves noradrenergic activation in the basolateral amygdala. Proceedings of the National Academy of Sciences, 94(25), 14048-14053.

Radley JJ, Arias CM, Sawchenko PE (2006) Regional Differentiation of the Medial Prefrontal Cortex in Regulating Adaptive Responses to Acute Emotional Stress. J Neurosci 26:12967-12976.
Radley JJ, Williams B, Sawchenko PE (2008) Noradrenergic innervation of the dorsal medial prefrontal cortex modulates hypothalamo-pituitary-adrenal responses to acute emotional stress. J Neurosci 28:5806-5816.
Radley JJ, Gosselink KL, Sawchenko PE (2009) A Discrete GABAergic Relay Mediates Medial Prefrontal Cortical Inhibition of the Neuroendocrine Stress Response. J Neurosci 29:7330-7340.
Radley JJ, Sawchenko PE (2011) A Common Substrate for Prefrontal and Hippocampal Inhibition of the Neuroendocrine Stress Response. J Neurosci 31:9683-9695.
Radley JJ (2012) Toward a limbic cortical inhibitory network: implications for hypothalamic-pituitary-adrenal responses following chronic stress. Front Behav Neurosci 6:7.
Radley JJ, Anderson RM, Hamilton BA, Alcock JA, Romig-Martin SA (2013) Chronic stress-induced alterations of dendritic spine subtypes predict functional decrements in an hypothalamo-pituitary-adrenal-inhibitory prefrontal circuit. J Neurosci 33:14379-14391.
Radley JJ, Sawchenko PE (2015) Evidence for involvement of a limbic paraventricular hypothalamic inhibitory network in hypothalamic-pituitary-adrenal axis adaptations to repeated stress. The Journal of Comparative Neurology 523:2769-2787.
Radley, J. J., & Johnson, S. B. (2018). Anteroventral bed nuclei of the stria terminalis neurocircuitry: Towards an integration of HPA axis modulation with coping behaviors-Curt Richter Award Paper 2017. Psychoneuroendocrinology, 89, 239-249.
Räikkönen K, Keltikangas-Järvinen L, Adlercreutz H, Hautanen A (1996) Psychosocial stress and the insulin resistance syndrome. Metabolism 45:1533-1538.
Redgate, E. S., & Fahringer, E. E. (1973). A comparison of the pituitary adrenal activity elicited by electrical stimulation of preoptic, amygdaloid and hypothalamic sites in the rat brain. Neuroendocrinology, 12(6), 334-343.
Rekkas, P. V., & Constable, R. T. (2005). Evidence that autobiographic memory retrieval does not become independent of the hippocampus: an fMRI study contrasting very recent with remote events. Journal of cognitive neuroscience, 17(12), 1950-1961.
Ressler, K. J. (2010). Amygdala activity, fear, and anxiety: modulation by stress. Biological Psychiatry, 67(12), 1117-1119.
Ressler, R. L., Goode, T. D., Evemy, C., & Maren, S. (2020). NMDA receptors in the CeA and BNST differentially regulate fear conditioning to predictable and unpredictable threats. Neurobiology of learning and memory, 174, 107281.
Reul, J. M. H. M., & de Kloet, E. D. (1985). Two receptor systems for corticosterone in rat brain: microdistribution and differential occupation. Endocrinology, 117(6), 2505-2511.
Reynolds SM, Zahm DS (2005) Specificity in the projections of prefrontal and insular cortex to ventral striatopallidum and the extended amygdala. J Neurosci 25:11757-11767.
Rivier C, Vale W (1983) Interaction of corticotropin-releasing factor and arginine vasopressin on adrenocorticotropin secretion in vivo. Endocrinology 113:939-942.

Robin, J., & Moscovitch, M. (2017). Details, gist and schema: hippocampal–neocortical interactions underlying recent and remote episodic and spatial memory. Current opinion in behavioral sciences, 17, 114-123.

Rodriguez-Romaguera, J., Ung, R. L., Nomura, H., Otis, J. M., Basiri, M. L., Namboodiri, V. M., ... & Stuber, G. D. (2020). Prepronociceptin-expressing neurons in the extended amygdala encode and promote rapid arousal responses to motivationally salient stimuli. Cell Reports, 33(6), 108362.

Rodríguez-Sierra OE, Turesson HK, Pare D (2013) Contrasting distribution of physiological cell types in different regions of the bed nucleus of the stria terminalis. Journal of Neurophysiology 110:2037-2049.

Roozendaall, B., Bohus, B., & McGaugh, J. L. (1996). Dose-dependent suppression of adrenocortical activity with metyrapone: effects on emotion and memory. Psychoneuroendocrinology, 21(8), 681-693.

Roozendaal, B., & McGaugh, J. L. (1996a). Amygdaloid nuclei lesions differentially affect glucocorticoid-induced memory enhancement in an inhibitory avoidance task. Neurobiology of Learning and Memory, 65(1), 1-8.

Roozendaal, B., & McGaugh, J. L. (1996b). The memory-modulatory effects of glucocorticoids depend on an intact stria terminalis. Brain research, 709(2), 243-250.

Roozendaal, B., Carmi, O., & McGaugh, J. L. (1996). Adrenocortical suppression blocks the memory-enhancing effects of amphetamine and epinephrine. Proceedings of the National Academy of Sciences, 93(4), 1429-1433.

Roozendaal, B., Portillo-Marquez, G., & McGaugh, J. L. (1996). Basolateral amygdala lesions block glucocorticoid-induced modulation of memory for spatial learning. Behavioral Neuroscience, 110(5), 1074.

Roozendaal, B., & McGaugh, J. L. (1997). Basolateral amygdala lesions block the memory-enhancing effect of glucocorticoid administration in the dorsal hippocampus of rats. European Journal of Neuroscience, 9(1), 76-83.

Roozendaal, B., Nguyen, B. T., Power, A. E., & McGaugh, J. L. (1999). Basolateral amygdala noradrenergic influence enables enhancement of memory consolidation induced by hippocampal glucocorticoid receptor activation. Proceedings of the National Academy of Sciences, 96(20), 11642-11647.

Roozendaal, B., Williams, C. L., & McGaugh, J. L. (1999). Glucocorticoid receptor activation in the rat nucleus of the solitary tract facilitates memory consolidation: involvement of the basolateral amygdala. European Journal of Neuroscience, 11(4), 1317-1323.

Roozendaal, B., Griffith, Q. K., Buranday, J., Dominique, J. F., & McGaugh, J. L. (2003). The hippocampus mediates glucocorticoid-induced impairment of spatial memory retrieval: dependence on the basolateral amygdala. Proceedings of the National Academy of Sciences, 100(3), 1328-1333.

Roozendaal, B., Hui, G. K., Hui, I. R., Berlau, D. J., McGaugh, J. L., & Weinberger, N. M. (2006). Basolateral amygdala noradrenergic activity mediates corticosterone-induced enhancement of auditory fear conditioning. Neurobiology of Learning and Memory, 86(3), 249-255.

Roozendaal, B., McEwen, B. S., & Chattarji, S. (2009). Stress, memory and the amygdala. Nature Reviews Neuroscience, 10(6), 423-433.

Roozendaal, B., McReynolds, J. R., Van der Zee, E. A., Lee, S., McGaugh, J. L., & McIntyre, C. K. (2009). Glucocorticoid effects on memory consolidation depend on functional interactions between the medial prefrontal cortex and basolateral amygdala. Journal of neuroscience, 29(45), 14299-14308.

Roozendaal, B., & McGaugh, J. L. (2011). Memory modulation. Behavioral neuroscience, 125(6), 797.

Roozendaal, B., & Mirone, G. (2020). Opposite effects of noradrenergic and glucocorticoid activation on accuracy of an episodic-like memory. Psychoneuroendocrinology, 114, 104588.

Rosen, J. B., Asok, A., & Chakraborty, T. (2015). The smell of fear: innate threat of 2, 5-dihydro-2, 4, 5-trimethylthiazoline, a single molecule component of a predator odor. Frontiers in Neuroscience, 9, 292.

Rosenkranz, J. A., Venheim, E. R., & Padival, M. (2010). Chronic stress causes amygdala hyperexcitability in rodents. Biological Psychiatry, 67(12), 1128-1136.

Rossi, M. A., & Stuber, G. D. (2018). Overlapping brain circuits for homeostatic and hedonic feeding. Cell Metabolism, 27(1), 42-56.

Rozeske, R. R., Valerio, S., Chaudun, F., & Herry, C. (2015). Prefrontal neuronal circuits of contextual fear conditioning. Genes, Brain and Behavior, 14(1), 22-36

Rozeske, R. R., Jercog, D., Karalis, N., Chaudun, F., Khoder, S., Girard, D., ... & Herry, C. (2018). Prefrontal-periaqueductal gray-projecting neurons mediate context fear discrimination. Neuron, 97(4), 898-910.

Rozanski A, Blumenthal JA, Kaplan J (1999) Impact of psychological factors on the pathogenesis of cardiovascular disease and implications for therapy. Circulation 99:2192-2217.

Rubin, R. T., Mandell, A. J., & Crandall, P. H. (1966). Corticosteroid responses to limbic stimulation in man: localization of stimulus sites. Science, 153(3737), 767-768.

Reul, J. M. H. M., & Kloet, E. D. (1985). Two receptor systems for corticosterone in rat brain: microdistribution and differential occupation. Endocrinology, 117(6), 2505-2511.

Sandi, C., & Rose, S. P. (1994). Corticosterone enhances long-term retention in one-day-old chicks trained in a weak passive avoidance learning paradigm. Brain Research, 647(1), 106-112.

Sandi, C., Loscertales, M., & Guaza, C. (1997). Experience-dependent facilitating effect of corticosterone on spatial memory formation in the water maze. European journal of neuroscience, 9(4), 637-642.

Sandi, C., & Pinelo-Nava, M. T. (2007). Stress and memory: behavioral effects and neurobiological mechanisms. Neural Plasticity, 2007.

Sangha, S., Diehl, M. M., Bergstrom, H. C., & Drew, M. R. (2020). Know safety, no fear. Neuroscience & Biobehavioral Reviews, 108, 218-230.

Saphier, D., & Feldman, S. (1987). Effects of septal and hippocampal stimuli on paraventricular nucleus neurons. Neuroscience, 20(3), 749-755.

Sapolsky, R. M., Krey, L. C., & McEwen, B. S. (1984). Glucocorticoid-sensitive hippocampal neurons are involved in terminating the adrenocortical stress response. Proceedings of the National Academy of Sciences, 81(19), 6174-6177.

Sapolsky, R. M., Armanini, M. P., Sutton, S. W., & Plotsy, P. M. (1989). Elevation of hypophysial portal concentrations of adrenocorticotropin secretagogues after fornix transection. Endocrinology, 125(6), 2881-2887.
Sapolsky RM (1992) Stress, the aging brain, and the mechanisms of neuron death: the MIT Press.
Sawchenko, P. E., Brown, E. R., Chan, R. K. W., Ericsson, A., Li, H. Y., Roland, B. L., & Kovacs, K. J. (1996). The paraventricular nucleus of the hypothalamus and the functional neuroanatomy of visceromotor responses to stress. Progress in brain research, 107, 201-222.
Sawchenko P, Swanson L (1983) The organization of forebrain afferents to the paraventricular and supraoptic nuclei of the rat. Journal of Comparative Neurology 218:121-144.
Schulz D, Canbeyli RS (2000) Lesion of the bed nucleus of the stria terminalis enhances learned despair. Brain Res Bull 52:83-87.
Schreurs, J., Seelig, T., & Schulman, H. (1986). β2-Adrenergic receptors on peripheral nerves. Journal of neurochemistry, 46(1), 294-296.
Schwerdtfeger RMH, Menard JL (2008) The lateral hypothalamus and anterior hypothalamic nucleus differentially contribute to rats' defensive responses in the elevated plus-maze and shock-probe burying tests. Physiology & Behavior 93:697-705.
Selye H (1936) A syndrome produced by diverse nocuous agents. Nature 138:32.
Selye H (1950) The physiology and pathology of exposure to stress.
Selye H (1979) The stress concept and some of its implications. Human stress and cognition: An information processing approach:11-32.
Selye H (1980) Stress in health and disease. Boston: Butterworths.
Seo, D. O., Zhang, E. T., Piantadosi, S. C., Marcus, D. J., Motard, L. E., Kan, B. K., ... & Bruchas, M. R. (2021). A locus coeruleus to dentate gyrus noradrenergic circuit modulates aversive contextual processing. Neuron, 109(13), 2116-2130.
Sesack SR, Deutch AY, Roth RH, Bunney BS (1989) Topographical organization of the efferent projections of the medial prefrontal cortex in the rat: an anterograde tracttracing study with Phaseolus vulgaris leucoagglutinin. The Journal of Comparative Neurology 290:213-242.
Sharp, B. M. (2017). Basolateral amygdala and stress-induced hyperexcitability affect motivated behaviors and addiction. Translational Psychiatry, 7(8), e1194-e1194.
Sharpe, M. J., Marchant, N. J., Whitaker, L. R., Richie, C. T., Zhang, Y. J., Campbell, E. J., ... & Schoenbaum, G. (2017). Lateral hypothalamic GABAergic neurons encode reward predictions that are relayed to the ventral tegmental area to regulate learning. Current Biology, 27(14), 2089-2100.
Sharpe, M. J., & Killcross, S. (2018). Modulation of attention and action in the medial prefrontal cortex of rats. Psychological review, 125(5), 822.
Sharpe, M. J., Batchelor, H. M., Mueller, L. E., Gardner, M. P., & Schoenbaum, G. (2021). Past experience shapes the neural circuits recruited for future learning. Nature Neuroscience, 24(3), 391-400.
Sheline YI, Wang PW, Gado MH, Csernansky JG, Vannier MW (1996) Hippocampal atrophy in recurrent major depression. Proceedings of the National Academy of Sciences of the United States of America 93:3908-3913.

Sherin, J. E., & Nemeroff, C. B. (2011). Post-traumatic stress disorder: the neurobiological impact of psychological trauma. Dialogues in clinical neuroscience, 13(3), 263.
Shin JW, Geerling JC, Loewy AD (2008) Inputs to the ventrolateral bed nucleus of the stria terminalis. Journal of Comparative Neurology 511:628-657.
Sierra-Mercado, D., Padilla-Coreano, N., & Quirk, G. J. (2011). Dissociable roles of prelimbic and infralimbic cortices, ventral hippocampus, and basolateral amygdala in the expression and extinction of conditioned fear. Neuropsychopharmacology, 36(2), 529-538.
Sotres-Bayon F, Quirk GJ (2010) Prefrontal control of fear: more than just extinction. Curr Opin Neurobiol 20:231-235.
Sousa, N., Lukoyanov, N. V., Madeira, M. D., Almeida, O. F. X., & Paula-Barbosa, M. M. (2000). Reorganization of the morphology of hippocampal neurites and synapses after stress-induced damage correlates with behavioral improvement. Neuroscience, 97(2), 253-266.
Southwick, S. M., Krystal, J. H., Morgan, C. A., Johnson, D., Nagy, L. M., Nicolaou, A., Heninger, G.R., & Charney, D. S. (1993). Abnormal noradrenergic function in posttraumatic stress disorder. Archives of General Psychiatry, 50(4), 266-274.
Spencer SJ, Buller KM, Day TA (2005) Medial prefrontal cortex control of the paraventricular hypothalamic nucleus response to psychological stress: possible role of the bed nucleus of the stria terminalis. The Journal of Comparative Neurology 481:363-376.
Starkman, M. N., Gebarski, S. S., Berent, S., & Schteingart, D. E. (1992). Hippocampal formation volume, memory dysfunction, and cortisol levels in patients with Cushing's syndrome. Biological Psychiatry, 32(9), 756-765.
Stujenske, J. M., Likhtik, E., Topiwala, M. A., & Gordon, J. A. (2014). Fear and safety engage competing patterns of theta-gamma coupling in the basolateral amygdala. Neuron, 83(4), 919-933.
Sullivan GM, Apergis J, Bush DEA, Johnson LR, Hou M, Ledoux JE (2004) Lesions in the bed nucleus of the stria terminalis disrupt corticosterone and freezing responses elicited by a contextual but not by a specific cue-conditioned fear stimulus. Neuroscience 128:7-14.
Sullivan RM, Gratton A (1999) Lateralized effects of medial prefrontal cortex lesions on neuroendocrine and autonomic stress responses in rats. J Neurosci 19:2834-2840.
Swanson LW, Sawchenko PE (1983) Hypothalamic integration: organization of the paraventricular and supraoptic nuclei. Annu Rev Neurosci 6:269-324.
Swanson, L. W. (2000). Cerebral hemisphere regulation of motivated behavior. Brain research, 886(1-2), 113-164.
Swanson LW (2004) Brain Maps: Structure of the Rat Brain. Amsterdam: Elsevier.
Tadel F, Baillet S, Mosher JC, Pantazis D, Leahy RM (2011) Brainstorm: A User Friendly Application for MEG/EEG Analysis Computational Intelligence and Neuroscience, vol. 2011, Article ID 879716, 13 pages, 2011.
Tappaz M, Oertel W, Wassef M, Mugnaini E (1982) Central GAB Aergic neuroendocrine regulations: pharmacological and morphological evidence. In: Progress in brain research, pp 77-96: Elsevier.

Tasker JG, Herman JP (2011) Mechanisms of rapid glucocorticoid feedback inhibition of the hypothalamic-pituitary-adrenal axis. Stress 14:398-406.
Tavares RF, Correa FM, Resstel LB (2009) Opposite role of infralimbic and prelimbic cortex in the tachycardiac response evoked by acute restraint stress in rats. J Neurosci Res 87:2601-2607.
Taylor, N. E., Pei, J., Zhang, J., Vlasov, K. Y., Davis, T., Taylor, E., ... & Brown, E. N. (2019). The role of glutamatergic and dopaminergic neurons in the periaqueductal gray/dorsal raphe: separating analgesia and anxiety. Eneuro, 6(1).
Tervo, D. G. R., Hwang, B. Y., Viswanathan, S., Gaj, T., Lavzin, M., Ritola, K. D., ... & Karpova, A. Y. (2016). A designer AAV variant permits efficient retrograde access to projection neurons. Neuron, 92(2), 372-382.
Thrivikraman, K. V., Su, Y., & Plotsky, P. M. (1997). Patterns of Fos-immunoreactivity in the CNS induced by repeated hemorrhage in conscious rats: correlations with pituitary-adrenal axis activity. Stress, 2(2), 145-158.
Tovote, P., Fadok, J. P., & Lüthi, A. (2015). Neuronal circuits for fear and anxiety. Nature Reviews Neuroscience, 16(6), 317-331.
Tovote P, Esposito MS, Botta P, Chaudun F, Fadok JP, Markovic M, Wolff SB, Ramakrishnan C, Fenno L, Deisseroth K, Herry C, Arber S, Luthi A (2016) Midbrain circuits for defensive behaviour. Nature 534:206-212.
Treit D, Aujla H, Menard J (1998) Does the bed nucleus of the stria terminalis mediate fear behaviors? Behavioral Neuroscience 112:379.
Ulrich-Lai YM, Herman JP (2009) Neural regulation of endocrine and autonomic stress responses. Nat Rev Neurosci 10:397-409.
Van De Werd HJ, Uylings HB (2008) The rat orbital and agranular insular prefrontal cortical areas: a cytoarchitectonic and chemoarchitectonic study. Brain Struct Funct 212:387-401.
Van Praag HM, de Kloet ER, van Os J (2004) Stress, the brain and depression: Cambridge University Press.
Veenema AH, Koolhaas JM, de Kloet ER (2004) Basal and stress-induced differences in HPA axis, 5-HT responsiveness, and hippocampal cell proliferation in two mouse lines. Annals of the New York Academy of Sciences 1018:255-265.
Veenema AH, Meijer OC, de Kloet ER, Koolhaas JM, Bohus BG (2003) Differences in basal and stress-induced HPA regulation of wild house mice selected for high and low aggression. Hormones and Behavior 43:197-204.
Verberne, A. J., Lewis, S. J., Worland, P. J., Beart, P. M., Jarrott, B., Christie, M. J., & Louis, W. J. (1987). Medial prefrontal cortical lesions modulate baroreflex sensitivity in the rat. Brain Research, 426(2), 243-249.
Vertes RP (2004) Differential projections of the infralimbic and prelimbic cortex in the rat. Synapse 51:32-58.
Vidal-Gonzalez I, Vidal-Gonzalez B, Rauch SL, Quirk GJ (2006) Microstimulation reveals opposing influences of prelimbic and infralimbic cortex on the expression of conditioned fear. Learn Mem 13:728-733.
Videbech P, Ravnkilde B (2004) Hippocampal volume and depression: A meta-analysis of MRI studies. Am J Psychiat 161:1957-1966.
Vogt BA, Peters A (1981) Form and distribution of neurons in rat cingulate cortex: areas 32, 24, and 29. The Journal of Comparative Neurology 195:603-625.

Vyas A, Bernal S, Chattarji S (2002a) Effects of chronic stress on dendritic arborization in the central and extended amgydala. Brain research 965:290-294.
Vyas A, Mitra R, Shankaranarayana Rao BS, Chattarji S (2002b) Chronic stress induces contrasting patterns of dendritic remodeling in hippocampal and amygdaloid neurons. The Journal of neuroscience : the official journal of the Society for Neuroscience 22:6810-6818
Vyas A, Jadhav S, Chattarji S (2006) Prolonged behavioral stress enhances synaptic connectivity in the basolateral amygdala. Neuroscience 143:387-393.
Walker DL, Davis M (1997) Double dissociation between the involvement of the bed nucleus of the stria terminalis and the central nucleus of the amygdala in startle increases produced by conditioned versus unconditioned fear. J Neurosci 17:9375-9383.
Walker DL, Toufexis DJ, Davis M (2003) Role of the bed nucleus of the stria terminalis versus the amygdala in fear, stress, and anxiety. Eur J Pharmacol 463:199-216.
Walker P, Carrive P (2003) Role of ventrolateral periaqueductal gray neurons in the behavioral and cardiovascular responses to contextual conditioned fear and poststress recovery. Neuroscience 116:897-912.
Walker, R. A., Wright, K. M., Jhou, T. C., & McDannald, M. A. (2020). The ventrolateral periaqueductal grey updates fear via positive prediction error. European Journal of Neuroscience, 51(3), 866-880.
Wallace, T., Schaeuble, D., Pace, S. A., Schackmuth, M. K., Hentges, S. T., Chicco, A. J., & Myers, B. (2021). Sexually divergent cortical control of affective-autonomic integration. Psychoneuroendocrinology, 129, 105238.
Wang, F., Flanagan, J., Su, N., Wang, L. C., Bui, S., Nielson, A., ... & Luo, Y. (2012). RNAscope: a novel in situ RNA analysis platform for formalin-fixed, paraffin-embedded tissues. The Journal of Molecular Diagnostics, 14(1), 22-29.
Watson, T. C., Cerminara, N. L., Lumb, B. M., & Apps, R. (2016). Neural correlates of fear in the periaqueductal gray. Journal of Neuroscience, 36(50), 12707-12719.
Wiltgen, B. J., Zhou, M., Cai, Y., Balaji, J., Karlsson, M. G., Parivash, S. N., ... & Silva, A. J. (2010). The hippocampus plays a selective role in the retrieval of detailed contextual memories. Current Biology, 20(15), 1336-1344.
Wichmann, S., Kirschbaum, C., Böhme, C., & Petrowski, K. (2017). Cortisol stress response in post-traumatic stress disorder, panic disorder, and major depressive disorder patients. Psychoneuroendocrinology, 83, 135-141.
Williams, C. L., Men, D., Clayton, E. C., & Gold, P. E. (1998). Norepinephrine release in the amygdala after systemic injection of epinephrine or escapable footshock: contribution of the nucleus of the solitary tract. Behavioral Neuroscience, 112(6), 1414.
Wingenfeld, K., & Wolf, O. T. (2014). Stress, memory, and the hippocampus. The Hippocampus in Clinical Neuroscience, 34, 109-120.
Winocur, G., & Moscovitch, M. (2011). Memory transformation and systems consolidation. Journal of the International Neuropsychological Society, 17(5), 766-780.
Wright KM, McDannald MA (2019) Ventrolateral periaqueductal gray neurons prioritize threat probability over fear output. eLife 8:e45013.

Xu, W., & Südhof, T. C. (2013). A neural circuit for memory specificity and generalization. Science, 339(6125), 1290-1295.
Yeh, L. F., Ozawa, T., & Johansen, J. P. (2021). Functional organization of the midbrain periaqueductal gray for regulating aversive memory formation. Molecular Brain, 14(1), 1-9.
Yizhar O, Fenno LE, Davidson TJ, Mogri M, Deisseroth K (2011) Optogenetics in Neural Systems. Neuron 71:9-34.
Yonelinas, A. P., Ranganath, C., Ekstrom, A. D., & Wiltgen, B. J. (2019). A contextual binding theory of episodic memory: systems consolidation reconsidered. Nature Reviews Neuroscience, 20(6), 364-375.
Yu, W., Pati, D., Pina, M. M., Schmidt, K. T., Boyt, K. M., Hunker, A. C., ... & Kash, T. L. (2021). Periaqueductal gray/dorsal raphe dopamine neurons contribute to sex differences in pain-related behaviors. Neuron, 109(8), 1365-1380.
Yuen, E. Y., Liu, W., Karatsoreos, I. N., Feng, J., McEwen, B. S., & Yan, Z. (2009). Acute stress enhances glutamatergic transmission in prefrontal cortex and facilitates working memory. Proceedings of the National Academy of Sciences, 106(33), 14075-14079.
Zhang, H., Zhao, Y., & Wang, Z. (2015). Chronic corticosterone exposure reduces hippocampal astrocyte structural plasticity and induces hippocampal atrophy in mice. Neuroscience Letters, 592, 76-81.
Zimmerman, J. M., & Maren, S. (2011). The bed nucleus of the stria terminalis is required for the expression of contextual but not auditory freezing in rats with basolateral amygdala lesions. Neurobiology of learning and memory, 95(2), 199-205.
Zingg, B., Chou, X. L., Zhang, Z. G., Mesik, L., Liang, F., Tao, H. W., & Zhang, L. I. (2017). AAV-mediated anterograde transsynaptic tagging: mapping corticocollicular input-defined neural pathways for defense behaviors. Neuron, 93(1), 33-47.